

**Energy-efficient Wastewater Treatment by Microbial Fuel Cells:  
Scaling Up and Optimization**

Zheng Ge

Dissertation submitted to the faculty of the Virginia Polytechnic Institute and  
State University in partial fulfillment of the requirements for the degree of

Doctor of Philosophy  
In  
Civil Engineering

Zhen He  
Gregory D. Boardman  
Amy Pruden  
Jactone Arogo Ogejo

October 12, 2015  
Blacksburg, VA

Keywords: microbial fuel cells, wastewater, energy recovery, optimization,  
scaling up

# **Energy-efficient Wastewater Treatment by Microbial Fuel Cells: Scaling Up and Optimization**

Zheng Ge

## **ABSTRACT**

Microbial fuel cells (MFCs) are potentially advantageous as an energy-efficient approach to wastewater treatment. For single-chamber tubular MFCs, anode effluent is used as catholyte instead of tap water or buffer solutions. Therefore, exposing cathode electrode to atmosphere could be also considered as a passive aeration for further aerobic oxidation of organics and nitrification. Based on several bench-scale studies, a 200-L scale MFC system with passive aeration process has been developed for treating actual municipal wastewater after primary clarification. The integrated system was able to remove over 80% organic contaminants and solid content from primary effluent. Through parallel and serial electricity connection, the power output of ~200 mW and the conversion efficiency of ~80% for charging capacitors were achieved by using commercially available energy harvesting device (BQ 25504). The treatment system is energy-efficient for the energy saving from aeration and sludge treatment while partial energy recovery as direct electricity can be utilized on site to power small electric devices. However, the post treatments are required to polish the effluent for nutrients removal.

## **ACKNOWLEDGEMENTS**

First of all, I would like to thank my advisor, Dr. Zhen He, for offering me such a precious opportunity of doing interesting research in microbial fuel cells and related wastewater technologies. Dr. He is a kind and knowledgeable mentor and he cares about us for the life, study, and career. Doing something about water seems to be my destiny that I love what I have chosen and I enjoy what I have been doing from deep down in my heart. Fortunately, I have a chance to work with Dr. He for my Ph.D study, and finally for being clear about what I will pursue as my life-time goal. I'm grateful to have Dr. He as my advisor during my graduate study. I would also like to thank my committee, Dr. Gregory D. Boardman, Dr. Amy Pruden, and Dr. Jactone Arogo Ogejo for their time and support in the research efforts.

Meanwhile, I would like to thank all of EBBL members, Dr. Zhenhai Wen, Dr. Cunyu Zhao, Dr. Yaobin Lu, Zeying Yuan, Zhemin Zhang, and Liao Wu for their support and assistance during my research journey, and especially our big brother Dr. Fei Zhang, who was always there to help me out with messy problems and encourage me to move forward.

I would like to thank my parents, for their unconditional support and constructive suggestions throughout the time of my graduate study in United States. The trust and believe on me are the most motivation of my efforts. I need thank my uncle's for their advices with a future vision from the aspect of a successful businessman. Also, a special thanks to my girlfriend Aili, for being with me during the last stressful year.

# CONTENTS

ABSTRACT.....	ii
ACKNOWLEDGEMENTS.....	iii
CONTENTS.....	iv
TABLES.....	viii
FIGURES.....	ix
ATTRIBUTION.....	xiii
CHAPTER 1.....	1
Introduction.....	1
1.1 Energy Demand and Wastewater Treatment.....	1
1.2 Principles and Applications of Microbial Fuel Cell.....	2
1.3 Scaling-up of MFC.....	5
1.4 Research Objectives.....	6
CHAPTER 2.....	9
Recovery of Electrical Energy in Microbial Fuel Cells: Brief Review.....	9
2.1 Introduction.....	9
2.2 Recovery of Electrical Energy in MFCs with Different Scales.....	12
2.3 Recovery of Electrical Energy from Different Substrates.....	15
2.4 Recovery of Electrical Energy in MFCs with or without Separators.....	18
2.5 Perspectives.....	19
CHAPTER 3.....	23
Effects of Draw Solutions and Membrane Conditions on Electricity Generation and Water Flux in Osmotic Microbial Fuel Cells.....	23
3.1 Introduction.....	23
3.2 Materials and Methods.....	26
3.2.1 OsMFC setup and general operation.....	26
3.2.2 General measurement and analysis.....	27
3.2.3 Specific testing conditions.....	27
3.3 Results and Discussion.....	30
3.3.1 Effects of draw solutions on the OsMFC performance.....	30

3.3.2 Effects of membranes on the OsMFC performance .....	38
3.4 Conclusions.....	42
CHAPTER 4 .....	43
Reducing Effluent Discharge and Recovering Bioenergy in an Osmotic Microbial Fuel Cell Treating Domestic Wastewater .....	43
4.1 Introduction.....	43
4.2 Materials and Methods.....	45
4.2.1 OsMFC setup .....	45
4.2.2 OsMFC startup.....	47
4.2.3 OsMFC fed on acetate solution.....	47
4.3.4 OsMFC fed on domestic wastewater .....	48
4.2.5 Measurement and analysis .....	48
4.3 Results and Discussion .....	50
4.3.1 OsMFC fed on acetate solution.....	50
4.3.2 OsMFC fed on domestic wastewater .....	53
4.3.3 FO membrane fouling.....	60
4.4 Conclusions.....	62
CHAPTER 5 .....	63
Hollow-fiber Membrane Bioelectrochemical Reactor for Domestic Wastewater Treatment .....	63
5.1 Introduction.....	63
5.2 Materials and Methods.....	65
5.2.1 MBER construction .....	65
5.2.2 Operating condition .....	67
5.2.3 Measurement and analysis .....	68
5.2.4 Energy estimation .....	70
5.3 Results.....	70
5.3.1 The MBER treating synthetic solution .....	70
5.3.2 The MBER treating wastewater.....	72
5.3.3 Energy balance.....	76
5.3.4 Membrane fouling.....	77

5.4 Conclusions.....	82
CHAPTER 6 .....	83
Long-Term Investigation of Microbial Fuel Cells Treating Primary Sludge or Digested Sludge .....	83
6.1 Introduction.....	83
6.2 Materials and Methods.....	85
6.2.1 MFC setup.....	85
6.2.2 MFC operation.....	86
6.2.3 Measurement and analysis .....	87
6.3 Results and Discussion .....	88
6.3.1 MFCs treating primary sludge or digested sludge .....	88
6.3.2 Two-stage MFC system treating primary sludge.....	92
6.3.3 Biogas and energy production .....	96
6.4 Conclusions.....	100
CHAPTER 7 .....	101
An Effective Dipping Method for Coating Activated Carbon Catalyst on The Cathode Electrodes of Microbial Fuel Cells .....	101
7.1 Introduction.....	101
7.2 Materials and Methods.....	103
7.3 Results and Discussion .....	104
7.4 Conclusions.....	113
CHAPTER 8 .....	114
Energy Extraction from A Large-Scale Microbial Fuel Cell System Treating Municipal Wastewater.....	114
8.1 Introduction.....	114
8.2 Materials and Methods.....	117
8.2.1 The MFC system.....	117
8.2.2 Electronic connections and energy harvesting device .....	117
8.2.3 Measurement and analysis .....	118
8.3 Results and Discussion .....	119
8.3.1 Performance of the MFC system .....	119
8.3.2 Energy extraction and conversion efficiency by using BQ 25504 .....	120

8.3.3 Charging and discharging .....	124
8.4 Conclusions.....	125
CHAPTER 9 .....	126
Perspectives.....	126
Reference .....	128
Appendices.....	140
Appendix A Supplemental Information to Chapter 4.....	140
Appendix B Supplemental Information to Chapter 5 .....	144
Appendix C Supplemental Information to Chapter 6 .....	149
Appendix D Supplemental Information to Chapter 8.....	152

## TABLES

Table 1.1 Standard potentials E0 and theoretical potentials for typical condition in MFCs (Logan et al., 2006).....	4
Table 4.1. The OsMFC performance with acetate solution or actual wastewater (WW). .	52
Table 4.2 The OsMFC performance during the step-decrease of wastewater HRT.....	55
Table 5.1. Characterization of the influent and the effluent of the MBER with different substrates and HRTs .....	73
Table 6.1 Characteristics of the primary sludge (PS) and the digested sludge (DS) in the Phase I.....	90
Table 6.2 Characteristics of the primary sludge (PS) and the treatment performance of the two MFCs in the Phase II.....	94
Table 6.3 Energy production (kWh/m <sup>3</sup> ) from the two-stage MFC system in the Phase II and energy production from biogas at South Shore Water Reclamation Facility.....	98
Table 7.1 Exchange current generated with the cathode electrodes with different initial AC input and multiple dipping times.....	109
Table 8.1 Performance of the MFC system (four groups in serial connection) in contaminants removal and current production.....	121
Table A1 The composition of the scaling compounds on the side of the FO membrane facing the anode (wastewater) .....	142
Table A2 The composition of the scaling compounds on the side of the FO membrane facing the cathode (draw solution).....	142
Table B1 Power consumption by the pumping system at different HRTs. ....	144
TABLE B2 Analysis of energy production and consumption of the MBER with different substrates and HRTs. ....	144
Table B3 Membrane cleaning methods and water flux during treatment of primary effluent. ....	145
Table B4 The mass ratio of the new and the fouled membrane.....	145

## FIGURES

Figure 1.1 Schematic of two-chamber microbial fuel cell.....	3
Figure 1.2 Schematic of electron transport from substrate to electrode in <i>G. sulfurreducens</i> biofilm (Sun et al., 2014).....	4
Figure 2.1 Electricity generation in MFCs with different anode liquid volumes: (A) power density, (B) normalized energy recovery, and (C) normalized energy recovery...	14
Figure 2.2 Normalized energy recovery (A) and power density (B) of the MFCs treating different types of substrates. WW means wastewater. Error bars represent the standard deviation.....	15
Figure 2.3 Comparison of normalized energy recovery from acetate between two concentration ranges. ....	17
Figure 2.4 Normalized energy recovery of the MFCs with or without separators and/or membranes. Error bars represent the standard deviation. ....	17
Figure 3.1 Experimental setup of an osmotic microbial fuel cell.....	27
Figure 3.2 The short-term (4 h) test of different draw solutions: (A) current generation and (B) water flux. ....	31
Figure 3.3 The effect of PPB concentrations on the OsMFC performance: (A) current generation and (B) water.....	34
Figure 3.4 Buffering the pH of the NaCl solution with dosing acid. The arrows indicate the addition of acid to the draw solution.....	35
Figure 3.5 Current generation in the OsMFC with FO membranes (an a CEM) under different conditions (A) and the 1-h test of the fouled & dried FO membrane (B). ....	37
Figure 3.6 Water flux (A) and current generation (B) during the test of backwash. The arrows indicate the addition of NaCl into the anode compartment. ....	40
Figure 4.1 Schematic of experimental setup of an osmotic microbial fuel cell.....	46
Figure 4.2 Polarization curves of the OsMFC treating acetate solution. ....	51
Figure 4.3 Batch operation of the OsMFC treating acetate solution: (A) the profile of current generation; and (B) the increase in water mass in a batch.....	52
Figure 4.4 Batch operation of the OsMFC treating wastewater: (A) the profile of current generation; and (B) the increase in water mass in a batch.....	55

Figure 4.5 Current generation of the OsMFC treating wastewater: (A) continuous operation; and (B) the step-decrease of wastewater HRTs. ....	56
Figure 4.6 Polarization curves of the OsMFC treating wastewater in continuous operation and at HRT 24 h. ....	56
Figure 4.7 Comparison between clean and fouled FO membranes: (A) Bode plot of electrochemical impedance spectroscopy; and (B) short-term water flux test (in a U-shape reactor shown in Fig. A1) .....	58
Figure 4.8 SEM pictures of the fouled FO membrane (A — active side; B — support side; C — cross-section) and a clean FO membrane (D — active side; E — support side; F — cross-section). ....	61
Figure 5.1. Schematic of a membrane bioelectrochemical reactor (MBER): 1 – influent reservoir, 2 – electric circuit, 3 – cathode electrode (carbon cloth), 4 – anode electrode (carbon brush), 5 – cation exchange membrane (CEM), 6 – gas collection, 7 – hol.....	66
Figure 5.2. Polarization curves (power and voltage) of the MBER with acetate solution (A) and wastewater (B). The wastewater polarization tests were conducted at two different organic loading rates: 0.04 and 0.28 kg TCOD m <sup>-3</sup> d <sup>-1</sup> .....	68
Figure 5.3 MBER performance with synthetic solution: (A) current generation, (B) transmembrane pressure (TMP), and (C) COD concentrations in the influent and the effluent. Arrow a: physical cleaning; arrow b: chemical cleaning. ....	74
Figure 5.4 MBER performance with wastewater (primary effluent): (A) current generation and COD loading rates; (B) transmembrane pressure (TMP); and (C) COD concentrations in the influent and the effluent. Arrow a: extremely low COD after a major storm; arrow b: the catholyte changed from tap water to the anode effluent. ....	75
Figure 5.5. Energy consumption and production in the MBER with different anode effluents at different HRTs. AS: acetate solution. PE: primary effluent. The number in parentheses indicates the HRT. ....	78
Figure 6.1 Schematic of the tubular MFC used for sludge treatment. ....	86
Figure 6.2 Current generation of individual MFC in Phase I with an HRT of 9 days in each reactor: (A) MFC-1 fed with primary sludge and (B) MFC-2 fed with digested sludge. ....	89
Figure 6.3 Current generation in the two-stage MFC system fed on primary sludge in Phase II with an HRT of 7 days in each reactor: (A) MFC-1 and (B) MFC-2. ....	93
Figure 6.4 Biogas production in the MFCs during Phase II. ....	97
Figure 7.1 The actual AC loading rates (Y axis) on the electrodes with different initial AC input of 2, 4, 8, and 12 g per 100 mL ethanol, and multiple dipping times. ....	106

Figure 7.2 Tafel plots of the cathode electrodes with different initial loading AC load (A) and different coating layers (CLs) by dipping (B).....	108
Figure 7.3 Variation of voltage and power density with current density in the MFC containing cathode electrode prepared in different ways: (A and B) cathode electrode coated with different initial AC input and one prepared by the brushing method for comp .....	109
Figure 7.4 Current generation during batch operation (A) and the production of total charge in a batch (B) with different initial AC inputs in a tubular MFC.....	112
Figure 8.1 Polarization curves of the MFCs with four types of serial connection: (A) S4 (R1357), (B) S3 (R 357), (C) S2 (R57), and (D) S1 (R5).....	120
Figure 8.2 Charging profiles of the ultracapacitors by the MFCs with four types of serial connection using BQ 25504.....	121
Figure 8.3 The efficiency of the BQ25504 with different voltage input under four types of connection: (A) S4 (R1357), (B) S3 (R 357), (C) S2 (R57), and (D) S1 (R5). .....	122
Figure 8.4 Charging and discharging of the ultracapacitors by the MFC system (S3 connection) and BQ25504. ....	124
Figure A1. The U-shape reactor used for the water flux test.....	141
Figure A2 EDS spectrum of the scaling compounds on the side of the FO membrane facing the anode (wastewater). ....	143
Figure A3 EDS spectrum of the scaling compounds on the side of the FO membrane facing the cathode (draw solution).....	143
Figure B1 Current generation in the MBER fed with the acetate solution at HRT 19 h. 146	
Figure B2 The TMP increase in the MBER fed with the acetate solution at HRT 19 h. 146	
Figure B3 Hollow-fiber membranes before (left) and after (right) chemical cleaning (day 202). ....	147
Figure B4 The weight percentages (WT%) of the elements in the new and the fouled membrane from EDS analysis: A) the interior and B) the exterior. ....	147
Figure B5 FTIR spectra of the new and the fouled membranes. ....	148
Figure C1 Power and voltage curves of the two MFCs during Phase I. MFC-1 was fed with the primary sludge and MFC-2 was supplied with the digested sludge. The scan rate was 0.1 mV/s.....	149
Figure C2 Current generation of MFC-1 with different recirculation rates in Phase I..	150

Figure C3 Current generation of MFC-1 buffered with two different solutions in Phase I. .... 150

Figure C4 Power and voltage curves of the two MFCs during Phase II: (A) using acidified water as a catholyte; and (B) using neutralized water as a catholyte. The scan rate was 0.1 mV/s..... 151

Figure D1 Schematic of MFCs system. .... 152

Figure D2 Schematic of electric connections: serial connections (top) and charging/discharging circuit connection (bottom). .... 153

Figure D3 Polarization curves of MFCs with various serial connections. .... 156

## ATTRIBUTION

*Each coauthor is duly credited for his or her contribution to this work, both in their sharing of ideas and technical expertise.*

Zhen He, Ph.D. Associate Professor of Civil and Environmental Engineering  
(Principal Investigator)

Department of Civil and Environmental Engineering, Virginia Polytechnic Institute  
and State University. Blacksburg, VA 24061

Coauthor of chapters 2, 3, 4, 5, 6, 7, 8

Jian Li, M.S., Doctoral Student

Department of Civil and Environmental Engineering, Virginia Polytechnic Institute  
and State University. Blacksburg, VA 24061

Coauthor of chapters 2

Yiran Tong, M.S., Doctoral Student

Department of Civil, Construction and Environmental Engineering, Marquette  
University. Milwaukee, WI 53233

Coauthor of chapters 2

Li Xiao, Ph.D.

Coauthor of chapters 2, 4

Qingyun Ping, Doctoral Student

Department of Civil and Environmental Engineering, Virginia Polytechnic Institute  
and State University. Blacksburg, VA 24061

Coauthor of chapters 4, 5

Fei Zhang, Ph.D., Research Scientist  
Cell-Free Bioinnovations, Inc. Blacksburg, VA 24061

Coauthor of chapters 6, 8

Julien Grimaud,  
Veolia Water North America, Indianapolis, IN 46204

Coauthor of chapters 6

Jim Hurst, P.E., Chief Technical Officer  
Veolia Water North America, Indianapolis, IN 46204

Coauthor of chapters 6

Liao Wu, Ph.D. student,  
College of Computer Science and Electronic Engineering, Hunan University,  
Changsha 410082, China

Coauthor of chapters 8

# **CHAPTER 1**

## **Introduction**

### **1.1 Energy Demand and Wastewater Treatment**

Currently, wastewater treatment technologies applied in many areas and countries are based on activated sludge process, an old but effective method for reducing pollutants in a short period. Although this century-old technology and its various modifications have been serving human society for environmental protection and pollution control successfully, a serious concern is the energy consumption that the energy demands keep increasing for the explosion of population and fast economic development. It may not be possible to reduce the generation of wastewater from human activities because of unsustainable utilization of raw materials and continuous growth of population, but more renewable energy sources can be explored for water treating and reusing. In U.S., about 3-4% of the electrical energy is consumed for wastewater treatment (Smith, 2002), however, domestic wastewater, itself, could be considered as an alternative renewable energy source for the high content of biodegradable organics. It was estimated that twice more energy could be recovered from organics in municipal solid waste than the operation (Mata-Alvarez et al., 2000).

Therefore, theoretically it should be possible to achieve energy-positive for wastewater treatment, or at least energy-neutral. Generally, 0.6 kWh per cubic meter treated wastewater is typically needed for a treatment facility employing aerobic activated sludge and anaerobic digestion process (McCarty et al., 2011). Such an energy-intensive process is mainly the result of the aeration for organic oxidation and nitrification in aeration tank,

and the following disposal of wasted sludge. Comparing with aerobic biological treatment, two distinguished advantages from anaerobic process are low energy consumption (no aeration) and less sludge production. To remove nitrogen, the subsequent ANAMMOX (anaerobic ammonium oxidation) would be an excellent alternative with low energy consumption as well as little sludge production (Lackner et al., 2014). In consequence, conventional aerobic biological treatment is completely replaceable by anaerobic process for organics degradation.

## **1.2 Principles and Applications of Microbial Fuel Cell**

Conventional anaerobic process (such as anaerobic digestion) is widely known for its capability of treating high concentration organic wastewater with positive energy recovery. However, for domestic wastewater treatment, low methane yield ( $0.16-0.25 \text{ L CH}_4 \text{ g}^{-1} \text{ COD}$ ) and high methane loss (28-39%) under ambient temperature conditions would be a challenging environmental issue (Kim et al., 2010; Plappally & Lienhard V, 2012).

Different from classic anaerobic process, as an emerging and promising technology of sustainable energy-efficient method for wastewater treatment, microbial fuel cell (MFC) is a device that degrades organics and simultaneously generates direct electricity with catalysis through bacteria (Logan et al., 2006). To distinguish from chemical fuel cell which is based on pure chemical reaction for the whole cell, a bio-anode in MFC is able to oxidize organics to obtain electrons, and then transfer the electrons to cathode to complete cathodic reduction reaction (Fig. 1.1). In most MFCs for treating wastewater, anode functions as a anaerobic bioreactor to degrade organic contaminants while anode electrode,

as electron acceptor, collect electrons and conduct them to cathode, which can be expressed as procedure in Fig. 1.2 (oxygen is final electron acceptor in cathode). The electrons obtained from substrate oxidation can be transported through NADH/NAD<sup>+</sup> and then to serial cytochrome agents in the outer cell membrane, and finally to anode electrode. The next step is electricity generation that the electrons from anode electrode will move toward high potential direction to cathode. Some typical half-cell reactions for anode and cathode in MFC are shown in Table 1.1. Therefore, the major difference between exoelectrogenic bacteria and other microorganisms is the pathway of electrons transport. In conventional definition, either anaerobic or aerobic respiration involves electron movement within the cells while the electron acceptors participate in metabolic activities which happen inside of the cells. However, for exoelectrogenic bacteria, electron reception is completed outside of the cells and the types of electron acceptors do not affect the metabolic pathway because the extracellular reception of electrons. It could be more accurate to understand exoelectrogens as anaerobic biological process with electrode respiration.

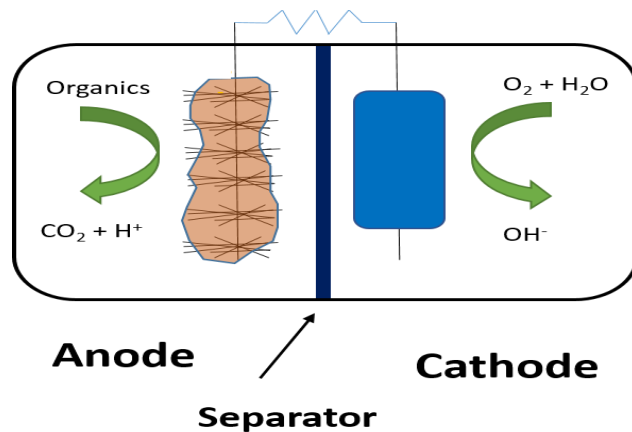


**Figure 1.1 Schematic of two-chamber microbial fuel cell**

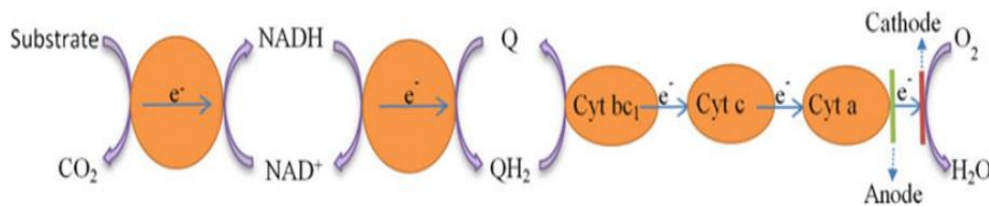


**Figure 1.2 Schematic of electron transport from substrate to electrode in *G. sulfurreducens* biofilm (Sun et al., 2014)**

**Table 1.1 Standard potentials  $E_0$  and theoretical potentials for typical condition in MFCs (Logan et al., 2006)**

Electrode	Reaction	$E_0$ (V)	Conditions	$E_{MFC}$ (V)
Anode	$2 \text{HCO}_3^- + 9 \text{H}^+ + 8 \text{e}^- \rightarrow \text{CH}_3\text{COO}^- + 4 \text{H}_2\text{O}$	0.187	$\text{HCO}_3^- = 5 \text{ mM}, \text{CH}_3\text{COO}^- = 5 \text{ mM}, \text{pH} = 7$	-0.296
Cathode	$\text{O}_2 + 4 \text{H}^+ + 4 \text{e}^- \rightarrow 2 \text{H}_2\text{O}$	1.229	$\text{pO}_2 = 0.2, \text{pH} = 7$	0.805
	$\text{O}_2 + 2 \text{H}_2\text{O} + 4 \text{e}^- \rightarrow 4 \text{OH}^-$	1.229	$\text{pO}_2 = 0.2, \text{pH} = 7$	0.805

An MFC oxidizing acetate in anode ( $\text{HCO}_3^- = 5 \text{ mM}, \text{CH}_3\text{COO}^- = 5 \text{ mM}, \text{pH} = 7$ ) and reducing oxygen in cathode ( $\text{pO}_2 = 0.2, \text{pH} = 7$ ) has a cell emf of 1.101 V.

No matter what mechanisms are for MFCs, researchers have developed various engineering systems, such as small cylinder (Liu & Logan, 2004; Rabaey et al., 2005a), H-shape bottle (Logan et al., 2005), MFC stacks (Aelterman et al., 2006), tubular MFC (Rabaey et al., 2005b), and etc., to achieve wastewater treatment and energy recovery based upon this innovative concept. Multiple studies have reported the applications of MFCs for wastewater treatment, including both domestic and industrial wastewater (Çetinkaya et al., 2015; Choi & Ahn, 2013; Fang et al., 2015; Feng et al., 2014a; Samsudeen et al., 2015; Ye et al., 2014). The long-term study also demonstrated the technical feasibility and reliability of MFC technology when dealing with real wastewater (Zhang et al., 2013). Meanwhile,

the technologies have been reviewed as one of the most promising alternatives to replace old-fashion activated sludge system by many researchers (Douglas C. Montgomery, 2011; Heidrich et al., 2011; Kim et al., 2011; Li et al., 2014). MFCs can be positioned as center unit for biological treatment instead of activated sludge process, functioning with necessary pretreatment and post polish treatment (Li et al., 2014).

### **1.3 Scaling-up of MFC**

One of the challenges in MFC development is the scaling-up of MFCs for practical applications, which includes increasing capacity of wastewater treatment and transferring energy from multiple cells in one MFCs system. To date, the most popular method to size up the reactor is to modularized single MFC unit. Tubular MFCs from Zhang (Zhang et al., 2013) and Ge's (Ge et al., 2015) studies have been demonstrated as reliable approach for treating municipal wastewater. Meanwhile, Dong has successfully developed stackable MFC modules with 90 L liquid capacity in total for brewery wastewater treatment (Dong et al., 2015). There are also three other reported work using similar configuration but applied in microbial electrolysis cells (MECs). However, comparing with thousands of publications from bench-scale MFC studies, few example over 50 L can be found till now. Even though some large MFCs (> 100 L) were reported but the performance was poor that neither organic removal nor energy recovery from organics were comparable with other small-scale studies (Feng et al., 2014b).

Generally, the power output decreases as the size of MFCs increases as reviewed in Chapter 2, probably due to the limitation of mass transfer in larger anode and cathode. Such “fuel

cell” concept determines that it requires more consideration on reactor design to reduce the mass transfer limits. Unlike a typical bioreactor with one chamber, MFCs require more attentions on balancing among anode, cathode, biofilm formation, and electricity production that any defects would limit the performance of the whole system because of interconnection between each components. Therefore, in MFCs, scaling-up does not only mean volume of anode (liquid capacity), but also involves the appropriate amplification of electrodes, separators, and catalyst coating.

## **1.4 Research Objectives**

The overall goal of this study is to develop a large-scale MFCs based on the understanding of small bench-scale studies to examine and optimize the performance of the compacted MFCs system on municipal wastewater treatment and energy recovery/utilization from organic degradation.

The first objective is to construct a MFCs platform with the effective anodic liquid volume of ~200 L, following by a post polish treatment with passive aeration. How to make MFC technology practical for dealing with large amount of influent flow is probably the most urgent challenge to date that most studies are still based on bench-scale reactors. Even though the liquid volume has been increased from milliliter to liter scale, there is few study reporting the performance of MFCs with larger scale (hundred liters to cubic meters) that conclusions from those studies may not work for large-scale system, or in another word, strategies successfully applied in small-scale system would not fit due to variance of reactor configuration. The three reported work based on large volume over 50 L were developed

based on two-chamber or membraneless air-cathode configurations (Dong et al., 2015; Feng et al., 2014b; Liang et al., 2013) but the complexity of “fuel cell” concept also enables the more potential alternatives for scaling-up that tubular reactor would also be one of potential candidate for future large-scale application. Therefore, it is important to evaluate the feasibility of large MFCs system with multiple tubular cells.

The second objective is the evaluation of treatment performance and electricity production based on the integrated MFCs system. The operation parameters such as hydraulic retention time (HRT) and catholyte distribution frequency would be two critical control factors regarding the organics removal and electricity generation. A general negative tendency observed is that large-scale MFCs produce lower power density normalized on effective liquid volume than that in small bench-scale reactors. For millimeter-scale MFCs, power density could reach  $\text{kW m}^{-3}$  level but for cells larger than 1 liter, power output is usually less than  $30 \text{ W m}^{-3}$  (Ge et al., 2013). The operation strategies could be quite different due to the high concentration gradient and limitation of mixing and mass transfer in larger reactors. In addition, buffer solution and other chemicals used under lab condition should be avoided for practical application but pH in final effluent has to be maintained neutral for either discharge or reuse.

Thirdly, energy recovery and utilization on site will be the final goal of the project. Actual electricity generation and energy balance analysis in large-scale system can give more reliable information regarding energy aspect than the results based on theoretical calculation from small MFCs, making steps towards developing pilot-scale tests and

commercial products more reasonable and confident. Although MFC is considered as a promising technology that is able to recovery direct electricity while treating wastewater, most studies did theoretical calculation based on lab conditions with small energy output which could not be able to power real utilities used in treatment process (such as pumps, mixers, or blowers). There are some publications reporting practical charging application in MFC and MDC systems (Dong et al., 2015; Ledezma et al., 2013; Zhang & He, 2012), which excited people about future of MFC and its possibility to use wastewater as energy source, however, it could be another challenge to power large appliances by extracting and managing energy from large-scale MFC system with multiple cells. In consequence, proper approach should be developed and investigated to transfer energy from MFCs to any energy storage media, which can be used further to power electronics and large utilities.

## CHAPTER 2

### Recovery of Electrical Energy in Microbial Fuel Cells: Brief Review

(This section has been published as: Ge, Z., Li, J., Xiao, L., Tong, Y. and He, Z.\* (2014) Recovery of electrical energy in microbial fuel cells. **Environmental Science & Technology Letters**. Vol 1, pp 137-141.)

#### 2.1 Introduction

One of the potential applications of microbial fuel cell (MFC) technology is to recover bioenergy from low-grade substrates such as wastewater (Logan & Rabaey, 2012). The electrical effects in a biological system were observed ~100 years ago, leading to the development of the MFC concept with intensive research conducted in the past decade (Arends & Verstraete, 2012). We have obtained a substantial amount of fundamental information about the microbiology, electrochemistry, and materials of MFCs. To examine the technical viability of MFCs, it is critical to understand their application niche, which is strongly related to their energy performance. It is widely acknowledged that the advantage of MFC technology is direct electricity generation; however, there is a lack of proper presentation of the energy data (He, 2013), and we are still not clear about how much energy MFCs can actually recover from wastewater.

There have been very few studies showing the data of energy recovery in reactor-type MFCs (excluding sediment and plant MFCs), although energy efficiency has been defined and reported in the literature (Liu & Logan, 2004; Logan et al., 2006; Rabaey et al., 2003). An early example reporting energy data in normalized energy recovery (NER) was a modular tubular MFC with an NER as high as 1.75 kWh/kg of the removed chemical oxygen demand (COD) (Kim et al., 2010a). In another study, by using a maximal power

point circuit, the researchers were able to extract  $2.13 \times 10^{-5}$  kWh from an MFC, much higher than  $2.77 \times 10^{-7}$  kWh when using a charge pump (Wang et al., 2012). In a novel osmotic MFC that extracted water from the anode through forward osmosis, energy recovery varied between 0.02 and 0.11 kWh/m<sup>3</sup> of treated wastewater, depending on the hydraulic retention time (Ge et al., 2013b). An MFC containing hollow-fiber ultrafiltration membranes for improved effluent quality generated much more energy from an acetate solution than from domestic wastewater (Ge et al., 2013a). During a long-term operation, the MFCs installed in a municipal wastewater treatment facility recovered less than 0.03 kWh/m<sup>3</sup> of the treated wastewater from the primary effluent (Zhang et al., 2013).

Those prior studies show the initial effort to understand the energy recovery in MFCs and also reveal the urgency of further studying this issue. To extract more information about energy recovery from previous MFC studies, we have examined and analyzed the MFC publications that have appeared in the past 12 years and used the reported data on power, flow rates, and organic concentrations to calculate the NER in various MFCs. By searching “microbial fuel cell” as a keyword in article titles in Web of Science (sediment-type or plant MFCs were excluded), we found 1412 MFC publications between 2000 and May 2013 and examined 840 papers for which we had access to the full text. Of the 194 papers reporting continuously operated MFCs, 128 papers were analyzed for NER because they contain sufficient information for energy analysis. Those papers are only a portion of the MFC-related publications (many of which could be missing because of the searching method, the available database, or the lack of data for energy analysis), but we think those that are analyzed can represent MFC research on continuously operated systems to a certain

degree for the past decade. Because of the difference in the presentation of data in the selected papers, in which some show the maximal power values (usually obtained from a polarization curve), some introduce the operating power data (with an external resistor), and some report both, we decided to use the operating power data for energy analysis or the maximal power values if no operating power data were reported. The concentrations of pure substrates such as acetate or glucose were converted into COD.

The NER is expressed in kilowatt hours per cubic meter [based on the volume of the water treated, or power divided by wastewater flow rate (eq. 2.1)], a common unit for discussing energy issues in wastewater treatment (Plappally & Lienhard V, 2012a), or kilowatt hours per kilogram of COD [based on organic removal, or power divided by wastewater flow rate and the difference in COD concentration (eq. 2.2)]. An MFC can achieve the maximal NER, which is affected by power output, wastewater flow rate, organic loading rate, and removal efficiency:

$$\begin{aligned} \text{NER} &= \frac{\text{power} \times \text{time } t}{[\text{wastewater volume (treated within time } t)]} \\ &= (\text{power}) / (\text{wastewater flow rate}) \end{aligned} \quad (2.1)$$

$$\begin{aligned} \text{NER} &= \frac{\text{power} \times \text{time } t}{[\text{COD (removed within time } t)]} \\ &= (\text{power}) / (\text{wastewater flow rate} \times \Delta \text{COD}) \end{aligned} \quad (2.2)$$

We focus on the studies of continuously operated MFCs because those with batch-operated MFCs usually report only the peak power values, which do not reflect the power production of a whole batch profile and cannot be used to estimate energy recovery in the absence of the raw data of the power–time profile. The energy data were statistically analyzed for comparison by using a two-sample t test (Douglas C. Montgomery, 2011). It must be noted

that, because of significant variations in MFC construction and operation among different studies, the conclusions drawn from the data may need further verification with strictly designed experiments. The objective of this brief review is to conduct initial literature analysis of energy performance of MFCs and encourage further investigation of this issue. Our analyses reveal a rough picture of energy recovery in MFCs affected by several factors, which has not been demonstrated before.

## **2.2 Recovery of Electrical Energy in MFCs with Different Scales**

The scale of MFC reactors has been a critical factor to MFC development, because it requires large-scale systems to demonstrate the technical and economical viability of MFC technology; however, most MFC studies were conducted in small reactors at milliliter levels. The desired scale for a successful demonstration will be from several hundreds to thousands of liters.

The prior studies usually use power density as a parameter to describe the “performance of electricity generation” in an MFC. The commonly used calculation of power density (eq. 3) is based on the anode liquid volume (or anodic net volume) and does not reflect either the volume of the treated wastewater or the removed COD like NER. The power densities of the selected studies are shown in Fig. 2.1A, in which the high power densities ( $>500$   $\text{W}/\text{m}^3$ ) are obtained from the MFCs with volumes of  $<50$  mL, and the highest (operating) power density of  $2150$   $\text{W}/\text{m}^3$  was reported in a  $0.34$  mL MFC. The MFCs producing  $100$ – $500$   $\text{W}/\text{m}^3$  generally have an anode liquid volume of  $<2000$  mL. When the MFC size is  $>2000$  mL, the power density is usually  $<30$   $\text{W}/\text{m}^3$ . The power density of the  $<100$  mL

MFC is significantly higher than the power density of those between 100 and 1000 mL and the power density of those larger than 1000 mL ( $p < 0.01$ ); the 100–1000 mL MFCs produce higher power densities than >1000 mL MFCs ( $p < 0.05$ ). Therefore, it seems that power densities decrease with an increase in MFC size.

$$\text{power density} = (\text{power})/(\text{anode liquid volume}) \quad (2.3)$$

However, the NER data exhibit different profiles. The high NER based on the volume of the treated water is more than 2.0 kWh/m<sup>3</sup> and achieved in MFCs with volumes ranging from 30 mL to 20 L (Fig. 2.1B). Most studies have NERs smaller than 0.3 kWh/m<sup>3</sup>. When expressing the NER based on organic removal (Fig. 2.1C), the highest NER of 1.95 kWh/kg of COD was obtained from a 230 mL MFC (Tugtas et al., 2011), which is 51% of the theoretical energy content (3.86 kWh/kg of COD) from COD oxidation to carbon dioxide and water (McCarty et al., 2011). Approximately 27% of the studies have an NER higher than 0.2 kWh/kg of COD, with reactor sizes ranging from 5 to 5800 mL. There is no statistical difference in NERs between the MFCs with different scales ( $p > 0.05$ ).

We have observed some discrepancies between the two NERs. For example, one study reported a very high NER based on the treated volume (2.25 kWh/m<sup>3</sup>) but had a medium value of 0.70 kWh/kg of COD; on the other hand, the study with a high NER based on COD removal (1.76 kWh/kg of COD) had a low NER based on the treated volume (0.026 kWh/m<sup>3</sup>). This may be caused by the different feeding rates and organic removal efficiencies and/or rates in those studies. We suggest that future studies that focus on energy recovery from wastewater should report NER values based on both the treated volume and the removed COD.

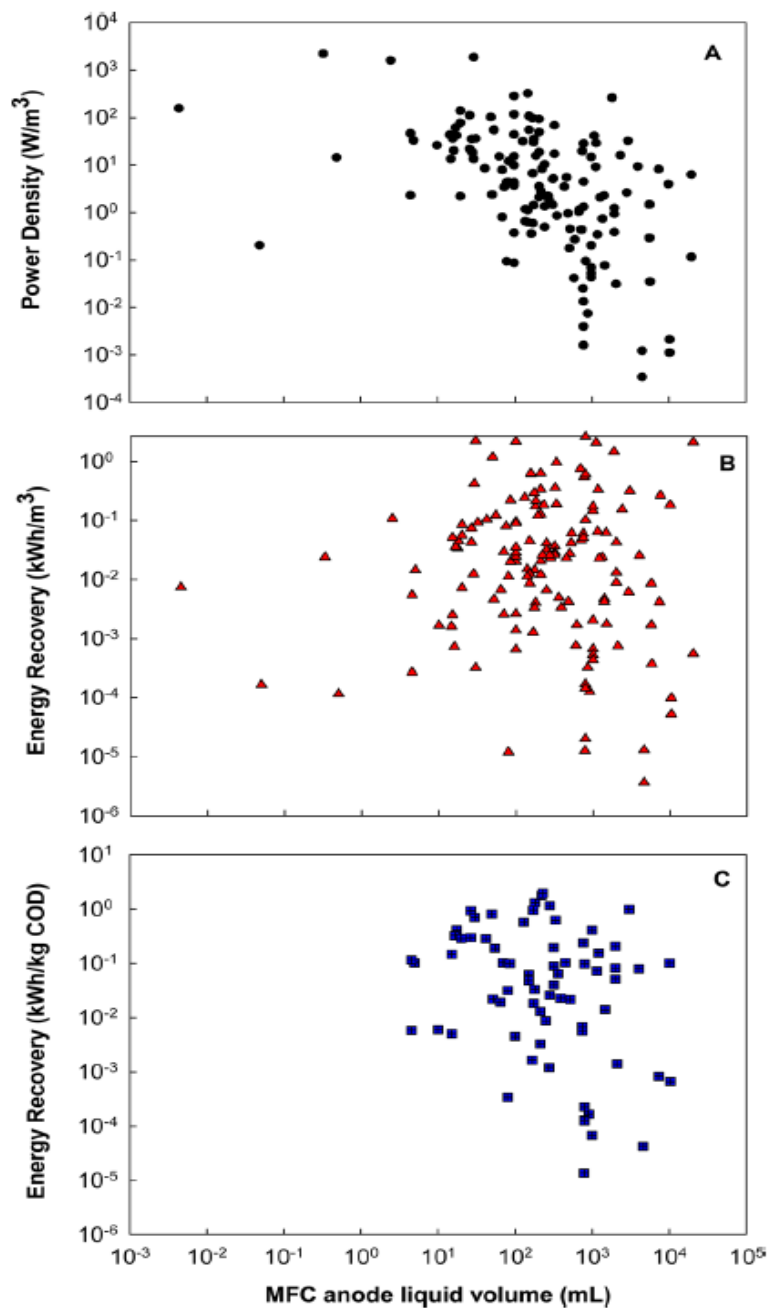
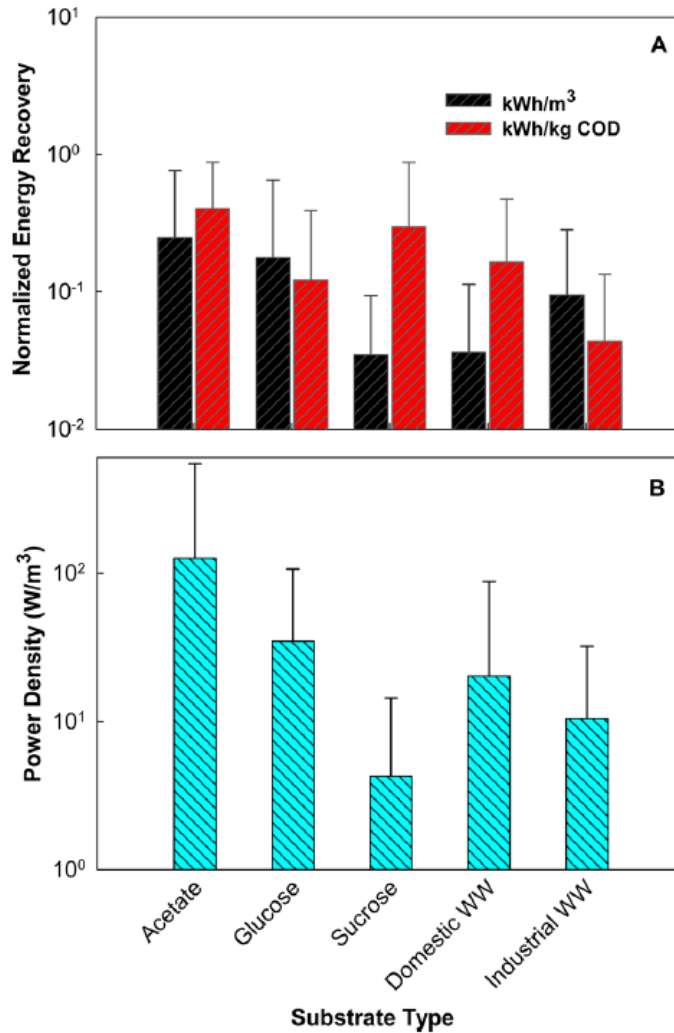


Figure 2.1 Electricity generation in MFCs with different anode liquid volumes: (A) power density, (B) normalized energy recovery, and (C) normalized energy recovery.



**Figure 2.2 Normalized energy recovery (A) and power density (B) of the MFCs treating different types of substrates. WW means wastewater. Error bars represent the standard deviation.**

### 2.3 Recovery of Electrical Energy from Different Substrates

Anode substrates, mostly organic compounds, are electron sources for electricity generation in MFCs. Substrates can significantly affect the anode potential, the microbial community, and the quality of the treated effluent, as well as the energy recovery. A wide range of substrates, including acetate, glucose, wastewater, and petroleum compounds, have been studied in MFCs for electricity generation (Pant et al., 2010).

Simple substrates such as acetate are expected to result in more electricity generation than complex ones, because of (relatively) simpler degradation pathways that could have less energy loss, which is demonstrated well in power production (Fig. 2.2B). For example, acetate, which may be the most often used substrate in MFC research, leads to much higher power densities than glucose ( $p < 0.03$ ), sucrose ( $p < 0.01$ ), or actual wastewaters ( $p < 0.01$ ) that are more complex. For energy recovery, acetate still exhibits a better performance than actual wastewaters ( $p < 0.05$ ), while the NERs from glucose are statistically similar to those from wastewater ( $p > 0.05$ ). The average NER with acetate is  $0.25 \text{ kWh/m}^3$  or  $0.40 \text{ kWh/kg}$  of COD, and that with glucose is  $0.18 \text{ kWh/m}^3$  or  $0.12 \text{ kWh/kg}$  of COD; the average NER with domestic wastewater is  $0.04 \text{ kWh/m}^3$  or  $0.17 \text{ kWh/kg}$  of COD, and industrial wastewater results in a value of  $0.10 \text{ kWh/m}^3$  or  $0.04 \text{ kWh/kg}$  of COD (Fig. 2.2A). Large variations associated with those values indicate the existence of some exceptional performances (either extremely high or low) in a few studies. Domestic wastewater generally has a low energy output based on the treated volume because of its low concentration, which, however, may also lead to an NER based on COD removal comparable to that of the pure organics, likely because of a better conversion of organics into electrical energy with low-concentration organics compared to that of a high-concentration organic stream.

To further examine the effect of substrate concentration on energy recovery, we plot NER versus acetate in two different concentration ranges (expressed in COD),  $<500$  and  $>500$  mg/L (Fig. 2.3). Acetate was chosen because of the availability of a large sample size for

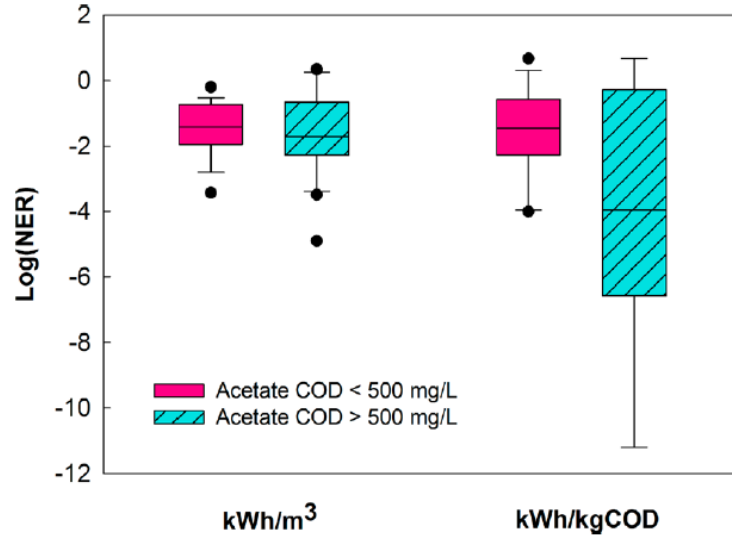


**Figure 2.3 Comparison of normalized energy recovery from acetate between two concentration ranges.**

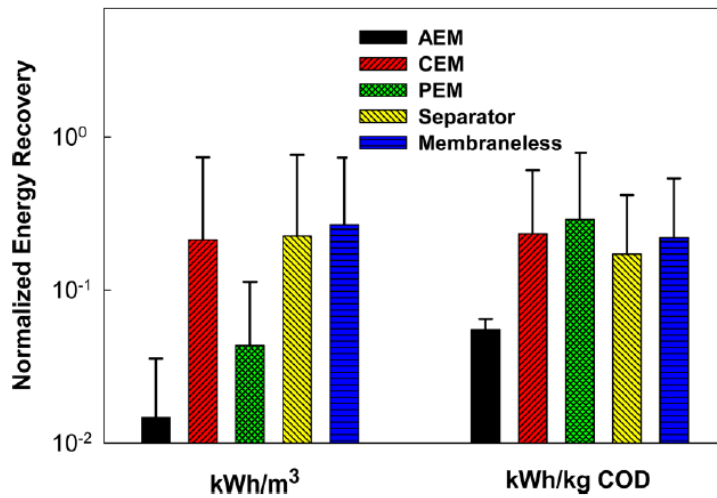


**Figure 2.4 Normalized energy recovery of the MFCs with or without separators and/or membranes. Error bars represent the standard deviation.**

statistical analysis, and 500 mg/L was arbitrarily used as a boundary value for the concentration of soluble organic compounds in domestic wastewater. The MFCs fed with <500 mg/L acetate generate an NER (kilowatt hours per cubic meter) similar to that of >500

mg/L acetate, but the NER expressed in kilowatt hours per kilogram of COD from <500 mg/L acetate is significantly higher than that from the higher range. The implication of these data may be that MFCs could be more suitable for treating low-strength wastewater, in terms of energy recovery efficiency; in particular, there have not been effective methods for recovering energy from low-strength wastewater, and anaerobic treatments are generally not applied. High-strength wastewater, however, should still be treated by the existing methods such as anaerobic digestion for the purpose of energy recovery, and MFCs are generally not applicable because of the low efficiency of energy conversion from high-strength substrates, for instance, compared with the efficiency of anaerobic digesters (Ge et al., 2013c), unless there are some economic advantages of using MFCs (e.g., eliminating gas collection and generator), which requires precise assessment, or in the places where the existing methods are not suitable (because of land use, operation, or other issues).

#### **2.4 Recovery of Electrical Energy in MFCs with or without Separators**

Because of different reactions conducted in the anode and the cathode of an MFC, a good separation between the two is required to prevent them from interfering with each other by the diffusion of oxygen, organic compounds, and other compounds. This separation is usually accomplished by using a solid electrolyte or oxygen gradient (e.g., in membrane-less MFCs). The commonly used solid electrolytes include ion exchange membranes [cation exchange membrane (CEM), anion exchange membrane (AEM), or proton exchange membrane (PEM)] and other materials like textiles, woven fabrics, and glass wool/beads as a separator (Li et al., 2011). The use of a separator may greatly affect an

MFC's structure and capital cost, as well as its performance in contaminant removal and energy recovery. Our analysis shows that, in general, the MFCs containing ion exchange membranes (including AEM, CEM, and PEM) have a lower NER based on the treated volume ( $0.14 \pm 0.40$  kWh/m<sup>3</sup>) than the membrane-less MFCs ( $0.23 \pm 0.46$  kWh/m<sup>3</sup>) ( $p < 0.05$ ), while they have similar NERs based on the removed COD ( $0.29 \pm 0.46$  kWh/kg of COD in the membrane-based MFCs vs  $0.17 \pm 0.30$  kWh/kg of COD in the membrane-less MFCs). We further analyzed the energy recovery with different separators, grouped into AEM, CEM, PEM (Nafion membrane), separators (non-ion exchange membranes), and membrane-less (Fig. 2.4). The MFCs with AEM exhibit lower energy recovery in both units, in contrast to the level of power production in the AEM MFCs that was found to be higher than that in the CEM MFCs (Li et al., 2011). However, the data from the AEM MFCs were excluded from statistical analysis because of a small sample size. The PEM MFCs have low energy recovery based on the treated volume, but comparable NER when COD removal is used for data expression. The CEM, separator, and membrane-less MFCs have similar energy performances.

## **2.5 Perspectives**

Our analysis has exhibited a rough picture of the amount of energy that MFCs can recover. We did not extend our analysis to other factors such as bacterial culture, different electron acceptors, or cathode catalysts because of the significant fluctuation in energy data due to the difference in reactor configuration, operation, bacterial culture, substrates, and other factors. There is only one small step from power calculation to energy calculation, but it really translates the research results into a language that the water/wastewater industry can

understand. NER may be a better parameter for comparison between different studies of MFCs that focus on energy recovery than other parameters that are commonly reported in MFC publications.

NER versus Power Density. Power density is the most widely reported parameter for describing the performance of MFCs with respect to electricity generation. It does not show energy recovery and does not involve factors such as the wastewater flow rate or the organic loading/removal rate, thereby making it nearly impossible to compare between different studies. In contrast, NER shows energy information and is based on wastewater characteristics that are not directly dependent on MFC dimensions. Of course, power production is still a critical factor and an essential parameter for calculating NER, and a higher power output generally results in a higher NER. Future studies focusing on energy recovery should work to improve NER, in addition to further improving power density.

NER versus Coulombic Efficiency (CE). CE is another parameter that is often used for comparison, and it represents the conversion of organics into electrical charge. However, a high CE does not necessarily mean a high energy recovery, because the CE calculation is related to electrical current, and a high current (e.g., close to short-circuit current) results in a high CE but very low power production (and thus a low energy recovery). Therefore, for MFCs with energy recovery as a major objective, NER will be a better parameter than CE for the purpose of comparison.

NER versus Energy Efficiency (EE). EE is the ratio of recovered energy to the heat of combustion of the organic substrates supplied within the time frame (Logan et al., 2006).

Because the heat of combustion of wastewater is hard to measure or estimate (Heidrich et al., 2011), EE is usually calculated for a synthetic solution with a known composition (Logan et al., 2006). Thus, for wastewater-fed MFCs, NER will allow a cross-wise comparison.

It should be noted that NER is a parameter with an emphasis on energy performance. Because of the complexity of MFCs, a thorough comparison between different MFCs should evaluate multiple parameters such as NER, Coulombic efficiency, power output, hydraulic retention time, organic loading rate, removal efficiency, and even economic factors (especially in future scaled-up systems).

The information about energy recovery helps to establish an energy balance, which can show us how far we are from an energy-neutral (or energy-positive) treatment process by using MFC technology. A precise estimation of energy consumption then becomes important. In a continuously operated MFC, the major energy consumers are pumps (e.g., feeding and recirculation), and there are approaches for the theoretical estimation of the energy requirement by pumps as described in the previous work (Kim et al., 2011b). As we can see from the analysis, MFCs do not recover much energy. For example, the theoretical energy content in organic compounds is  $\sim 3.86$  kWh/kg of COD, and MFCs recover less than 2.0 kWh/kg of COD (most studies have NER values of  $< 1.0$  kWh/kg of COD). Further improvement of energy recovery through optimizing configuration, operation, microbiology, and materials will make MFCs more attractive. On the other hand, adopting proper strategies to reduce the energy requirement of MFC operation may

compensate for low energy recovery; for example, a batch mode (e.g., a sequence batch reactor) or intermittent mixing in a continuous mode may decrease the extent of energy consumption by recirculation pumps. In addition, we may maximize the benefits of MFC technology by incorporating it with other energy-producing processes such as anaerobic digestion (Pham et al., 2006) and algal bioreactors (Xiao et al., 2012) or modifying it for producing other energy carriers like hydrogen gas (Logan et al., 2008) or for creating additional functions such as desalination (Kim & Logan, 2013), nutrient recovery (Kuntke et al., 2012), and production of valuable chemicals (Rozenal et al., 2009).

## CHAPTER 3

### Effects of Draw Solutions and Membrane Conditions on Electricity Generation and Water Flux in Osmotic Microbial Fuel Cells

(This section has been published as: Ge, Z. and He, Z.\* (2012) Effects of draw solutions and membrane conditions on electricity generation and water flux in osmotic microbial fuel cells. **Bioresource Technology**. Vol 109, pp 70-76.)

#### 3.1 Introduction

The mission of wastewater treatment has transformed from simple contaminant removal to a more sustainable task with a goal of less energy consumption and more water recovery. “Less energy consumption” requires a more efficient treatment process, and/or recovery of energy from contaminants. Bioenergy can be produced from wastewater by means of anaerobic digestion, microbial fuel cells, or photo-algal bioreactors (Angenent et al., 2004), but none of those technologies can extract high-quality water from wastewater for water reuse. “More water recovery” employs extensive post-treatments, usually through membrane processes, to extract clean water for reuse. Those membrane processes such as microfiltration, ultrafiltration, nanofiltration, and reverse osmosis consume intensive energy due to the requirement of high hydraulic pressures and they encounter rapid membrane fouling because of complex constituents present in wastewater (Shannon et al., 2008). The energy contents in organic compounds are not harvested during those membrane processes. Therefore, there is a strong need to develop a technology that can take advantage of both energy-producing and water-extracting processes and integrate them into a single process. A novel osmotic microbial fuel cell (OsMFC) has been developed to simultaneously treat wastewater, extract clean water, and produce bioelectricity (Zhang et al., 2011). To better understand OsMFCs, two important

components – forward osmosis and microbial fuel cells – are briefly introduced in the following. Forward osmosis (FO) is water movement through a semi-permeable membrane (e.g., FO membrane) from high water potential (feed solution) to low water potential (draw solution) (Cath et al., 2006). Draw solution is a concentrated solution that has a high osmotic pressure. Such a water movement does not require external energy input like that in reverse osmosis; thus, FO is a low-energy process. FO has been studied and applied to treat industrial wastewater and landfill leachate (Chung et al., 2011). Low membrane fouling was observed with an FO membrane in an osmotic membrane bioreactor treating the synthetic feed solution (Achilli et al., 2009). Microbial fuel cells (MFCs) are bioelectrochemical reactors that can use microbial metabolisms to produce bioelectricity (Logan et al., 2006). Anaerobic organisms in the anode of an MFC oxidize contaminants and produce protons and electrons. Electrons transfer through an external circuit to the cathode where they reduce oxygen to water; meanwhile, ions move across an ion exchange membrane to keep a charge balance. MFCs have been investigated to treat various wastewaters (Pant et al., 2010) or modified for beneficial functions such as hydrogen production (Logan et al., 2008), caustic soda production (Rabaey et al., 2010) or desalination (Cao et al., 2009).

OsMFCs integrate both FO and MFCs into one bioreactor by replacing ion exchange membranes with FO membranes. This change helps to realize the extraction of high-quality water from the wastewater during the electricity-generating process. The previous study examined the feasibility of the OsMFC concept and found that OsMFCs could extract water using either NaCl or seawater as a draw solution while still producing electricity (Zhang et

al., 2011). Electricity generation in OsMFCs was actually higher than that in conventional MFCs, because of active proton movement with water flux. OsMFCs hold great promise as a sustainable wastewater treatment technology. The key to developing an OsMFC system is to combine FO (e.g., water flux) and MFC (e.g., electricity generation) into a robust process. Before stepping into practical issues such as reactor configuration and scaling up, it is necessary to understand the fundamental problems associated with this combination, for instance, whether draw solutions that are commonly used in FO processes can function as catholytes for electricity generation, how FO membrane fouling is affected by the anolyte and affects OsMFC performance, and how the membrane can be cleaned without much influence on microbial activities in the anode. It also should be noted that the condition of an OsMFC is more complex than a conventional FO process because of microorganisms, electrode installation, cathode aeration and electricity generation; therefore, the difference is expected between the two processes in issues such as membrane fouling and reversal salt flux, which require an extensive research investigation.

In this study, several representative draw solutions were examined in an OsMFC for both electricity generation and water flux. The effect of draw solutes' concentrations and pH controlling via acid addition was also investigated. FO membranes under different conditions (new, fouled, and/or dried) were tested in the OsMFC. Backwash of FO membrane was conducted by dosing NaCl into the anolyte.

## 3.2 Materials and Methods

### 3.2.1 OsMFC setup and general operation

The OsMFC system consisted of two equal-size compartments of anode and cathode (Fig. 3.1). The total liquid volume of each compartment was 140 mL. The liquid volume of the catholyte was 240 mL, including the cathode compartment and a flask attached to the cathode. The compartments were glass bottles connected by an FO membrane (Hydration Technology Innovations, LLC, Albany, OR, USA). Before use, FO membranes were soaked in deionized water for 30 min according to the manufacturer's instructions. For comparison, some studies replaced the FO membrane with a cation exchange membrane-CEM (Membrane International Inc., Ringwood, NJ, USA) to form a conventional MFC. The surface area of each membrane was about 6.4 cm<sup>2</sup>. More details of the anode and cathode electrodes can be found in a previous publication (Zhang et al., 2011). The electrodes were connected by copper wires to an external resistor of 10  $\Omega$ . Both compartments were continuously stirred with magnetic bars. A 100 mL flask placed on a digital balance was used to scale the water moved through the FO membrane into the cathode compartment. The OsMFC was operated under a room temperature of ~20  $^{\circ}\text{C}$ .

The anode was fed continuously with a solution that was prepared containing (per L of deionized water): sodium acetate, 2 g; NH<sub>4</sub>Cl, 0.15 g; MgSO<sub>4</sub>, 0.015 g; CaCl<sub>2</sub>, 0.02 g; NaHCO<sub>3</sub>, 0.1 g; KH<sub>2</sub>PO<sub>4</sub>, 0.53 g; K<sub>2</sub>HPO<sub>4</sub>, 1.07 g; and trace element, 1 mL (He et al., 2006). The cathode was operated in batch mode in all experiments and the catholyte was recirculated at 20 mL/min. The cathode compartment was aerated with the air at a flow rate of 30 mL/min. This aeration could reduce water production via evaporation but the loss was not significant in the present study.



Four draw solutions at a concentration of 1 M each, including NaCl, potassium phosphate buffer (PPB), CaCl<sub>2</sub> and glucose, were tested individually. One mole of PPB contained 53 g of KH<sub>2</sub>PO<sub>4</sub> and 107 g of K<sub>2</sub>HPO<sub>4</sub>. The anode was continuously fed at a hydraulic retention time (HRT) of 2 h. The data were collected from the short-term (4 h) tests of both water flux and electricity generation and the change of catholyte weight was recorded hourly. The pH and conductivity of the catholyte was measured before and after each test.

#### 3.5.3.2 PPB concentrations

Four PPB solutions (50, 100, 200 and 500 mM) were tested to investigate the effect of solute concentrations. The initial pH of those buffer solutions was about 7. The HRT of the anolyte was adjusted to 10 h for this test. The data of electricity generation were collected in a 24 h testing period. The weight of the catholyte was recorded hourly in the first 4 h duration and the last 2 h duration and the pH and conductivity of catholyte were collected at hours 0, 4, and 24.

#### 3.5.3.3 pH controlling with acid addition

To control the pH of the NaCl catholyte, 5 mL of 50-fold dilution of 37% HCl was dosed into the catholyte every 12 h. The pH and conductivity of catholyte were recorded every 12 h. The total volume of the catholyte was kept at about 240 mL after HCl dosing. The initial NaCl concentration in the cathode of this test was 0.8 M. The HRT of the anolyte was 10 h.

#### 3.5.3.4 Membrane conditions

The FO membranes were tested under several conditions, including new membrane, new membrane that was dried after soaking (“new & dried”), fouled membrane, and fouled membrane that was dried (“fouled & dried”). For comparison, a new CEM also was evaluated in the OsMFC. The performance of the OsMFC with those membranes was monitored for 22 h. A 1 h short-term experiment was carried out to investigate the fouled and dried membrane. Electricity generation, conductivity of anolyte and catholyte, weight of overflow catholyte and pH were measured. The HRT of the anolyte was 10 h in those tests.

#### 3.5.3.5 FO membrane backwash

In the backwash test, NaCl was dosed into the anode compartment acting as a draw solute and deionized water was fed into the cathode compartment as a feed solution. The OsMFC was operated for 24 h before the first backwash. Five backwash cycles (6 operation cycles for the OsMFC) were conducted using 0.2, 0.3, 0.3, 0.5, and 0.5 M of NaCl for the backwash period of 1, 1, 2, 1 and 1 h, respectively. The anode operation was switched to batch during the backwash and then resumed to continuous operation after the backwash. When adding 0.5 M NaCl, the anolyte was replaced with a fresh feeding solution after the backwash. During the backwash electricity generation and water flux were measured. The digital balance was connected to a PC through a USB cable controlled by software (Logger Pro, Vernier Software & Technology, Portland, OR, USA) to record the change of catholyte weight. The recording rate was one data point/min and two data points/min for the OsMFC operation and the backwash, respectively.

### 3.3 Results and Discussion

#### 3.3.1 Effects of draw solutions on the OsMFC performance

##### 3.3.1.1 Types of draw solutions

Four representative draw solutions (1 M each) were tested as catholytes in the OsMFC. Sodium chloride (NaCl) is the most commonly used draw solute in FO processes (Achilli et al., 2010); PPB is widely applied in MFC operations (Logan et al., 2006); calcium chloride (CaCl<sub>2</sub>) is a divalent chemical that has exhibited a high osmotic pressure compared with other draw solutes (Cath et al., 2006); and glucose represents sugar-based draw solutes that can be applied to the food industry without the need of being re-concentrated. Electricity generation was observed with three draw solutes but not with glucose (Fig. 3.2A). The highest current (>2.5 mA) was generated from the PPB catholyte, while the NaCl and CaCl<sub>2</sub> catholytes produced a slightly lower electric current. Water flux, on the other hand, behaved differently from electricity generation (Fig. 3.2B). An increasing water flux was obtained with the PPB and NaCl catholytes and at the end of the 1 h testing period, both achieved water flux of 2.51–2.69 LMH. However, the opposite trend of water flux occurred with the CaCl<sub>2</sub> and glucose catholytes, dropping to ~0.56 LMH after 4 h. An extended test to 20 h showed that water flux with the CaCl<sub>2</sub> and glucose catholytes remained below 0.45 LMH. During the same period, the PPB catholyte maintained a water flux of ~2.42 LMH and the NaCl catholyte had a decreased water flux to 1.82 LMH. To understand why those draw solutions (catholytes) produced different results of electricity generation and water flux, the variation of catholyte pH and conductivity during the testing period was monitored. The oxygen reduction in the cathode of an MFC can elevate pH and a higher catholyte pH will cause a larger overpotential, thereby reducing electricity

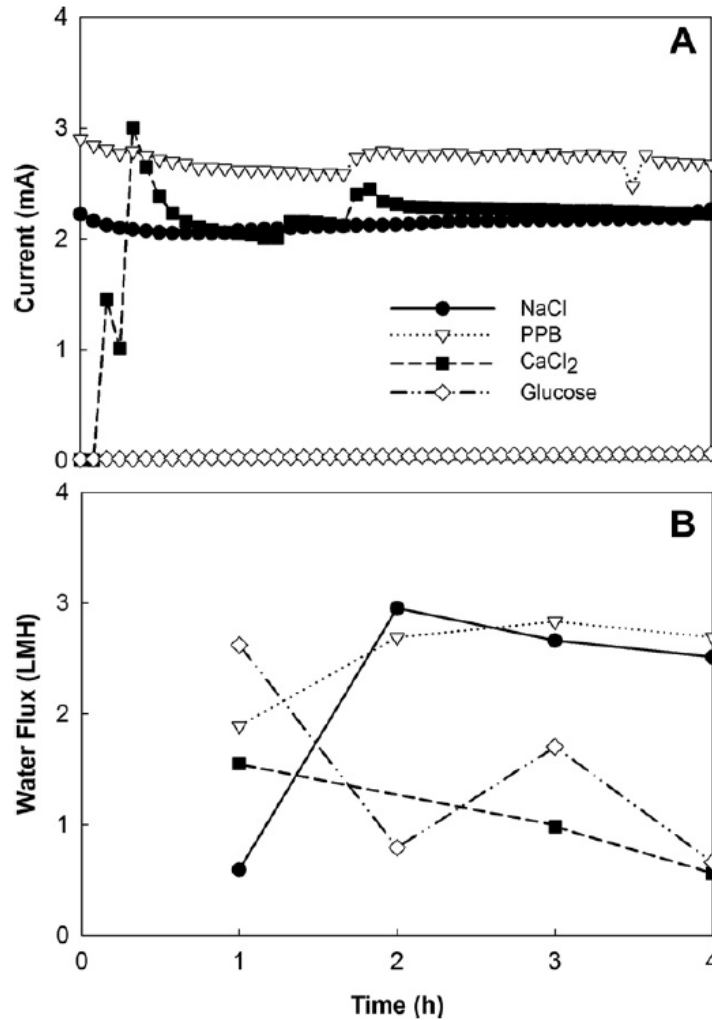


**Figure 3.2 The short-term (4 h) test of different draw solutions: (A) current generation and (B) water flux.**

generation (Rozendal et al., 2006). The pH of the NaCl catholyte increased from 7.0 to 9.6 within 4 h. The CaCl<sub>2</sub> catholyte had a final pH of 9.7. Those high catholyte pHs could result in a weaker electricity generation, as suggested by the present results and a previous study (Zhang et al., 2011). Meanwhile, the pH of the PPB catholyte that produced the highest current varied between 7.2 and 7.3, because of its strong buffer capacity. Although the glucose catholyte had the lowest pH of 6.0–6.7, it produced very little electricity

because of extremely low conductivity. It is known that increasing catholyte conductivity can improve electricity generation in MFCs (Gil et al., 2003). The current generation with the glucose catholyte actually increased slightly from 0.01 to 0.06 mA within 4 h, possibly because water flux from the anode compartment introduced ions into the catholyte and thus added a little conductivity. Due to this water flow, the glucose concentration in the cathode was reduced by about 5.4% (from 1230 to 1163 mg COD/L). With the dilution effect from water flux, the conductivities of the other three draw solutions also decreased (data not shown).

It was unexpected that the CaCl<sub>2</sub> catholyte had much less water flux than the NaCl catholyte while producing a similar amount of electricity (Fig. 3.2). Previous FO studies found that CaCl<sub>2</sub> has a higher osmotic pressure than NaCl at the same concentration (Cath et al., 2006). When using the CaCl<sub>2</sub> catholyte, chemical precipitation appeared (in gray) on the FO membrane facing the anode. It is likely that calcium ions migrated from the cathode compartment into the anode compartment and combined with phosphate or carbonates in the anolyte to form precipitation on the membrane surface. Such reverse salt flux has been reported in FO processes (Phillip et al., 2010). In addition, the CaCl<sub>2</sub> catholyte had a high initial pH of 10, which should be unfavorable for oxygen reduction. However, this high initial pH did not obviously impede electricity generation, compared with the NaCl catholyte, likely due to the higher conductivity of the CaCl<sub>2</sub> catholyte. One mole of the CaCl<sub>2</sub> catholyte had a conductivity of 120.1 mS/cm; at the end of the 4 h test, its conductivity was still 116.8 mS/cm. Meanwhile, one mole of the NaCl catholyte had a conductivity of 83.5 mS/cm, which dropped to 77.7 mS/cm after the 4 h test. Those results

suggested that  $\text{CaCl}_2$ , although a good draw solution for FO processes, may not be suitable as a catholyte chemical in OsMFCs.

The study demonstrated that an ideal draw solution (catholyte) for OsMFC application should possess a certain ability of pH buffering, have a high conductivity, and not form membrane scaling. Another important criterion (in some applications) is how efficiently it can be reconcentrated after dilution in FO processes. The common approach for reconcentration is to use reverse osmosis, which consumes intensive energy (Chung et al., 2011). Researchers have discovered new solutes such as ammonia–carbon dioxide (McCutcheon et al., 2005) and soluble magnetic nanoparticles (Ling et al., 2010) that can be recovered through low-energy processes. Ammonia–carbon dioxide was not tested in the OsMFC because the high pH due to cathode reactions and aeration with air bubbles would drive ammonia out of the solution, similar to ammonia stripping (Quan et al., 2009). The loss of ammonia will decrease ammonium concentration and thus water flux. It remains to be explored whether soluble magnetic nanoparticles can be applied as cathode solutes in OsMFCs. The draw solution that does not require reconcentration, such as seawater and fertilizer (Phuntsho et al., 2011), will also be of strong interest to OsMFC development.

#### 3.6.1.2 PPB concentrations

The PPB catholyte exhibited an advantage in both electricity generation and water flux. Thus, the PPB catholyte was further investigated at different concentrations varying from 50 to 500 mM. Clearly, the PPB concentrations affected the OsMFC performance, and a

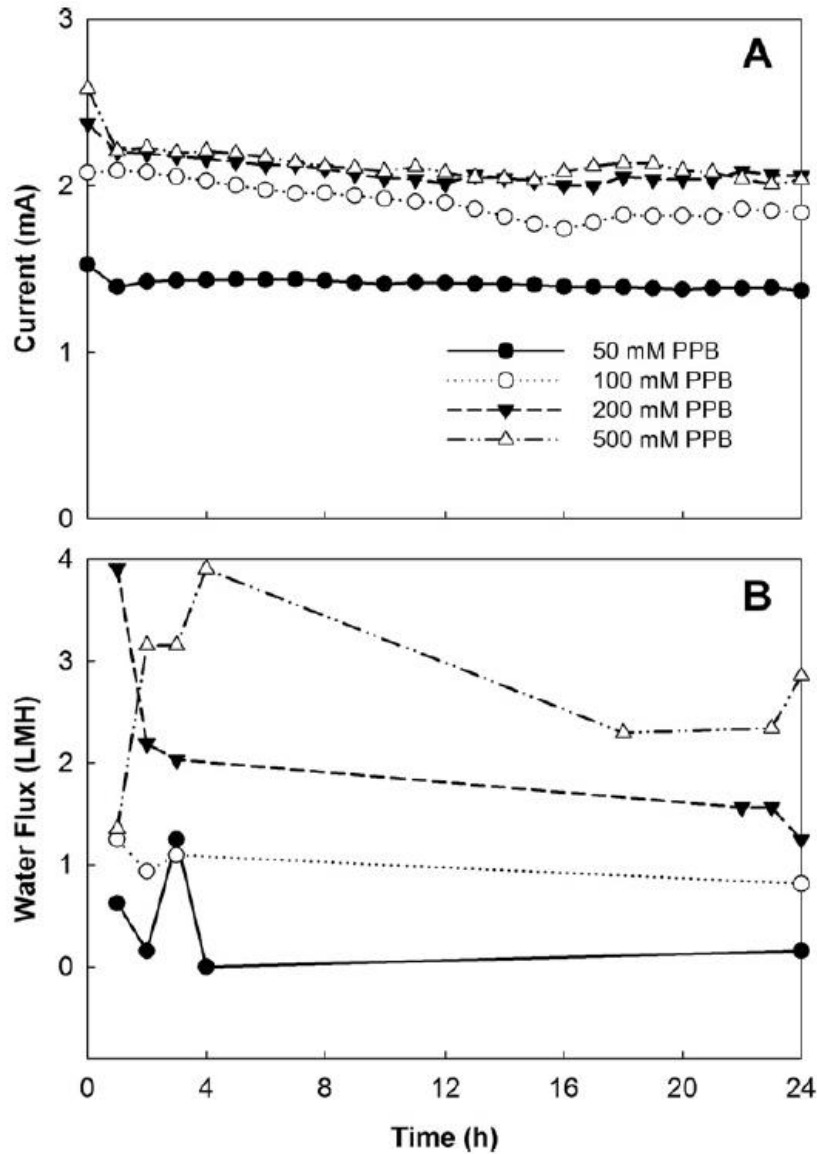


**Figure 3.3 The effect of PPB concentrations on the OsMFC performance: (A) current generation and (B) water**

higher PPB concentration led to a better result of both current generation and water flux (Fig. 3.3). It was also found that current generation, compared with water flux, received less influence from the PPB concentration. The pHs of the PPB catholytes that were between 100 and 500 mM remained about 7.3 during the 24 h testing period. The 50 mM

PPB had a slightly higher final pH of 7.6, because of a weaker buffering capacity. Although the 500 mM PPB catholyte contained conductivity more than twice that of the 200 mM PPB catholyte, the two catholytes produced a similar amount of electricity, indicating that increasing catholyte conductivity beyond a certain point would not help to increase electricity generation. Water flux was affected more significantly by the PPB concentration, as a higher concentration can create a larger osmotic pressure, which is the driving force of water flux. The 50 mM PPB catholyte had the lowest water flux because of its low conductivity of 7.7 mS/cm that created the smallest difference of osmotic pressure between the anolyte and the catholyte among the tested PPB concentrations. This low conductivity could also contribute to low electricity generation. The results indicated that when determining the concentration of draw solution for OsMFCs, the anolyte conductivity should be considered. Some special wastewaters such as food wastewater contain high salinity and will require a much higher conductivity in the draw solution.

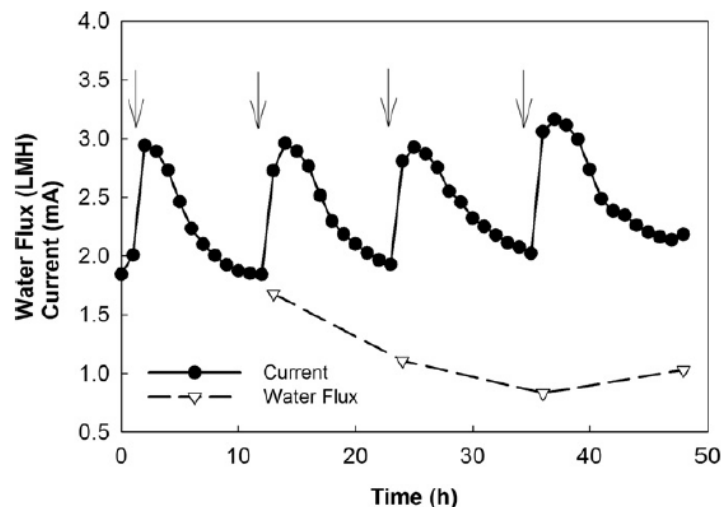


**Figure 3.4 Buffering the pH of the NaCl solution with dosing acid. The arrows indicate the addition of acid to the draw solution.**

### 3.3.1.3 Acidified NaCl catholyte

As a simple and low cost chemical, NaCl is the most commonly used draw solute in FO processes. However, the lack of pH buffering capacity hinders its application in OsMFCs. To overcome this problem, the pH of the NaCl catholyte was adjusted with hydrochloric acid (HCl). When the pH of the NaCl catholyte increased to above 9.0, HCl was added to reduce the pH to 2.5. This action increased the current generation by almost 50% in a short period and then the current decreased because of increased pH caused by oxygen reduction (Fig. 3.4). However, water flux was not significantly affected by HCl addition. The decreased water flux was likely a result of both the decreased conductivity (from 65.1 to 50.7 mS/cm) and membrane fouling. Adding HCl would increase conductivity, but this increase was negligible compared with conductivity reduction by water dilution, because of the small volume of HCl added.

Although adding HCl to neutralize the alkalinity may complicate the OsMFC operation, the NaCl–HCl combination has some advantages compared with the PPB catholyte. First, the cost of the NaCl–HCl combination is much lower than that of the PPB catholyte. Based on the price information from Sigma–Aldrich (St. Louis, MO, USA) from whom the chemicals were purchased and the quantities used in this study, it is estimated that the chemicals cost \$0.25/day for the NaCl–HCl combination and \$1.76/day for the PPB catholyte for operating the present OsMFC. If HCl is added more frequently, for instance 10 times the current frequency, to maintain a constantly high current generation, the cost will increase to \$0.36/day, still significantly lower than the cost of the PPB. This cost difference will substantially affect operating expense at full scale applications. Second, the

use of the NaCl–HCl combination is more environmentally friendly than the PPB catholyte. Because of reverse salt flux during FO processes, phosphate could migrate into the anode compartment and be discharged with the anode effluent (treated wastewater). Phosphorous is a key inorganic contaminant and its concentration must be maintained at a low level in wastewater effluent. An overload of phosphorous (with other nutrients) can cause eutrophication that deteriorates natural water bodies.

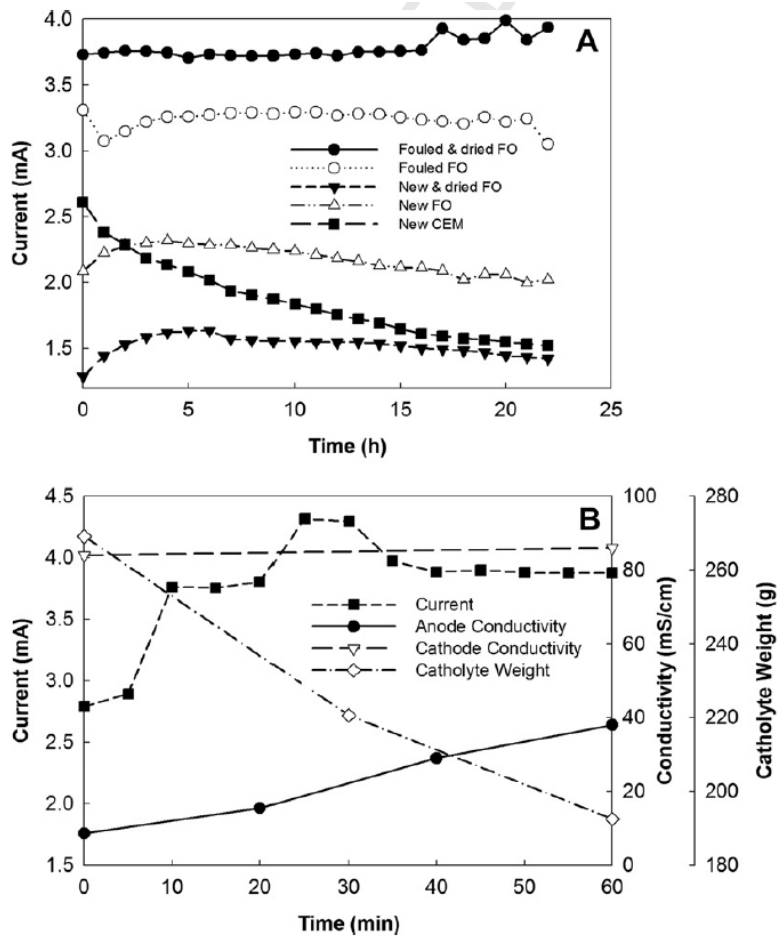


**Figure 3.5** Current generation in the OsMFC with FO membranes (an a CEM) under different conditions (A) and the 1-h test of the fouled & dried FO membrane (B).

### 3.3.2 Effects of membranes on the OsMFC performance

#### 3.3.2.1 Membrane conditions and types

The OsMFC performance was investigated with FO membranes under different conditions that were compared with cation exchange membrane (CEM) (Fig. 3.5A). The NaCl solution was used as the draw solution in those tests. The electricity production with a new FO membrane was higher than that with a new CEM, confirming the finding in a previous study (Zhang et al., 2011). This difference was attributed to a proactive proton transport with water flux through the FO membrane. Increasing electricity generation in MFCs via the improved proton movement has also been realized by using ammonium ions as a proton shuttle (Cord-Ruwisch et al., 2011). No obvious water flux was observed with the CEM (data not shown). It was expected that the OsMFC operation would cause FO membrane fouling, but the fouled FO membrane led to higher electricity generation (50% more) than the new FO membrane. When the fouled membrane was dried in the air and then reused in the OsMFC, the current generation was further increased to ~4 mA. For comparison, a new FO membrane was soaked in water, dried and then used in the OsMFC. This new and dried FO membrane resulted in lower electricity production than a new FO membrane (soaked in water and then used in the OsMFC). Water flux with the new and dried membrane was about 0.39 LMH after 22 h operation, much lower than 2–3 LMH with a new FO membrane. Those results demonstrated that a soak-dry process would seriously damage the FO membrane, which is in agreement with the manufacturer's suggestion that FO membranes should be stored in water after the first-time soaking.

No water flux was observed with the fouled FO membranes, although they had more electricity generation. On the contrary, water loss occurred in the cathode compartment in

the presence of the fouled and dried membrane. To further confirm and understand this phenomenon, electricity, conductivity and water loss was monitored with the fouled and dried FO membrane (Fig. 3.5B). During the 1 h test, current generation was mostly above 3.5 mA, similar to the 22 h test shown in Fig. 3.5A. The conductivity of the catholyte (85.1 mS/cm) did not obviously change, but the conductivity of the anolyte clearly increased from 8.6 to 38.0 mS/cm. Meanwhile, the weight of the catholyte decreased from 269 to 193 g. Those results indicated that the fouled and dried FO membrane had completely lost FO function; it allowed the catholyte to intrude into the anode compartment and this high-salinity flux increased the conductivity of the anolyte, which explained why higher electricity was produced with the fouled and dried FO membrane. The results also indicated that the anode (freshwater) microbes could tolerate salt flux to a certain degree and maintained a stable performance of electricity generation under a saline condition (a conductivity of 38.0 mS/cm is equivalent to about 22 g NaCl/L). This could be an important implication for the future application of OsMFCs, because reverse salt flux often happens during the FO process. This feature might also help conduct membrane backwash, which is addressed in the following.

### 3.3.2.2 Membrane backwash

The fouling of the FO membrane occurred during OsMFC operation, revealed by both direct observation of the membrane condition and a decrease in water flux. Backwash was employed to reduce membrane fouling. Unlike a conventional FO reactor that can apply a high-salinity solution in its feeding side for backwash, OsMFCs contain a microbial community in the anode (the feeding side) that would be adversely affected by a shock

from a high salt solution. Thus, a low concentration of NaCl (0.2–0.5 M) was added to the anolyte as draw solution and deionized water in the cathode as feed solution. As shown in Fig. 3.6, backwash did not obviously alleviate the decrease in water flux. A longer backwash time (e.g., 2 h backwash during the second addition of 0.3 M NaCl) led to a faster decrease after backwash. A higher concentration of NaCl (0.5 M) did not result in a better water flux, compared with 0.2 and 0.3 M of NaCl. As expected, the overall trend of water flux decreased, likely due to the accumulated fouling (Fig. 3.6A). The generation of electric current was clearly improved after each backwash (Fig. 3.6B), possibly because of the increased conductivity of the anolyte with the additional salt.

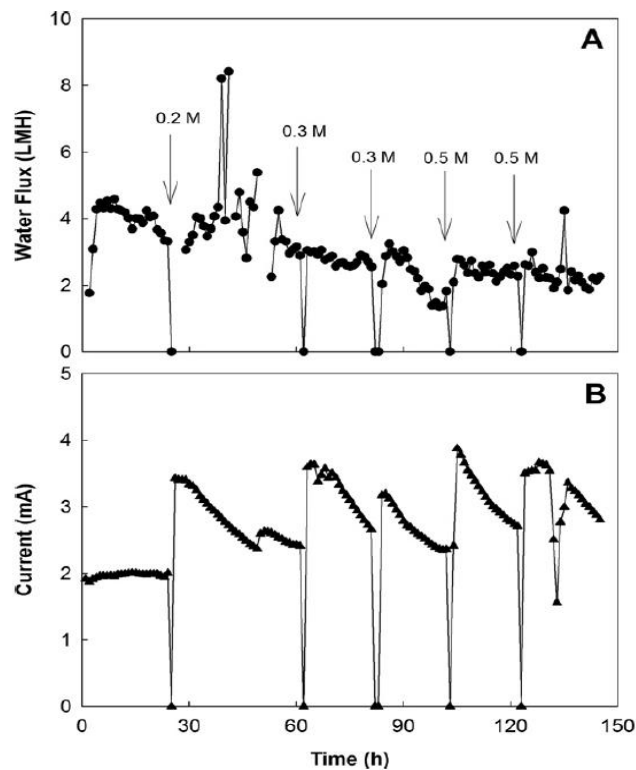


**Figure 3.6 Water flux (A) and current generation (B) during the test of backwash. The arrows indicate the addition of NaCl into the anode compartment.**

This study was an early attempt to reduce FO membrane fouling in OsMFCs and the results demonstrated the challenge of cleaning an FO membrane in OsMFCs because of the need to maintain microbial functions during the cleaning process. A strong acid/base solution that is commonly used to clean membranes is not appropriate in OsMFCs because of the severe effect on microbes, unless FO membranes can be removed from the reactor. Future approaches to clean FO membranes in OsMFCs may consider the use of chemicals that are less harmful to microbes at high concentrations, improved membrane design for anti-fouling, recirculation of biogas in the anode to reducing fouling (similar to that in anaerobic membrane bioreactors), and/or design of removable anode electrodes to accommodate the cleaning process. In addition, a reliable FO membrane is one of the key factors to the successful application of OsMFCs. The membrane used in this study is sensitive to fouling and dehydration. The CEM, on the other hand, is more durable. A stable performance of electricity generation in MFCs could be achieved with a CEM that was soaked and dried multiple times (unpublished data). Moreover, membrane fouling is also less serious with CEM because of the mechanism of ion exchange. MFCs with CEM could be continuously operated for 1 year and no significant decrease in electricity production was observed (Zhang et al., 2010). However, CEM does not have the function of extracting clean water from the anolyte (e.g., wastewater). The cost of FO membranes (\$30/m<sup>2</sup> according to the manufacturer) is also significantly lower than that of CEM (\$97/m<sup>2</sup>). Therefore, FO membranes have both functional and economic advantages over CEM and will be applicable in OsMFCs if an effective strategy can be developed to reduce membrane fouling.

### **3.4 Conclusions**

This study demonstrated that an optimal catholyte for OsMFCs should meet several criteria, including low cost, high conductivity for both water flux and electricity generation, and be environmentally friendly. A good draw solution used in an FO or a good catholyte applied in an MFC does not always work well in an OsMFC and must be examined for its suitability for OsMFCs. The FO membrane fouling adversely affected water flux; adding salt into the anode for backwash did not obviously alleviate membrane fouling. Those findings will help to understand the critical factors towards developing a practical OsMFC system.

## CHAPTER 4

### **Reducing Effluent Discharge and Recovering Bioenergy in an Osmotic Microbial Fuel Cell Treating Domestic Wastewater**

(This section has been published as: Ge, Z., Ping, Q., Xiao, L. and He, Z.\* (2013) Reducing effluent discharge and recovering bioenergy in an osmotic microbial fuel cell treating domestic wastewater. **Desalination**. Vol 312, pp 52-59.)

#### **4.1 Introduction**

Development of sustainable wastewater treatment aims to recover energy and useful resource from wastewater with more efficient contaminant removal (McCarty et al., 2011). Among the emerging developments, microbial fuel cells (MFCs) is a promising technology for direct electricity production from wastewater through microbial oxidation of organic contaminants (Logan et al., 2006). MFCs can effectively treat various contaminants/substrate (Pant et al., 2010) and generate bioelectricity that is potentially useful (McCarty et al., 2011); research has moved toward scaling up the MFC system for examining its feasibility of practical application (Logan, 2010). In addition to MFCs' conventional functions of contaminant removal and bioelectricity generation, a new function is proposed regarding effluent discharge: recovering high-quality water for water reuse (He, 2012). Membrane separations are usually considered for this type of application but they are energy intensive because of high hydraulic pressures; membrane fouling is another major concern. Forward osmosis (FO), as a low-energy and low-fouling technology (Cath et al., 2006; Chung et al., 2012; Hoover et al., 2011), is of special interest to MFC development, and in fact, FO has been integrated into an MFC for simultaneous bioenergy production and water extraction (Zhang et al., 2011).

The MFC using an FO membrane as a separator between its anode and cathode is called osmotic microbial fuel cell (OsMFC) (Zhang et al., 2011). Such cooperation between MFCs and FO takes advantages of both processes and can accomplish multiple functions within one system. The use of FO membrane improved electricity generation in an OsMFC, compared with a conventional MFC that contained a cation exchange membrane. It was found that active movement of water due to osmosis promoted proton transport and buffered the pH of the catholyte, both of which are important to electricity generation in MFCs (Rozendal et al., 2006). A higher salinity of the catholyte (and thus a higher osmotic pressure) benefited both electricity generation and water flux (Zhang et al., 2011). The OsMFC worked with both sodium chloride and artificial seawater. Further investigation demonstrated that, among four draw solutes that were tested, sodium chloride resulted in the best performance of both electricity generation and water flux (Ge & He, 2012). Phosphate buffer solution that is commonly used in the MFC studies did not appear to be a suitable draw solute because of high cost and potential release of phosphorus due to reverse salt flux; neither calcium chloride nor glucose led to a good electricity production, because of fouling or low conductivity. The concept of OsMFCs is also applied to microbial desalination cells (MDCs) (Cao et al., 2009; Jacobson et al., 2011), creating an osmotic MDC (OsMDC) (Zhang & He, 2012). The OsMDC achieved a better salinity reduction in saline water than an FO process, because of the combined water flux (dilution) and electricity generation (salt removal). Compared with a conventional MDC, the OsMDC can recover more water for the purpose of water reuse.

While the OsMFCs appear promising, we must understand the challenges associated with its development. Compared with an FO process, it is more difficult to clean the membrane fouling in an OsMFC because of the presence of electrodes and biofilm that complicates its structure and raises the issue of microbial effects (Ge & He, 2012). The requirement of aeration (or a terminal electron acceptor) to complete the cathode reaction restricts the application of some popular draw solutes such as ammonia-carbon dioxide (McCutcheon et al., 2005). Reverse salt flux (Phillip et al., 2010) could introduce undesired ions into wastewater effluent, which will affect the receiving water body. Nevertheless, those challenges and others warrant further investigation.

Our previous studies of OsMFCs (or OsMDCs) adopted synthetic organic solution as the anode feeding solution. To examine OsMFCs' compatibility with more complex substrates, we tested actual domestic wastewater in this study. A synthetic acetate solution was still used to start up the OsMFC and to investigate the effect of recirculation rates. After a stable performance was achieved with acetate solution, the anode feeding solution was switched to domestic wastewater. We monitored both electricity generation and water flux with the wastewater and studied the influence of hydraulic retention time. Membrane fouling was characterized using electrochemical techniques and chemical analysis.

## **4.2 Materials and Methods**

### **4.2.1 OsMFC setup**

The OsMFC consisted of two equal-size compartments ( $14 \times 7 \times 3.7 \text{ cm}^3$ /each) as the anode and the cathode, separated by an FO membrane (Fig. 4.1). The liquid volume of each

compartment was 360 mL. Before use, the FO membrane (Hydration Technology Innovations, LLC, Albany, OR, USA) was soaked in deionized water for 30 min according to the manufacturer's instructions. The surface area of membrane was about 98 cm<sup>2</sup>. The active layer of membrane was facing the anode feeding solution. Stainless steel mesh and carbon cloth was placed on both sides of the FO membrane as support and the cathode electrode (the ones in the cathode compartment). Two carbon brushes (Gordon Brush Mfg. Co. Inc., Commerce, CA, USA) were inserted into the anode compartment as the anode electrodes. Before use, those brushes were pre-treated by immersion in acetone overnight and heated at 450 °C for 30 min. The electrodes were connected by copper wires to an external resistor of 10 Ω. A 1000-mL glass bottle containing the catholyte as a reservoir was placed on a digital balance to measure the the water flux. The cathode compartment was aerated with the air to provide oxygen for cathode reaction and create turbulence of flow. The OsMFC was operated at a room temperature of ~ 22 °C.

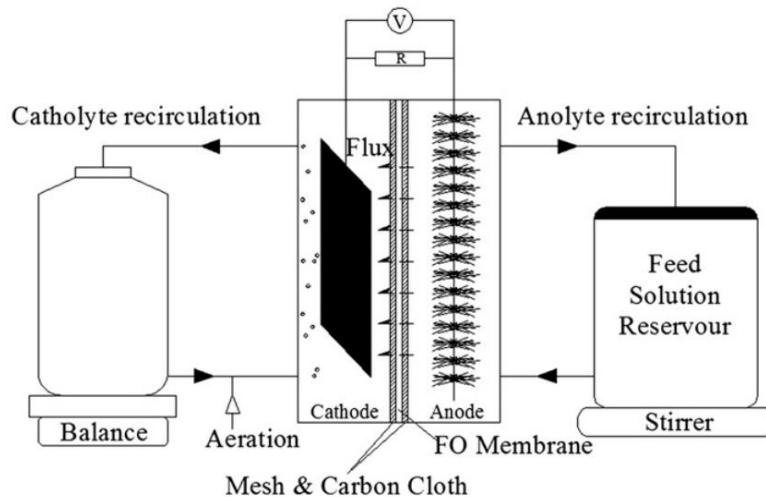


**Figure 4.1 Schematic of experimental setup of an osmotic microbial fuel cell.**

#### 4.2.2 OsMFC startup

To develop the desired biofilm on the anode electrodes, the OsMFC began as a conventional MFC using a cation exchange membrane (CEM, Membrane International Inc., Ringwood, NJ, USA) between the anode and the cathode compartments. The anode was inoculated by using raw sludge from a primary sedimentation and digestion sludge (Southshore Wastewater Treatment Plant, Milwaukee, WI, USA). To increase current generation, the external resistance was adjusted gradually from 2000 to 10  $\Omega$ . The catholyte was 50–100 mM of phosphate buffer solution. Once a stable current output was achieved, the MFC reactor was opened and the CEM was replaced by the FO membrane while keeping the anode and the cathode electrodes intact. In that way, the MFC was converted to an OsMFC.

#### 4.2.3 OsMFC fed on acetate solution

The OsMFC was first operated on an acetate solution to examine the system performance and the effect of recirculation rates. The anode was fed in a batch mode with an acetate solution containing (per L of DI water): sodium acetate, 2 g;  $\text{NH}_4\text{Cl}$ , 0.15 g;  $\text{MgSO}_4$ , 0.015 g;  $\text{CaCl}_2$ , 0.02 g;  $\text{NaHCO}_3$ , 0.1 g;  $\text{KH}_2\text{PO}_4$ , 0.53 g;  $\text{K}_2\text{HPO}_4$ , 1.07 g; and trace element, 1 mL (He et al., 2006). Sodium chloride solution (2 M) was used as the catholyte and supplied in a batch mode. Both anolyte and catholyte were recirculated by peristaltic pumps at the same rate ranging from 100 mL/min to 400 mL/min. At the end of a cycle (22–24 h), the anolyte and catholyte remaining in the reservoir bottles were replaced with 500 mL fresh acetate solution and fresh 2 M NaCl solution, respectively. The cathode compartment

was filled with DI water for 2 h to rest the FO membrane before refilling with the new catholyte.

#### 4.3.4 OsMFC fed on domestic wastewater

Domestic wastewater (primary effluent) was collected from Southshore Wastewater Treatment Plant (Milwaukee, WI, USA) and used as the anode feed solution. The OsMFC was first operated in a batch mode: the anolyte (wastewater) was replaced every 24 h and the cathode (2 M NaCl) solution was completely replaced after a 46-h cycle. After several cycles, the reactor was then operated in continuous flow mode. The HRT of the anode feed was 10 h (based on the anode liquid volume) for the first 10-day duration and then adjusted to 24 h for 9 days by changing the anode feeding flow rate. The recirculation rates for both the anolyte and catholyte were 100 mL/min. To examine the effect of recirculation rate on water flux, the catholyte recirculation rate was raised to 3000 mL/min without aeration for several hours. At the same time, the anolyte HRT was adjusted to about 3 h to ensure a sufficient supply of the anode feed solution. The tests of high catholyte recirculation rate were conducted with and without the carbon cloth that was initially installed on both sides of the FO membrane (Fig. 4.1).

#### 4.2.5 Measurement and analysis

The cell voltage was recorded every 3 min by a digital multimeter (2700, Keithley Instruments Inc., Cleveland, OH, USA). The pH was measured using a benchtop pH meter (Oakton Instruments, Vernon Hills, IL, USA). The conductivity was measured by a benchtop conductivity meter (Mettler-Toledo, Columbus, OH, USA). The polarization

curve was performed by a potentiostat (Reference 600, Gamry Instruments, Warminster, PA, USA) at a scan rate of 0.2 mV/s. The volumetric densities of power and current were calculated based on the liquid volume of the anode compartment, according to a previous study (Zhang et al., 2010). The concentration of chemical oxygen demand (COD) was measured using a colorimeter (Hach DR/890, Hach Company, Loveland, CO, USA). Water flux into the cathode ( $L\ m^{-2}\ h^{-1}$ , LMH) was calculated by the change of weight recorded on the balance. The water flux test procedures and the measurements using energy dispersive spectrometer (EDS), electrochemical impedance spectroscopy (EIS), and scanning electron microscopy (SEM) can be found in the supplementary data. The efficiency of organic-to-electricity was expressed by coulombic recovery (CR) and coulombic efficiency (CE), calculated as follows:

$$CR = \frac{Q_{output}}{Q_{input}} = \frac{\sum I(A)t(s)}{96485\left(\frac{C}{mol\ e^{-}}\right) \times COD_{total}(mol) \times 4\left(\frac{mol\ e^{-}}{mol\ O_2}\right)} \quad (4.1)$$

$$CE = \frac{Q_{output}}{Q_{input-r}} = \frac{\sum I(A)t(s)}{96485\left(\frac{C}{mol\ e^{-}}\right) \times COD_{removed}(mol) \times 4\left(\frac{mol\ e^{-}}{mol\ O_2}\right)} \quad (4.2)$$

where  $Q_{output}$  is the produced charge,  $Q_{input}$  is the total charge available in the added organic compounds,  $Q_{input-r}$  is the total charge available in the removed organic compounds,  $I$  is electric current and  $t$  is time.  $COD_{total}$  is the total COD input to the anode compartment in the period of time  $t$ , and calculated based on the initial COD concentration multiplied by the initial anolyte volume.  $COD_{removed}$  is the removed COD within time  $t$ . The removed COD was also expressed in percentage as a ratio of initial COD input and final COD remained.

Energy consumption in the OsMFC was mainly due to the recirculation of the anolyte and the catholyte by pumps. The power required for the recirculation pump was estimated as Eq. 4.3 (Kim et al., 2011):

$$P = \frac{Q\gamma E}{1000} \quad (4.3)$$

where P is power requirement (kW), Q is flow rate (m<sup>3</sup>/s),  $\gamma$  is 9800 N/m<sup>3</sup>, and E is the hydraulic pressure head (m). For the OsMFC, Q was  $1.67 \times 10^{-6}$  m<sup>3</sup>/s (100 mL/min) for both anode and cathode recirculation, and the measured hydraulic pressure head loss was 0.01 m; thus, the total power required for the recirculation pumps was  $1.6 \times 10^{-7}$  kW.

## 4.3 Results and Discussion

### 4.3.1 OsMFC fed on acetate solution

The OsMFC generated electricity and produced water flux with the acetate solution. Polarization test demonstrated that the open circuit potential was 0.6 V (Fig. 4.2). The maximum current density was 136.3 A/m<sup>3</sup> and the maximum power density was 28.2 W/m<sup>3</sup>, much higher than that of our previous OsMFC fed with the similar acetate solution (Zhang et al., 2011). This increased performance of electricity generation resulted from an optimized configuration of the present OsMFC, compared with the previous one that consisted of two glass bottles with a small membrane surface area and was inefficient for electricity generation. The batch operation exhibited a current profile affected by the organic substrate: the current increased upon the replacement of the anode solution, fluctuated (between 40 and 50 A/m<sup>3</sup>) for more than 20 h and decreased due to the depletion of the organic substrates (Fig. 4.3A). The OsMFC removed  $83.5 \pm 8.5\%$  of COD at an initial COD loading rate of  $0.6 \pm 0.1$  kg/m<sup>3</sup>/d, and achieved a CE of  $28.9 \pm 7.3\%$  and a CR

of  $23.8 \pm 5.7\%$  (Table 4.1). Increasing the recirculation rates of both the anolyte and the catholyte from 100 to 200 mL/min clearly improved electricity generation with an increased electric charge from 716.2 to 1222.8 C; however, further increase in the recirculation rates to 300 and 400 mL/min did not obviously affect electricity generation, suggesting that mixing intensity above 200 mL/min might be sufficient for substrate distribution within the anode compartment. A similar result of recirculation rate was observed in our previous studies of a conventional MFC (Zhang et al., 2010). The pH of the catholyte increased to  $9.9 \pm 0.4$ , because of the cathodic oxygen reduction reaction (Zhao et al., 2006); while the pH of the anolyte slightly decreased to  $6.4 \pm 0.3$  in a cycle of 22-h operation (Table 4.1).

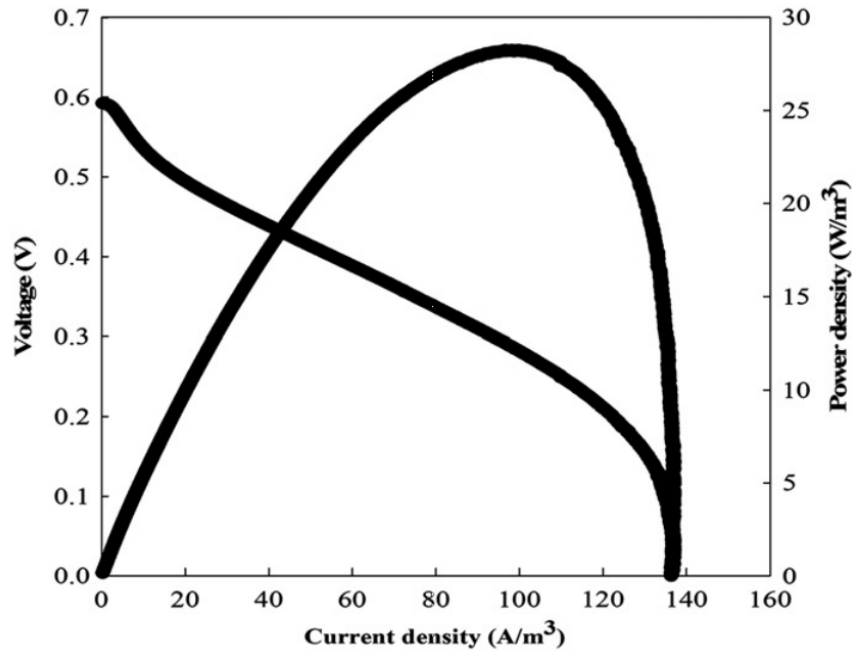


**Figure 4.2 Polarization curves of the OsMFC treating acetate solution.**

**Table 4.1. The OsMFC performance with acetate solution or actual wastewater (WW)**

Operation	Substrate	pH		SCOD Removal (%)	CE (%)	CR (%)	Average Flux (LMH)	Effluent Reduction (%)
		Anode	Cathode					
Batch mode	Acetate (22 h)	6.4±0.3	9.9±0.4	82.5±9.0	20.9±6.9	17.1±5.6	1.22±0.13	57.8±6.0
	WW (46 h)	7.6	8.4	N/A	N/A	N/A	1.30	64.2
Continuous mode	WW (10 h)	N/A	8.6±0.1	50.0±18.1	83.8±38.2	37.3±8.0	1.26±0.07	34.2±2.0
	WW (24 h)	6.9±0.3	8.4±0.3	74.8±3.9	56.4±13.3	42.1±9.1	1.06±0.16	69.5±10.5

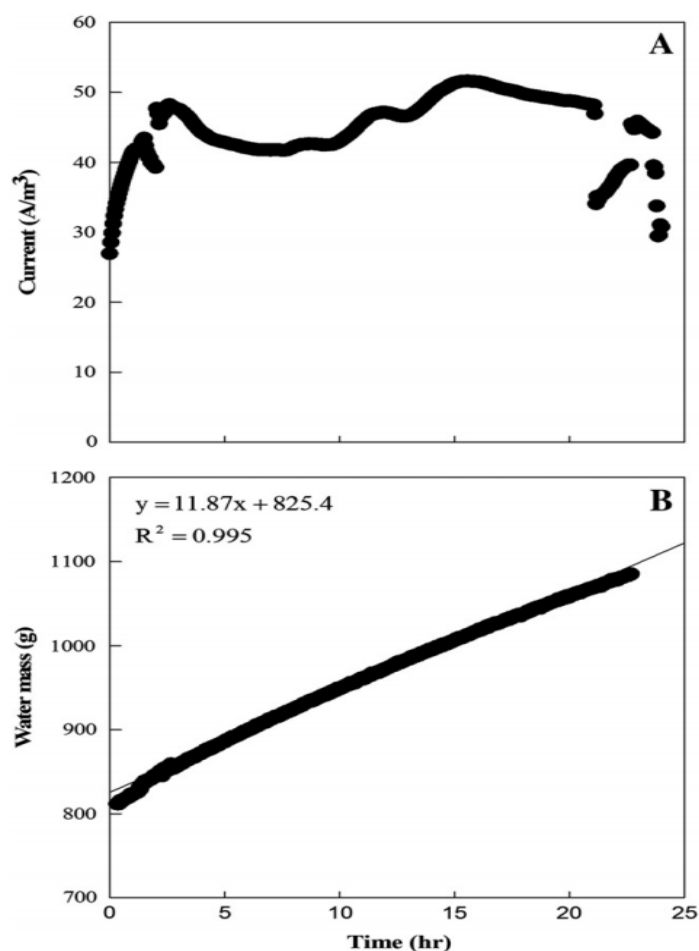


**Figure 4.3 Batch operation of the OsMFC treating acetate solution: (A) the profile of current generation; and (B) the increase in water mass in a batch.**

Water movement across the FO membrane was observed with an increased water mass in the cathode compartment (Fig. 4.3B). This water flux diluted the catholyte and resulted in a lower conductivity of  $84.1 \pm 6.5$  mS/cm at the end of an operation cycle. The anolyte conductivity, on the other hand, was doubled to  $15.2 \pm 2.5$  mS/cm, because of concentrated effect from water loss (to the cathode compartment); reverse permeation of draw solute into the anode compartment might also increase the conductivity of the anolyte (Hancock & Cath, 2009; Phillip et al., 2010). The OsMFC achieved water flux of  $1.22 \pm 0.13$  LMH, much lower than those in previous FO studies (Achilli et al., 2009; Yang et al., 2009; Yip et al., 2010). This low water flux could be due to a large concentration polarization (CP) resulted from a low cross-flow velocity and FO membrane fouling. It is known that CP can severely affect water flux and higher cross flow velocity helps to reduce external concentration polarization (ECP). At a recirculation rate of 400 mL/min, the cross-flow velocity in the OsMFC was about 0.26 cm/s, much lower than 2.3 - 58 cm/s employed in FO studies (Cath et al., 2010; Lee et al., 2010; Li et al., 2012; Mi & Elimelech, 2008; Phuntsho et al., 2011; Zou et al., 2011). Biofilm formation on the active layer of the FO membrane facing the anode (feeding) side might also adversely affect water flux. We will address those issues in more details in the following sections.

#### 4.3.2 OsMFC fed on domestic wastewater

##### 4.3.2.1 Batch mode

When the actual wastewater (primary effluent) was fed into the anode compartment in a batch mode, the OsMFC exhibited a current profile with a sharp peak current of  $\sim 9$  A/m<sup>3</sup> followed by a quick decrease (Fig. 4.4A). The total charged accumulated in a cycle was

155.8 C. Within the similar operating cycle, electricity generation from the actual wastewater was much lower than that of the acetate solution, most likely due to a lower organic input. The wastewater contained soluble COD varying between 64 and 96 mg/L, significantly lower than 1500 mg/L of the acetate solution. In addition, the organic compounds in wastewater are more complex than acetate and thus more difficult to be biologically degraded. Water flux, however, was not obviously affected by the change of the acetate solution to the wastewater, and the increase in water mass in the cathode compartment was slightly more than that with the acetate solution (Fig. 4.4B). The OsMFC achieved water flux of 1.30 LMH (Table 4.1). The improved water flux was because of a lower conductivity of the wastewater, thereby creating larger osmotic difference across the FO membrane and thus a higher osmotic pressure to drive water movement. Water flux from the anode into the cathode decreased the volume of wastewater from 1000 to 358 mL, 64.2% reduction in effluent discharge.

#### 4.6.2.2 Continuous operation

The continuous supply of wastewater to the OsMFC constantly produced electricity; because of complicated composition and the low organic concentration of the wastewater, the current generation fluctuated at a low level around 2 A/m<sup>3</sup> (Fig. 4.5A). Extending the HRT from 10 to 24 h slightly decreased the current production. Similar to current generation, the polarization curve showed some unstable responses during the voltage scanning, but useful information could still be extracted: the open circuit voltage was 0.63 V, the maximum power density was about 4.5 W/m<sup>3</sup> and the maximum current density reached 37 A/m<sup>3</sup> (Fig. 4.6). During a short-period test of step increase in the organic

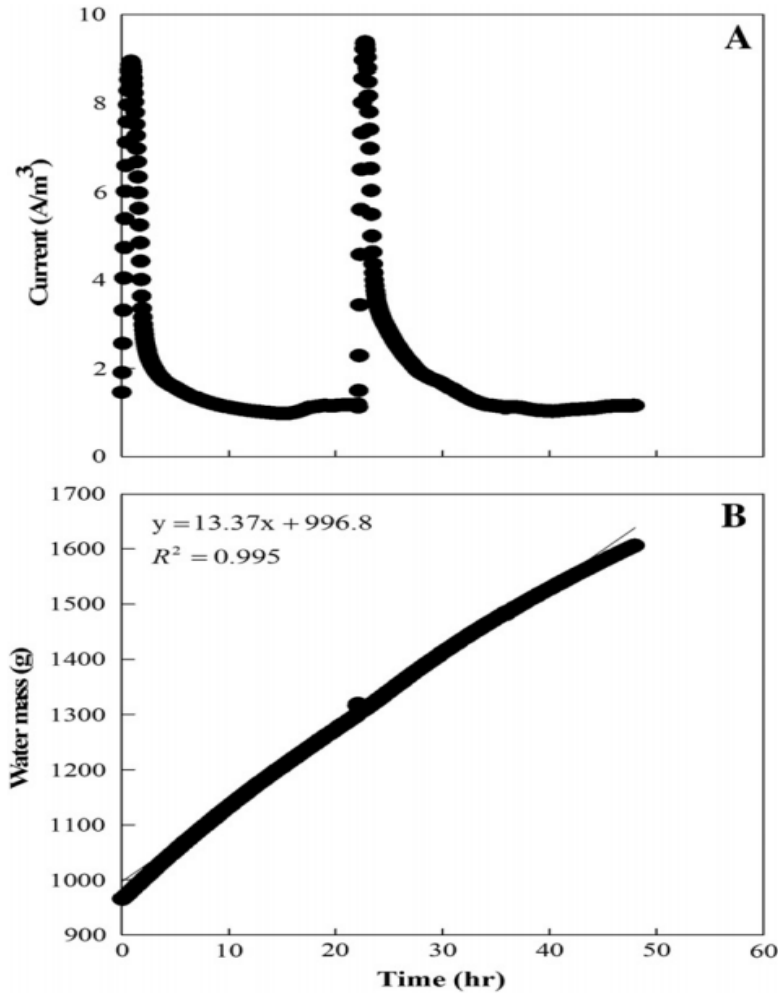


Figure 4.4 Batch operation of the OsMFC treating wastewater: (A) the profile of current generation; and (B) the increase in water mass in a batch.

Table 4.2 The OsMFC performance during the step-decrease of wastewater HRT

HRT (h)	SCOD Loading (kg/m <sup>3</sup> /d)	Current Density (A/m <sup>3</sup> )	Power Density (W/m <sup>3</sup> )	Energy Production (kWh/m <sup>3</sup> )	Energy Production* (kWh/m <sup>3</sup> )	Energy Consumption (kWh/m <sup>3</sup> )	Average Flux (LMH)	Effluent Reduction (%)
24	0.15	5.3	0.10	$2.4 \times 10^{-3}$	0.108	0.011	1.11	72.5
12	0.31	10.0	0.36	$4.3 \times 10^{-3}$	0.054	0.005	1.33	43.4
6	0.62	15.1	0.82	$4.9 \times 10^{-3}$	0.027	0.003	1.49	24.3

\*potential maximum power produced by OsMFC ( $4.5 \text{ W/m}^3$ ,  $1.6 \times 10^{-3} \text{ W}$ )

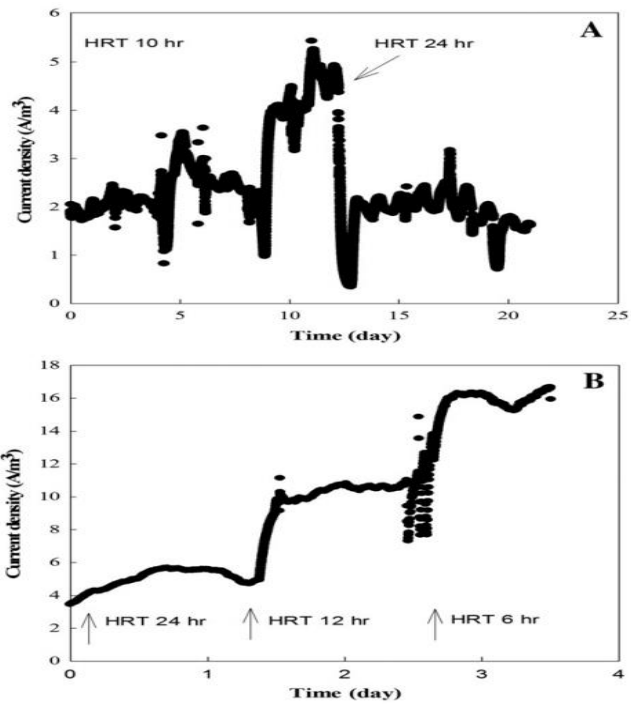


Figure 4.5 Current generation of the OsMFC treating wastewater: (A) continuous operation; and (B) the step-decrease of wastewater HRTs.

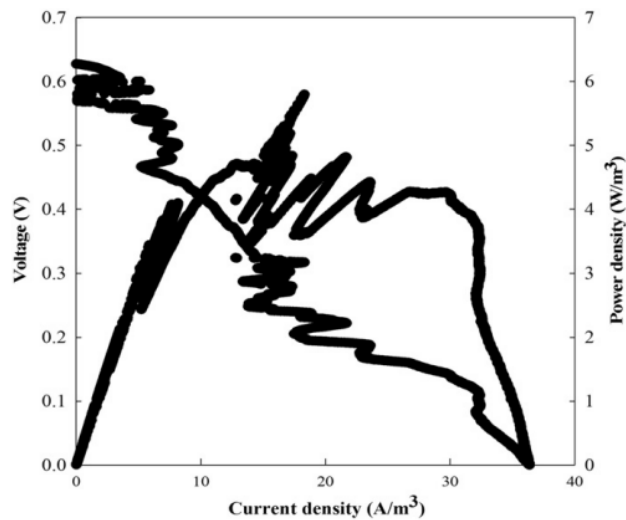


Figure 4.6 Polarization curves of the OsMFC treating wastewater in continuous operation and at HRT 24 h.

loading rate (decrease in HRT from 24 to 12 and then 6 h), it was clearly observed that electricity generation increased with the increasing organic loading, indicating that current generation was limited by organic supply (Fig. 4.5B and Table 4.2). The average SCOD concentration in wastewater during the step-increase test was about 154 mg/L, resulting in a higher current generation at HRT 12 h (Fig. 4.5B) than that at HRT 10 h (Fig. 4.5A).

Higher organic loading rates also improved energy production: at HRTs 12 and 6 h, the total energy production was 0.004 kWh/m<sup>3</sup> and 0.005 kWh/m<sup>3</sup>, respectively, both of which are close to the energy consumed by the pumps, suggesting the possibility of a self-sustained OsMFC system in terms of energy. It must be noted that the OsMFC was not operated at its maximum power output during those tests; according to Fig. 4.6, the maximum power output at HRT 24 h was about 4.5 W/m<sup>3</sup>, which could be even higher at a shorter HRT because of the larger substrate supply. Assuming the OsMFC runs at 4.5 W/m<sup>3</sup>, the energy production will be much higher than the energy consumed (Table 4.2). The key factors to accomplish such an energy-neutral system include energy production that can be further improved through optimizing OsMFC configuration and increasing organic supply, and energy consumption that is mainly determined by the recirculation of electrolytes. We must understand that it is very difficult to establish a precise energy balance for bench-scale OsMFCs, especially energy consumption by the pumping system. Our effort of energy analysis was to obtain a rough picture of energy production and requirement involved in the OsMFC at a small scale, which would guide further development of this system.

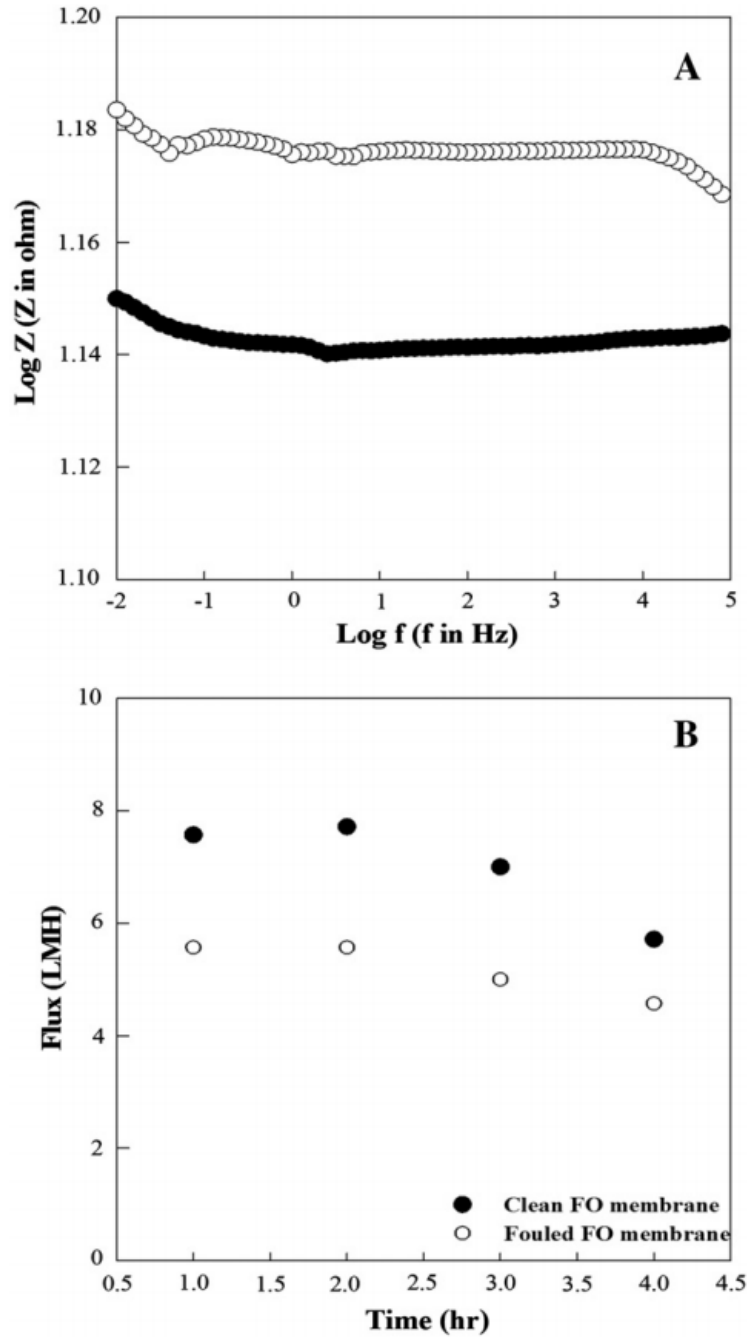


Figure 4.7 Comparison between clean and fouled FO membranes: (A) Bode plot of electrochemical impedance spectroscopy; and (B) short-term water flux test (in a U-shape reactor shown in Fig. A1)

Water flux increased slightly with decreasing HRTs (Table 4.1 and Table 4.2), possibly because the faster supply of low-salinity wastewater at a lower HRT reduced concentration polarization on the active layer of FO membrane facing the anode, compared with a high HRT that had a slower wastewater influent and accumulated salts due to water loss and reverse salt flux. However, the reduction in wastewater effluent decreased with decreasing HRTs, because more wastewater was fed into the anode at a lower HRT. At HRT 10–12 h, which is similar to that of aerobic biological wastewater treatment, the OsMFC reduced 30–40% of wastewater effluent (Table 4.1 and Table 4.2). This reduction, or increased water reuse, will help accomplish sustainable water management while reducing freshwater use, achieving both environmental and economic benefits (Anderson, 2003).

The recirculation rates of electrolytes could affect the shear condition on the surface of the FO membrane and concentration polarization, thereby influencing water flux. The OsMFC achieved low water flux (< 1.50 LMH) in both batch and continuous operation; to explore whether water flux can be improved by a higher recirculation rate, the recirculation rate of catholyte was increased to 3000 mL/min. The recirculation rate of anolyte was maintained unchanged, because a high rate could disturb the biofilm that formed on the anode electrode and thus affect the anode performance. In addition, it was found that a better mixture on the drawing side may reduce concentration polarization (Gruber et al., 2011). Unfortunately, we did not observe a significant increase in water flux to a level comparable to that in previous FO studies. The OsMFC achieved 1.97 LMH at high recirculation of the catholyte, which increased to 2.15 LMH when the carbon cloths on both sides of the FO membrane were removed. The low water flux was likely due to an inefficient configuration

(large and thick compartment) of the OsMFC that did not create a high cross-flow velocity. At 3000 mL/min, the cross-flow velocity was only 2 cm/s; adding mesh on both sides of the FO membrane did not help improve flow turbulence, possibly due to its small pore size. In addition, it is well known that internal concentration polarization (ICP), which is hardly reduced by increasing flow rate or turbulence, can greatly reduce water flux (Zhao et al., 2012).

#### 4.3.3 FO membrane fouling

After operating the OsMFC for more than 100 days (about 50% of the time on wastewater and the other 50% on acetate solution), the FO membrane was removed to analyze any fouling. The EIS data showed an increase in impedance of the fouled membrane compared with the clean membrane (Fig. 4.7A), suggesting the appearance of the fouling (Gao et al., 2013). The 4-h water flux test revealed that the fouled membrane achieved a lower average water flux of 5.2 LMH than 7.1 LMH of a clean membrane (Fig. 4.7B). It was observed in the SEM pictures that the anode side of the FO membrane contained a large number of microorganisms (Fig. 4.8A), while the cathode side of the membrane was covered by abiotic scaling (Fig. 4.8B). The cross-section of the fouled membrane was filled with fouling compounds (Fig. 4.8C). EDS analysis showed that various compounds, including phosphate, iron, and calcium, were detected on both sides of the membrane (Fig. A2 and S4.3) and the dominant species (by weight) were phosphate, nitrogen, oxygen, sulfur, and calcium (Table A1 and A2). The weight percentages of those compounds differed between the two sides of the membrane.

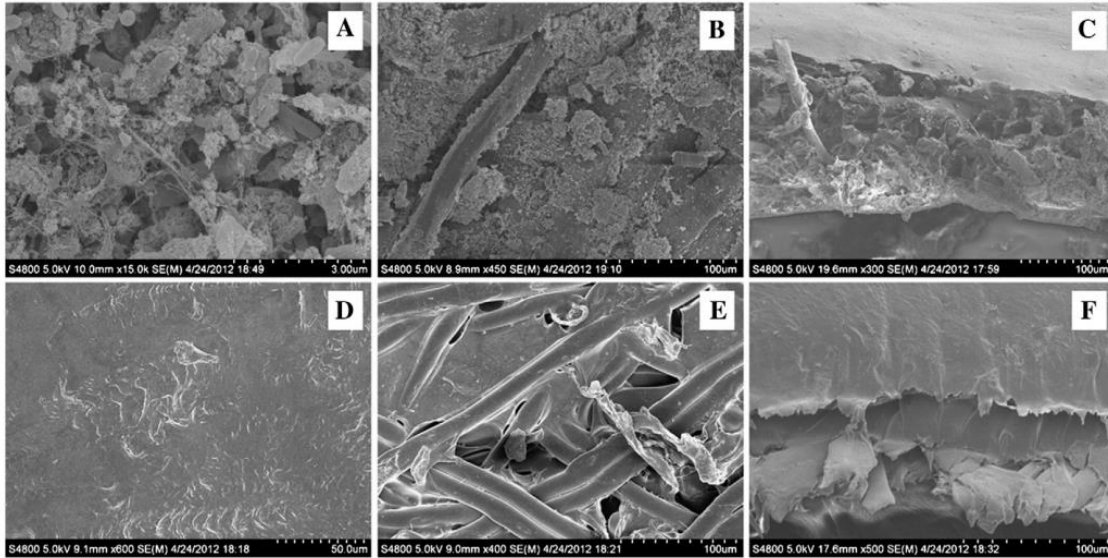


**Figure 4.8 SEM pictures of the fouled FO membrane (A — active side; B — support side; C — cross-section) and a clean FO membrane (D — active side; E — support side; F — cross-section).**

A major challenge of applying FO membranes in wastewater treatment is membrane fouling. Our results clearly showed both biofouling and abiotic scaling caused by microorganisms and organic/inorganic compounds in wastewater, which adversely affected the membrane performance. Unlike an osmotic membrane bioreactor that can take advantage of aeration to alleviate fouling, the anode of an OsMFC is anaerobic and has no gas bubbling; therefore, the fouling can be more serious. Our previous study suggested that backwash has a limited effect on reducing the fouling in an OsMFC (Zhang et al., 2011). Therefore, a suitable method for membrane cleaning is critical for application of OsMFCs. The possible approaches include recirculating biogas produced in the anode to remove fouling, optimizing the anode compartment to improve the shear effect of water flow, and designing a removable membrane for external cleaning. On the other hand, our results also

demonstrated the durability of the FO membrane. Without major cleaning (except for periodic, short-term soaking of one side of the membrane in DI water), the FO membrane worked for more than 100 days under a tough condition (in the presence of microorganisms and various organic and inorganic compounds), which proves that FO membranes are low-fouling membranes.

#### **4.4 Conclusions**

The results of this study demonstrated that an OsMFC can recover bioenergy from domestic wastewater through bioelectrochemical reactions and reduce wastewater effluent via water extraction by forward osmosis. Electricity generation was affected by organic loading rates (both organic concentration and hydraulic retention time). Water flux was influenced by recirculation rate (e.g., low shear effect due to inefficient reactor configuration), membrane fouling, and concentration polarization. Reduction of the effluent could increase the concentrations of nutrients such as nitrogen and phosphorus (while the total amount of nutrients will not be changed); therefore, a post-treatment step to polish the effluent by removing nutrients will be required. To implement OsMFCs' environmental and energy sustainability (e.g., water reuse and energy neutral), future studies will optimize the reactor configuration, examine anti-fouling or membrane cleaning methods, and scale-up the system.

## CHAPTER 5

### **Hollow-fiber Membrane Bioelectrochemical Reactor for Domestic Wastewater Treatment**

(This section has been published as: Ge, Z., Ping, Q. and He, Z.\* (2013) Hollow-fiber membrane bioelectrochemical reactor for domestic wastewater treatment. **Journal of Chemical Technology & Biotechnology**. Vol 88, pp 1584-1590.)

#### **5.1 Introduction**

Microbial fuel cells (MFCs) have been widely studied as a potential approach for simultaneous wastewater treatment and bioenergy production (Rinaldi et al., 2008). The research has been focused on improving electricity generation in MFCs via investigating their architecture and operation, electrode and membrane materials, substrates, electrochemistry, microbiology and new functions (Logan & Regan, 2006; Logan, 2010; Pant et al., 2010; Zhao et al., 2009; Zhou et al., 2011). The primary function of an MFC is wastewater treatment; however, the issues about the MFC effluent quality are not sufficiently addressed, possibly because most studies fed the MFCs using synthetic solutions that are “purer” than actual wastewater. A few studies that adopted actual wastewater have demonstrated an effective organic removal by MFCs (Pant et al., 2010), but the information of the treated effluent quality such as turbidity is very limited. MFCs are designed to replace the secondary treatment (Rabaey & Verstraete, 2005), which usually requires a tertiary treatment such as filtration and/or disinfection for further purifying the treated effluent (Masters & Ela, 2008). To produce a high-quality effluent for either direct discharge or water reuse will make MFCs more competitive as a wastewater treatment technology.

The existing wastewater treatment can achieve high-quality effluents using membrane bioreactors (MBR), which integrate membrane filtration using microfiltration (MF) or ultrafiltration (UF) membranes with suspended growth bioreactors. The MBR technology has been commercialized for municipal or industrial wastewater treatment (Marrot et al., 2004; van Nieuwenhuijzen et al., 2008). The filtration elements can be either submerged (internal) in a bioreactor such as an activated sludge tank, or installed as a sidestream (external). To recover energy from wastewater, anaerobic MBR (AnMBR) is developed with the production of methane gas (Smith et al., 2012). More details about the MBR technology can refer to several in-depth review publications (Brindle & Stephenson, 1996; Gander et al., 2000; Judd, 2008; Liao et al., 2006; Yang et al., 2006).

Filtration membranes have also been studied in MFCs, mostly as separators between the anode and the cathode, instead of filtration media (Li et al., 2011). Because the larger pore size of filtration membranes facilitates ion transport, the use of filtration membranes such as MF/UF membranes greatly improved power production (Sun et al., 2009; Zuo et al., 2007). However, the increased permeation of oxygen and the loss of substrate across filtration membranes constrain their applications in MFCs (Li et al., 2011). Recent development of osmotic MFCs use forward osmosis membrane as both the separator for electrodes and the medium for water filtration (driven by an osmotic pressure) (Ge & He, 2012; Zhang et al., 2011), but the recovered water needs post-treatment such as reverse osmosis.

A possible strategy to involve filtration membranes in MFCs is to use MF/UF membranes as filtration media, installed either inside or outside the anode compartment similarly to that in MBRs. Ion exchange membranes are still required to separate the electrodes, unless a membrane-less MFC is employed. In this study, we developed a membrane bioelectrochemical reactor (MBER) by installing hollow-fiber membranes inside a tubular MFC. The MBER is expected to produce high-quality water while generate electric energy from organic oxidation. The MBER is significantly different from recent studies of bioelectrochemical membrane reactors using biofilm formed on stainless steel mesh or nylon mesh as the filtration material in MFCs with aerated cathodes (Wang et al., 2011; Wang et al., 2012). We have operated the MBER with both synthetic solution and actual wastewater for more than 200 days, and examined electricity generation, trans-membrane pressure and the effluent quality.

## **5.2 Materials and Methods**

### **5.2.1 MBER construction**

The MBER was constructed based on a tube made of cation exchange membrane (CEM - Ultrex CMI7000, Membranes International, Inc., Glen Rock, NJ) (Fig. 5.1). Ten 20-cm long PVDF hollow-fiber (HF) membranes (150,000 Dalton, Litree Purifying Technology Co., Ltd, China) was installed around the carbon brush (Gordon Brush Mfg. Co., Inc., Commerce, CA), which was used as the anode electrode materials and pretreated by being heated at 450 °C for 30 min (Wang et al., 2009). The HF membranes have pore size of 0.2 µm and a surface area of about 0.011 m<sup>2</sup> in total. The cathode electrode consisted of one layer of carbon cloth (PANEX<sup>®</sup>30-PW03, Zoltek, Corporation, St Louis, MO) and catalyst

layers ( $0.3 \text{ mg Pt / cm}^2$ ). The powder of Pt/C (10%, Etek, Somerset, NJ, USA) was mixed with Nafion binder and deionized water, and applied to the surface (the side facing CEM) of carbon cloth using a brush. The cathode catalysts were air-dried for 24 hours at room temperature before operation. Both anode and cathode electrodes were connected by copper wires to an external circuit across a resistance decade box (Tenma 7270, Springboro, OH, USA). The resistance was adjusted according to polarization curve. The anode liquid volume was  $\sim 920 \text{ mL}$ .

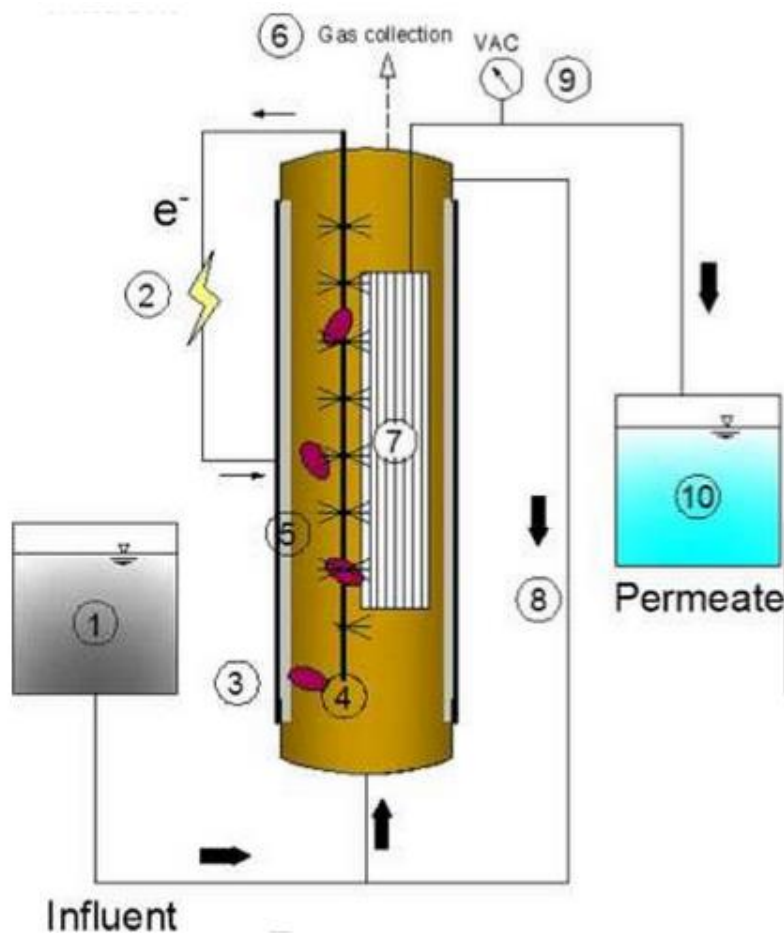


**Figure 5.1. Schematic of a membrane bioelectrochemical reactor (MBER): 1 – influent reservoir, 2 – electric circuit, 3 – cathode electrode (carbon cloth), 4 – anode electrode (carbon brush), 5 – cation exchange membrane (CEM), 6 – gas collection, 7 – hol**

### 5.2.2 Operating condition

The MBER was inoculated using anaerobic digester sludge from a local wastewater treatment facility (South Shore, Oak Creek, WI), and operated under a room temperature of  $\sim 20$  °C. The MBER operation started with a synthetic solution that was fed into the anode compartment from the bottom of the MBER and the permeated water (effluent) was sucked by peristaltic pump. The synthetic wastewater contained (per L of tap water): sodium acetate, 0.75 g;  $\text{NH}_4\text{Cl}$ , 0.15 g;  $\text{NaCl}$ , 0.5 g;  $\text{MgSO}_4$ , 0.015 g;  $\text{CaCl}_2$ , 0.02 g;  $\text{NaHCO}_3$ , 0.1 g;  $\text{KH}_2\text{PO}_4$ , 0.53 g;  $\text{K}_2\text{HPO}_4$ , 1.07 g; and trace element, 1 mL (He et al., 2006). The HF membrane was operated intermittently to minimize membrane fouling (4 min suction and 1 min rest). The flow rate was 0.7-1.4 mL/min, resulting in a hydraulic retention time (HRT) of  $\sim 27$ -15 h. The anode solution was recirculated at 50 mL/min. After about 70 days, the synthetic solution was changed to the primary effluent collected from the South Shore Wastewater Treatment Plant. Tap water was used to rinse the cathode electrode from the top to the bottom for 110 days and then the catholyte was changed to the anode effluent.

During the operation, the permeation flux was kept constant while the trans-membrane pressure (TMP) across the membrane was measured by a vacuum pressure meter. According to the instruction of HF membrane manufacturer, the operation TMP should be kept below 30 kPa. Therefore, Off-line cleaning was carried out when TMP exceeded 30 kPa. The membrane were removed and soaked in pH 12 solution (500 ppm  $\text{NaOH}$  and 100-500 ppm  $\text{NaOCl}$ ) for 30 min, and then backwashed for 30 min using the same chemical solution.

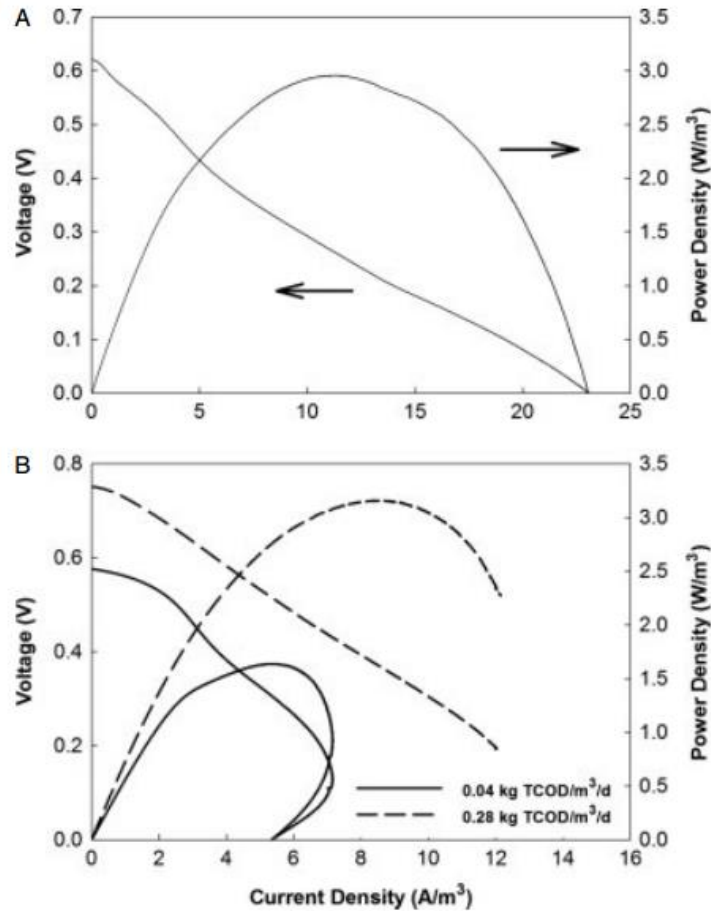


**Figure 5.2. Polarization curves (power and voltage) of the MBER with acetate solution (A) and wastewater (B). The wastewater polarization tests were conducted at two different organic loading rates: 0.04 and 0.28 kg TCOD m<sup>-3</sup> d<sup>-1</sup>.**

### 5.2.3 Measurement and analysis

The cell voltage was recorded every 3 min by a digital multimeter (2700, Keithley Instruments, Inc., Cleveland, OH). The pH was measured using a benchtop pH meter (Oakton Instruments, Vernon Hills, IL, USA). The concentrations of chemical oxygen demand (COD), ammonium, nitrite, and nitrate were measured using a colorimeter according to the manufacturer's procedure (Hach DR/890, Hach Company, Loveland, CO, USA). The turbidity was measured using turbidimeter (DRT 100B, HF Scientific, Inc., Fort

Myers, FL, USA). The polarization tests were performed by a potentiostat (Reference 600, Gamry Instruments, Warminster, PA, USA) at a scan rate of 0.2 mV s<sup>-1</sup>. The power density and current density were calculated based on the anode liquid volume. The water flux from the HF membrane filtration was calculated through pumping flow rate and expressed as liter per surface area of the membrane per hour (L m<sup>-2</sup> h<sup>-1</sup> - LMH). Elemental analysis was performed on an X-ray energy dispersive spectrometer (EDS) (TopCon ABT-32). The EDS was conducted with an accelerating voltage of 15 kV and a working distance of 30 mm. The target elements included nitrogen, oxygen, sodium, magnesium, aluminum, silicon, phosphate, calcium, and copper. Fourier transform infrared spectroscopy (FTIR) measurements were conducted on an infrared spectrophotometer (Brucker Corp VECTOR 22) equipped with diamond Attenuated Total Reflection within a range 4000–600 cm<sup>-1</sup>. The efficiency of organic-to-electricity was expressed by coulombic recovery (CR) and coulombic efficiency (CE), which were calculated according to the following equations:

$$\begin{aligned}
 CR &= \frac{Q_{output}}{Q_{input}} \\
 &= \frac{\sum I(A)t(s)}{96485\left(\frac{C}{mol\ e^{-}}\right) \times COD_{total}(mol) \times 4\left(\frac{mol\ e^{-}}{mol\ O_2}\right)} \quad (6.1)
 \end{aligned}$$

$$\begin{aligned}
 CE &= \frac{Q_{output}}{Q_{input-r}} \\
 &= \frac{\sum I(A)t(s)}{96485\left(\frac{C}{mol\ e^{-}}\right) \times COD_{removed}(mol) \times 4\left(\frac{mol\ e^{-}}{mol\ O_2}\right)} \quad (6.2)
 \end{aligned}$$

where  $Q_{output}$  is the produced charge,  $Q_{input}$  is the total charge available in the added organic compounds,  $Q_{input-r}$  is the total charge available in the removed organic compounds,  $I$  is electric current and  $t$  is time.  $COD_{total}$  is the total COD input to the anode compartment in the period of time  $t$ , and  $COD_{removed}$  is the COD removed within time  $t$ .

## 5.2.4 Energy estimation

Energy consumption in the MBER was mainly due to recirculation of the anolyte and the catholyte by pumps. The power required for the recirculation pump was estimated as eq.

5.3 (Kim et al., 2013):

$$P = \frac{Q\gamma E}{1000} \quad (5.3)$$

where P is power requirement (kW), Q is flow rate ( $\text{m}^3 \text{s}^{-1}$ ),  $\gamma$  is  $9800 \text{ N m}^{-3}$ , and E is the hydraulic pressure head (m). For example, for the MBER treating the primary effluent at HRT of 19 h, Q was  $8.33 \times 10^{-7} \text{ m}^3 \text{ s}^{-1}$  ( $50 \text{ mL min}^{-1}$ ) and  $1.03 \times 10^{-7}$  ( $6.2 \text{ mL min}^{-1}$ )  $\text{m}^3 \text{ s}^{-1}$  for anode and cathode recirculation, respectively, and the hydraulic pressure head loss was assumed to be 0.098 m; thus, the total power required for the recirculation pumps was  $9 \times 10^{-7} \text{ kW}$ . The energy for membrane filtration was calculated based on average vacuum pressure (22 kPa) and permeate flow ( $2 \times 10^{-8} \text{ m}^3 \text{ s}^{-1}$ ), yielding a suction pumping power requirement of  $4.31 \times 10^{-7} \text{ kW}$  (Table B1). The influent pumping power requirement was  $4.73 \times 10^{-8} \text{ kW}$ , according to the hydraulic head loss of 0.35 m and average inflow rate of  $1.38 \times 10^{-8} \text{ m}^3 \text{ s}^{-1}$ . In total, the power requirement for pumping was  $1.38 \times 10^{-6} \text{ kW}$ . Divided by influent flow rate, the total energy requirement was  $2.78 \times 10^{-2} \text{ kWh m}^{-3}$  (or 0.028 in  $\text{kWh m}^{-3}$  in Table B2).

## 5.3 Results

### 5.3.1 The MBER treating synthetic solution

The MBER started as a conventional MFC in which a synthetic solution was actively fed into the bottom of the reactor and flowed out from the top. In the first 20 days, the external

resistance was gradually decreased from 1000 to 10  $\Omega$ , and the current generation increased to  $\sim$ 16 mA. Then, the operation was switched to the 'MBER' mode and the hollow-fiber membranes began water extraction. At an HRT of 19 h and water flux of 5.45 LMH, the current generation varied mostly between 10 and 17 mA (Fig. B1) and the COD removal was about 45% at a loading rate of 0.61 kg m<sup>-3</sup> d<sup>-1</sup>. Depending on the current output, the CE was between 30 and 40% and the CR was 14–20%. The TMP increased very rapidly to 40–50 kPa within 20 h, indicating the occurrence of membrane fouling (Fig. B2). Backwash was conducted using the anode effluent for 1 h when the TMP was above 40–50 kPa; however, the increasing trend was not obviously changed (Fig. B2).

To alleviate the TMP increase and membrane fouling, the HRT was increased to 27 h on day 39, and thus water flux decreased to 3.82 LMH. Figure 5.2A shows the overall electricity generation as a polarization curve. The operating current was maintained around 10 mA, lower than that at HRT 19 h because fewer organic compounds were supplied to the anode (Fig. 5.3A). The pace of the TMP increase clearly slowed, and it took about 1 week to increase the TMP from 5 to 26 kPa (Fig. 5.3B). Then, the membranes were taken out of the MBER and rinsed with DI water to remove the fouling layer. Before resuming the operation, the MBER was backwashed for 1 h at water flux of 5.45 LMH (arrow a on Fig. 5.3B). After physical cleaning, the TMP increased from zero to 37 kPa in six days. Then, a chemical cleaning of the membranes was conducted (arrow b on Fig. 5.3B), in which membranes were soaked in pH 12 NaOH solution for 2 h followed by a 30-min backwash with DI water. When the operation resumed, the TMP increased from zero to 32 kPa in 8 days, indicating that chemical cleaning restored membrane function better than

physical cleaning. At an organic loading rate of  $0.51 \text{ kg m}^{-3} \text{ d}^{-1}$ , the MBER removed 58% of the COD and produced an effluent containing  $246 \pm 39 \text{ mg COD L}^{-1}$  (Fig. 5.3C and Table 5.1). The CE and the CR were about 30% and 17%, respectively. The turbidity of the effluent was  $0.41 \pm 0.19 \text{ NTU}$ .

### 5.3.2 The MBER treating wastewater

The influent of the MBER was switched to real wastewater (primary effluent) on day 75, and the operation consisted of four phases based on the HRTs: 36, 26, 19, and 15 h (corresponding water flux of 3.82, 4.91, 6.55, and 7.75 LMH). The wastewater obtained from the South Shore Wastewater Treatment Plant contained low organic concentration varying with time, which significantly affected electricity generation (Fig. 5.2B). The soluble COD concentration could be as low as  $20 \text{ mg L}^{-1}$  after major storms (arrow a in Fig. 5.4C).

Phase 1 with an HRT 36 h was operated for 46 days. A strategy of integrated periodic backwash and membrane relaxation was adopted to slow down TMP increase and membrane fouling: the MBER was backwashed for 1 min at  $4 \text{ mL min}^{-1}$  every 29 min forward operation, and water filtration was stopped for 1 min every 4 min. The MBER produced a current of 1–1.5 mA (Fig. 5.4.A), significantly lower than that of the synthetic solution, because of lower organic input (Fig. 5.4A and 5.4C). The influent wastewater

**Table 5.1. Characterization of the influent and the effluent of the MBER with different substrates and HRTs**

Substrate	HRT (h)	R <sub>ext</sub> (Ω)	Influent TCOD (mg/L)	Influent SCOD (mg/L)	Influent NH <sub>4</sub> <sup>+</sup> -N (mg/L)	Effluent TCOD (mg/L)	Effluent NH <sub>4</sub> <sup>+</sup> -N (mg/L)	Effluent Turbidity (NTU)	R <sub>TCOD</sub> (%)	CE (%)
Acetate Solution	19	10	485 ± 16	-	-	265 ± 10	-	-	45.3	36.4
Acetate Solution	27	10	583 ± 5	-	-	246 ± 39	-	0.41 ± 0.17	57.8	29.8
Primary Effluent	36	60	152 ± 38	83 ± 22	20 ± 6	20 ± 7	17 ± 3	0.75 ± 0.31	86.9	10.8
Primary Effluent	26	45	158 ± 106	72 ± 53	24 ± 3	16 ± 6	12 ± 1	0.48 ± 0.29	90.1	17.1
Primary Effluent	19	45	235 ± 122	105 ± 71	20 ± 9	23 ± 8	18 ± 3	0.45 ± 0.03	90.2	13.6
Primary Effluent	15	45	199 ± 8	71 ± 3	22 ± 2	21 ± 7	20 ± 1	0.53 ± 0.15	89.4	16.0

R<sub>ext</sub>: external resistance  
R<sub>TCOD</sub>: TCOD removal efficiency

contained total COD (TCOD) of 152 ± 38 mg L<sup>-1</sup> and SCOD of 83 ± 22 mg L<sup>-1</sup> (Table 5.1). The TCOD concentration in the MBER effluent was 20 ± 7 mg L<sup>-1</sup>. The CE was ~11% and the CR was about 9% (based on TCOD). On day 110, the catholyte was changed from tap water (without any pH control) to the anode effluent, and current generation was not obviously affected (arrow b in Fig. 5.4A). The MBER slightly decreased ammonium concentration from 20 ± 6 to 17 ± 3 mg NH<sub>4</sub><sup>+</sup>-N/L, probably due to the ammonia loss through bacterial growth and/or cation exchange membrane (Kim et al., 2008). The nitrate concentration in both the influent and effluent of the MBER remained low at ~ 0.2 mg NO<sub>3</sub><sup>-</sup>-N/L. The total phosphate was unchanged by the MBER operation. The turbidity of the effluent was 0.75 ± 0.31 NTU, much lower than the 10–20 NTU of the effluent of the MFCs without UF membranes when treating the same wastewater (unpublished data). It took 43 days for the TMP to increase from zero to 15 kPa (Fig. 5.4B), much slower than with the synthetic solution. This slow increase can be attributed to three reasons: first, a

lower water flux (longer HRT) slowed down the membrane fouling; second, a lower organic concentration in the wastewater resulted in less microbial growth and thus less microbial fouling of the membrane; and third, the strategy of both periodic backwash and membrane relaxation greatly relieved membrane fouling.

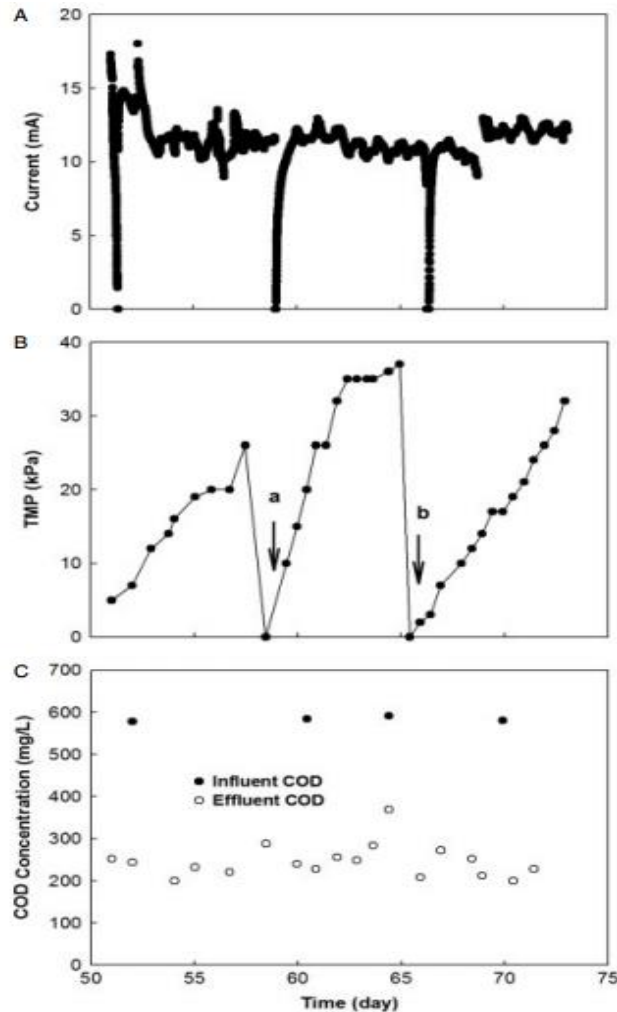


**Figure 5.3 MBER performance with synthetic solution: (A) current generation, (B) transmembrane pressure (TMP), and (C) COD concentrations in the influent and the effluent. Arrow a: physical cleaning; arrow b: chemical cleaning.**

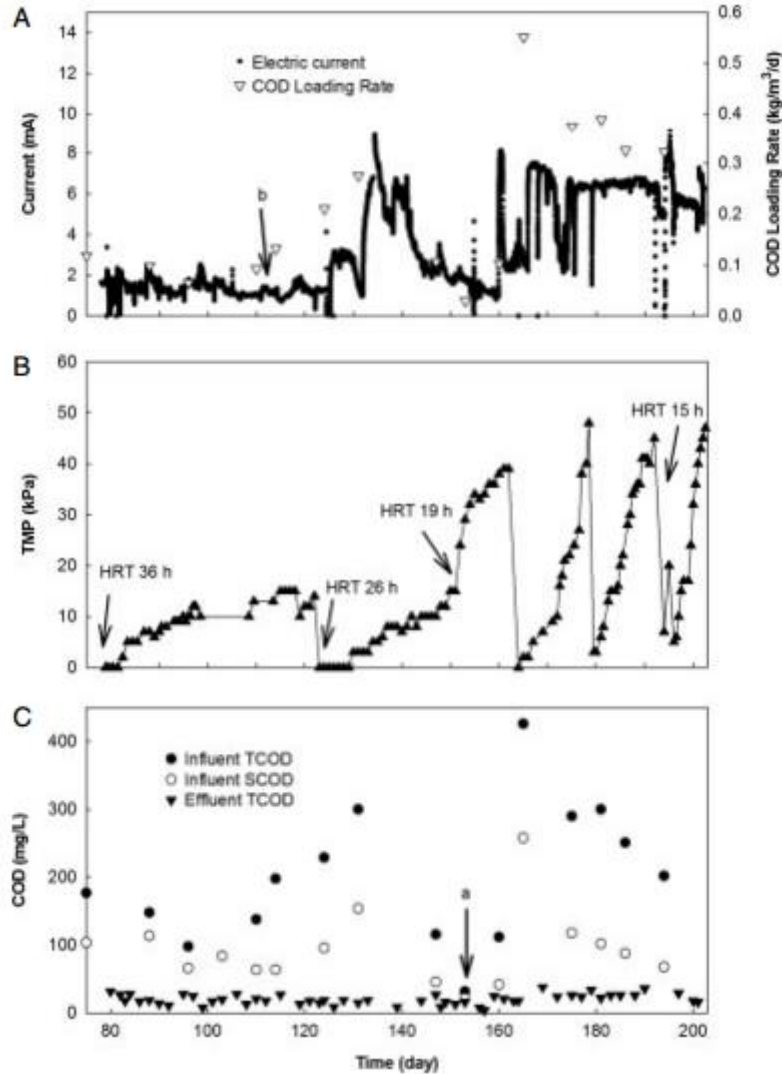


**Figure 5.4 MBER performance with wastewater (primary effluent): (A) current generation and COD loading rates; (B) transmembrane pressure (TMP); and (C) COD concentrations in the influent and the effluent. Arrow a: extremely low COD after a major storm; arrow b: the catholyte changed from tap water to the anode effluent.**

In Phase 2, the HRT was reduced to 26 h. Before the new operation, the membranes were removed from the MBER and cleaned using a pH 12 NaOH solution (Table B3). The TMP increased from zero to 15 kPa in 28 days, faster than Phase I (Fig. 5.4B). The current was generally higher than the previous phase due to higher organic loading in a shorter HRT,

and largely affected by the actual organic concentration in the wastewater. A high peak of 8 mA was observed, because of a high TCOD ( $300 \text{ mg L}^{-1}$ ) and SCOD ( $152 \text{ mg L}^{-1}$ ) in the feed at day 130. Despite the higher organic influx, the MBER effluent contained a TCOD concentration of about  $20 \text{ mg L}^{-1}$ , indicating stable performance of the organic removal. During this period, the CE and the CR based on TCOD was 17% and 15%, respectively. The average turbidity was below 0.5 NTU (Table 5.1). In Phase 3, operation with a new HRT of 19 h started on day 151 without cleaning the membrane. The TMP dramatically increased from 15 to 24 kPa on day 152 and continued to rise to 39 kPa over the next 10 days. Then, the hollow-fiber membranes were removed for cleaning (Table B3). At restart of the MBER TMP exhibited an increase to 45–50 kPa in 14–15 days. The effluent quality (COD removal and turbidity) was similar to the previous operation (Table 5.1). A brief Phase 4 was operated at an HRT of 15 h, and a quick increase of TMP to 45 kPa in 7 days was observed; at this rate, the membrane would require frequent cleaning and thus make this operation unsustainable.

### 5.3.3 Energy balance

The energy balance was estimated by analyzing energy consumption and production ( $\text{kWh m}^{-3}$ ) in the MBER, as summarized in Table B2 and shown in Fig. 5.5. Energy consumption in the MBER is mainly due to the pumping system, which consists of three parts: influent feed, permeate (vacuum pumping), and recirculation of the anolyte and the catholyte. The power required for the pumps shown in Table B1 was estimated according to a previous study (Kim et al., 2011) and more details can be found in the Supporting Information. It was found that recirculation consumed the most energy (Table B2), and a longer HRT

resulted in more energy consumption, because the recirculating pumps were operated for a longer period of time to treat every cubic meter of wastewater. The estimated energy requirement varied between 0.027 and 0.040 kWh m<sup>-3</sup> at HRTs of 15–36 h (Table B2). The energy produced in the MBER was calculated by integrating power over time and was affected by organic loading rates. The MBER fed with the acetate solution that had a higher COD produced 0.036–0.038 kWh m<sup>-3</sup>, much higher than 0.003–0.025 kWh m<sup>-3</sup> with the wastewater (Table B2). According to the estimation of energy consumption, the MBER could theoretically produce enough energy to support the pumping system when treating the acetate solution. The energy production from wastewater was lower than the energy requirement, and at the shortest HRT of 15 h production was close to the consumption (Fig. 5.5). The low organic content in the wastewater used in this study led to low energy production.

#### 5.3.4 Membrane fouling

Due to the lack of active anti-fouling methods, reducing membrane fouling in an MBER is important for successful operation. In this study, both high organic loading rates and high water flux accelerated membrane fouling. Physical cleaning with DI water to remove fouling layers had a limited effect on membranes when treating wastewater. Chemical cleaning employing a high pH solution (pH 12), sodium hypochlorite, and backwash generally restored the water flux (Table B3) and cleaned the membrane surface (Fig. B3). The EDS spectrum revealed that the fouled membrane contained more elements, such as nitrogen, calcium, magnesium, copper, aluminum, silicon, and chloride, than the new membrane and there was almost no difference between the interior and the exterior

membranes, except that calcium was detected on the interior side of the membrane (Fig. B4). The significant presence of nitrogen (16–18%) in the fouled membrane was possibly due to protein and inorganic nitrogen contaminants in the wastewater.

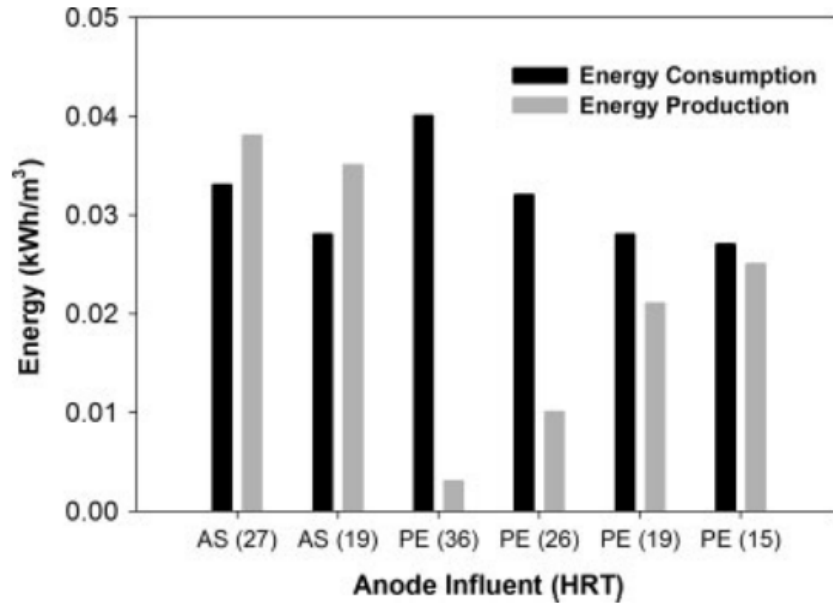


**Figure 5.5. Energy consumption and production in the MBER with different anode effluents at different HRTs. AS: acetate solution. PE: primary effluent. The number in parentheses indicates the HRT.**

The two main components of the PVDF membrane, carbon and fluoride, also changed in weight. Using the mass of fluoride as a reference, the C/F ratio increased from 1.01 of the new membrane to 1.16 of the fouled membrane for the exterior membrane, and from 0.83 to 0.88 for the interior membrane (Table B4). The ratio of oxygen-to-fluoride also increased from 0.49–0.53 in the new membrane to 0.68 in the fouled membrane (Table B4). The excessive carbon, nitrogen, and oxygen in the fouled membrane indicated biofouling (Rabiller-Baudry et al., 2002); which was also confirmed by the FTIR spectra, which

showed a new peak on the fouled membrane at  $1642\text{ cm}^{-1}$  (Fig. B5), related to the amide I ( $\text{C}=\text{O}$  and  $\text{C}-\text{N}$  stretching), suggesting the presence of proteins (Xu et al., 2012).

## 5.7 Discussion

This study has demonstrated the proof of concept of a membrane bioelectrochemical reactor and provided an alternative approach to anaerobic treatment of domestic wastewater. During membrane cleaning, the anode electrode was taken out from the MBER and exposed to the air. It was observed that current generation was restored quickly after the anode electrode was installed back in the MBER (Fig. 5.3A), suggesting that the anode microbes could tolerate oxygen for a short period of time, which gives the MBER more flexibility in response to operational fluctuation such as oxygen exposure due to either a leak or system maintenance. The experiments with actual wastewater demonstrated that the MBER could achieve good treatment performance with low COD concentration and turbidity in the effluent; however, the results also revealed serious membrane fouling (more details in the following section), which was affected by organic loading rates resulting from both HRT and the COD concentration in the influent. In general, the MBER could maintain good COD removal from primary effluent while producing bioelectricity.

A conventional MFC that treated similar wastewater produced an effluent with turbidity 10–20 NTU and 20–40 mg VSS  $\text{L}^{-1}$  (unpublished data); through integrating hollow-fiber membranes, the MBER improved the effluent quality with low turbidity ( $\sim 1$  NTU) and almost no suspended solids. The concentration of pathogens was not examined in the

present system; however, with a pore size of 0.02  $\mu\text{m}$ , the hollow-fiber membranes could prevent the discharge of bacteria in the final effluent.

Limited nitrogen removal is one of the major barriers to the application of anaerobic treatment (e.g. AnMBR (Kim et al., 2011)). Nitrogen, mainly ammonia, cannot be removed under anaerobic conditions unless ANAMMOX is developed. In this study, the ammonium concentration slightly decreased in the anode effluent, because of microbial growth and/or ammonium diffusion through the CEM. However, after the anode effluent was used as catholyte to rinse the cathode, an obvious reduction of ammonium concentration to  $2 \pm 1 \text{ mg L}^{-1}$  was observed in the catholyte; meanwhile, the nitrate concentration increased to  $10 \pm 6 \text{ mg L}^{-1}$ , indicating the presence of nitrification on the surface of the cathode electrode. It is likely that nitrifying bacteria took advantage of oxygen and formed biofilm on the cathode electrode. This ‘fixed-biofilm’ nitrification did not significantly increase the suspended solids in the catholyte, and the turbidity of the catholyte was  $\sim 1$  NTU, slightly higher than the 0.5 NTU of the anode effluent. Nitrate removal is critical to lowering the concentration of total nitrogen, but bioelectrochemical denitrification is not expected on the cathode because of the presence of oxygen. Previous denitrifying biocathode in MFCs (Clauwaert et al., 2007) raises the possibility that the cathode of an MBER may be specially designed to provide a partially anoxic condition to accomplish both nitrification and denitrification; to achieve this, shortcut nitrification–denitrification (Gao et al., 2009) will be more advantageous. Phosphorus, on the other hand, could not be removed in the MBER. Like other anaerobic treatments of low-strength wastewater that are being studied, the MBER would require post-processes to remove or recover nutrients (Kim et al., 2011).

It should be noted that a precise energy analysis for a bench-scale system is very difficult, and the present information attempts to promote more (future) work related to energy analysis, because of the lack of systematic analysis of energy balance in MFCs. The accuracy of an energy balance in the present system is largely affected by the energy required for the pumping system, and our theoretic calculation could underestimate the energy consumption. If an AnMBR is used as a reference, because of the similarity between AnMBR and MBER, our system (treating actual wastewater) produced less than 15% of the energy that the pumping system consumes ( $0.2 \text{ kWh m}^{-3}$ ) in a full-scale AnMBR. (Prieto AL et al, 2011) The present MBER generated a low (operating) power density  $< 2 \text{ W m}^{-3}$  with the wastewater; it is possible to further improve its power output by increasing organic loading rate and optimizing reactor configuration and operation. If the power output can be improved by 10 times to  $20 \text{ W m}^{-3}$ , an MBER will produce sufficient energy to provide an energy-neutral treatment system.

Although the HRTs of 15–36 h applied to the MBER are within the range of AnMBRs treating domestic wastewater (Smith AL et al., 2012), a shorter HRT (and higher organic loading rate) will benefit wastewater treatment with less land footprint of the facility. To maintain a short HRT, membrane fouling must be reduced; in future studies, one can consider reducing sludge retention time (SRT) and involving active anti-fouling methods. The SRT of the present MBER was more than 180 days, and the previous study found that a short SRT (e.g. 30–60 days) could greatly slow down membrane fouling (Huang et al., 2011). Using biogas to remove foulants is a common approach to control fouling in

AnMBRs; however, the use of a carbon brush electrode in an MBER isolated hollow-fiber membranes from contact with gas bubbles and could also trap bubbles with carbon fibers. Fluidized granular activated carbon (GAC) that has been used to control fouling (Kim et al., 2011) will be considered to maintain a low TMP in a future MBER.

#### **5.4 Conclusions**

This study has demonstrated a proof of concept of an MBER for wastewater treatment. Further MBER development must understand and address some key challenges. For instance, the low CE and CR with real wastewater could be due to other electron sinks such as sulfate reduction and methanogenesis, and constructing a carbon balance would help understand the electron flow. It will be of strong interest to examine the treatment of wastewater with high COD content and stability of the MBER system during long-term operation. Membrane fouling must be effectively reduced. The results have suggested that installing membranes within the anode compartment may not be an optimal approach to integrate membranes with MFCs, due to the difficulty of membrane cleaning. Future MBERs will consider fluidized GAC when membranes are inside the anode compartment, or a side-stream membrane system that is placed sequentially to MFCs.

## CHAPTER 6

### Long-Term Investigation of Microbial Fuel Cells Treating Primary Sludge or Digested Sludge

(This section has been published as: Ge, Z., Zhang, F., Grimaud, J., Hurst, J. and He, Z.\* (2013) Long-term investigation of microbial fuel cells treating primary sludge or digested sludge. **Bioresource Technology**. Vol 136, pp 509-514.)

#### 6.1 Introduction

Sewage sludge is a byproduct of municipal wastewater treatment and generated from primary and secondary sedimentation. In municipal wastewater treatment plants, the treatment and disposal of sewage sludge can comprise up to 50% of the operation costs (Appels et al., 2008). There are several approaches for treating sludge to reduce solid contents and to stabilize biomass; however, anaerobic digestion (AD) is generally preferred because of its cost-effectiveness and bioenergy production. Digested sludge can be further composted for agriculture uses, and biogas can be converted into electricity and/or heat through combustion and thus compensate for some energy use in a wastewater treatment plant. Because of a large amount of organic contents, primary sludge contains about 66% of the energy content of wastewater (Ting and Lee, 2007), and about 81% of biodegradable organic energy may be converted to methane (McCarty et al., 2011). Despite the great energy potential with biogas production, several issues limit successful AD application; for instance, electric generators and their maintenance are costly, and biogas may need pre-treatment to remove contaminants such as hydrogen sulfide (Appels et al., 2008). In addition, energy will be lost during methane conversion, because the common efficiency of methane-to-electricity is about 33%. Therefore, it is of great interest to explore alternative technologies for sludge treatment and energy recovery.

The use of microbial fuel cells (MFCs) is a promising approach for direct production of electric energy or other energy carriers such as hydrogen gas from various organic substrates (Logan et al., 2006 and Pant et al., 2010). Sewage sludge has also been studied in MFCs for electricity generation. A single-chamber MFC with a baffle inside its anode compartment generated low power from anaerobic sludge due to a large internal resistance caused by the baffle (Hu, 2008). Because hydrolysis is considered to be a limiting step in AD (Halalsheh et al., 2011), appropriate pretreatment is expected to improve the contents of soluble and small-particle organics that can be better used by microorganisms. The ultrasonic and alkaline pretreatment of sludge improved its degradability and resulted in a higher power output of  $12.5 \text{ W/m}^3$ , with 61.0% and 62.9% reduction of total chemical oxygen demand (TCOD) and volatile solids (VS), respectively (Jiang et al., 2009 and Jiang et al., 2010). Likewise, improved power output and solid production was observed in an MFC after pretreatment with sterilization and alkalization (Xiao et al., 2011). When an MFC was linked to an anaerobic digester to form an integrated recirculation loop, it was found that methane production was higher than the digester alone (Inglesby and Fisher, 2012), because a high concentration of ammonium/ammonia will inhibit methanogenic activity (Sung and Liu, 2003). The improved biogas production, resulting from the use of a recirculation loop, was likely due to the migration of ammonium ions from the digester to the cathode compartment of the MFC driven by electricity generation in the MFC, which was also demonstrated previously (Kim et al., 2008). A recent study reported the performance of MFCs in treating a fermentation solution from primary sludge, in which higher power production was obtained when treating a mixture of fermentation supernatant

and primary effluent, because of elevated concentrations of soluble COD and volatile fatty acids after the fermentation process (Yang et al., 2013).

In general, previous research on using MFCs to treat sludge focused on the short-term performance of power production and COD removal, and few studies have examined biogas production and solid reduction in great detail. Furthermore, no studies have really shown the production of electric energy (in kWh) from sludge; power is not an energy parameter (He, 2013). In this study, we conducted a long-term (almost 500 days) investigation of MFCs treating sewage sludge for energy production, organics removal, and solid reduction. The experiment consisted of two phases: in Phase I, two tubular MFCs were operated with primary sludge and digested sludge, respectively, for more than 10 months; in Phase II, both MFCs were operated as a two-stage system to treat primary sludge for about 6 months. We examined biogas production in the MFCs and compared energy production between MFCs and anaerobic digesters. The results helped to better understand the application niche of MFC technology in wastewater treatment.

## **6.2 Materials and Methods**

### **6.2.1 MFC setup**

Two identical tubular MFCs were constructed based on a tube made of cation exchange membrane (Ultrex CMI7000, Membranes International, Inc., Glen Rock, NJ, USA) (Fig. 6.1). The membrane tube had a diameter of 6 cm and a height of 70 cm. A carbon brush (Gordon Brush Mfg. Co., Inc., Commerce, CA, USA) was used as an anode electrode and installed inside the membrane tube, resulting in an anode liquid volume of 1.8 L. The

cathode electrode was carbon cloth (PANEX® 30-PW03, Zoltek, Corporation, St. Louis, MO, USA) coated with Pt/Carbon catalyst (0.2 mg Pt/cm<sup>2</sup>). The cathode electrode wrapped the membrane tube and connected to the anode electrode by titanium wire and copper wire across a resistance decade box.

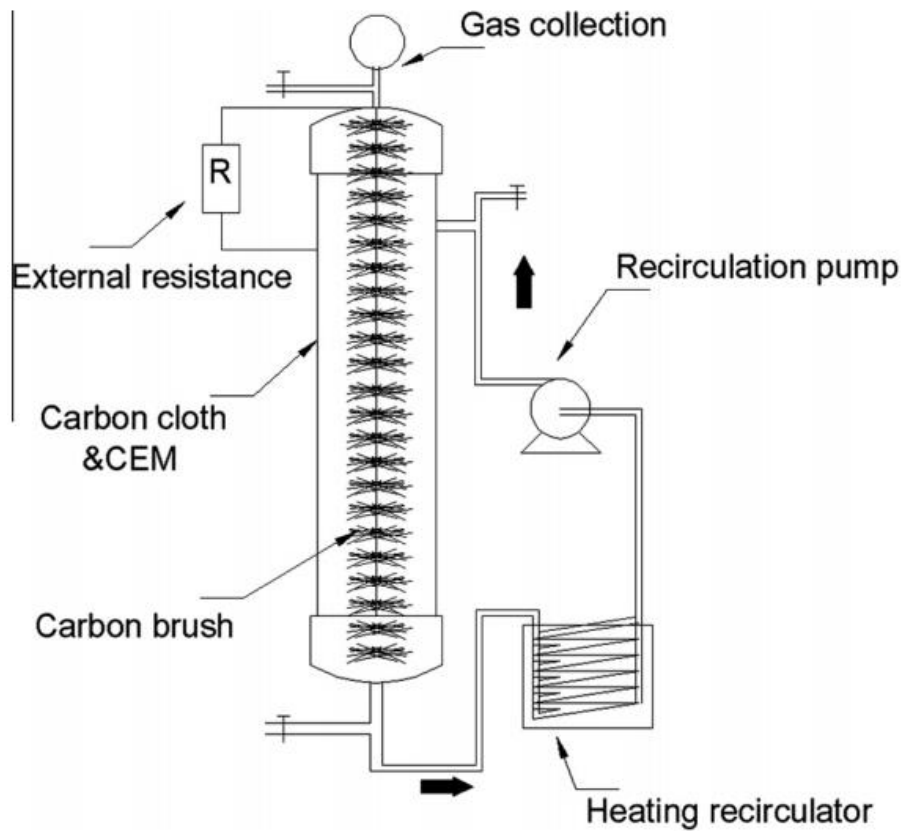


**Figure 6.1 Schematic of the tubular MFC used for sludge treatment.**

### 6.2.2 MFC operation

Both MFCs (MFC-1 and MFC-2) were inoculated with raw sludge from a primary sedimentation tank (South Shore Water Reclamation Facility, Milwaukee, WI, USA). In Phase I, two MFCs were operated at an HRT of 9 days in each reactor: MFC-1 used the

primary sludge as an anode substrate, while MFC-2 was fed with the digested sludge from the anaerobic digesters at South Shore Water Reclamation Facility. In Phase 1, the large particles in the sludge were removed using a 4-mm sieve before feeding. In Phase II, the two MFCs formed a two-stage MFC system, in which the primary sludge was first fed into MFC-1, and then the treated effluent of MFC-1 was transferred into MFC-2. Each MFC had an HRT of 7 days, resulting in a total HRT of 14 days in the two-stage MFC system. An electric blender was used to break the large particles in the primary sludge, and then the sludge was screened through a 3.3-mm sieve. To buffer the pH of the anolytes in the two MFCs, 1.68–3.36 g of NaHCO<sub>3</sub> was added at the beginning of each feed cycle. The anolytes were recirculated at 150 and 100 mL/min in Phase I and II, respectively. The temperature of the anolytes was maintained around 35 °C by using a heating recirculator (Model 1104; VWR International, LLC, USA), which heated a water bath housing the recirculation of the anolyte. The acidified tap water (pH = 2, adjusted using sulfuric acid) was recirculated at ~45 mL/min as the catholyte for both MFCs.

### 6.2.3 Measurement and analysis

The MFC voltage across an external resistor was measured using a multimeter (Model 2700; Keithley Instruments, Inc.). Biogas was collected and measured by the water replacement method. The composition of biogas (mainly CO<sub>2</sub> and CH<sub>4</sub>) was analyzed by using a gas chromatography (Focus GC, Thermo Fisher Scientific, Waltham, MA, USA). TCOD concentrations were measured using a COD digester and colorimeter according to the manufacturer's instructions (Hach Company, Loveland, CO, USA). Total suspended solids (TSS) and volatile suspended solids (VSS) were measured using standard methods

(Clesceri et al., 1998). The pH was measured using a Benchtop pH meter (UB-10, Denver Instrument, Denver, CO, USA). Polarization curves were constructed using a Gamry Reference 600 potentiostat (Gamry Instruments, Warminster, PA, USA). The power density and current density were calculated based on the anode liquid volume. Coulombic efficiency (CE) was calculated according to a previous study (Ge et al., 2013). The calculation of energy from power can be found in the Supplementary data.

## **6.3 Results and Discussion**

### **6.3.1 MFCs treating primary sludge or digested sludge**

Both MFCs were acclimated for about 2 months at an initial external resistor of 2000  $\Omega$  (which was changed to 40  $\Omega$  later) to reach a condition with stable electricity generation, and then polarization analysis was carried out to determine the internal resistance. Although the maximum power densities obtained from polarization curves were very different, 6.4 and 3.2  $\text{W/m}^3$  for MFC-1 and MFC-2, respectively (Fig. C1), the two MFCs had a similar internal resistance of  $\sim 20 \Omega$ . These power densities were in the typical range of 2.4–7.8  $\text{W/m}^3$  from the MFCs using sludge as substrates (Wang et al., 2012). Subsequently, the external resistance of both MFCs was adjusted to 20  $\Omega$  for the maximum power output during the remaining period of Phase I. Fig. 6.2 shows the current generation at an HRT of 9 days for more than 250 days. The fluctuation in current generation was due to the large variation in the sludge characteristics of TCOD and the solid contents in the feeding sludge (Table 6.1). The primary sludge contained more than 80% of volatile organics, whereas about only half of the solid content was volatile in the digested sludge because of the stabilization during anaerobic digestion. The pH of the primary sludge was

relatively acid because of hydrolysis and fermentation in the sedimentation tank, but the digested sludge had a neutral pH, possibly due to the alkalinity addition during anaerobic digestion.

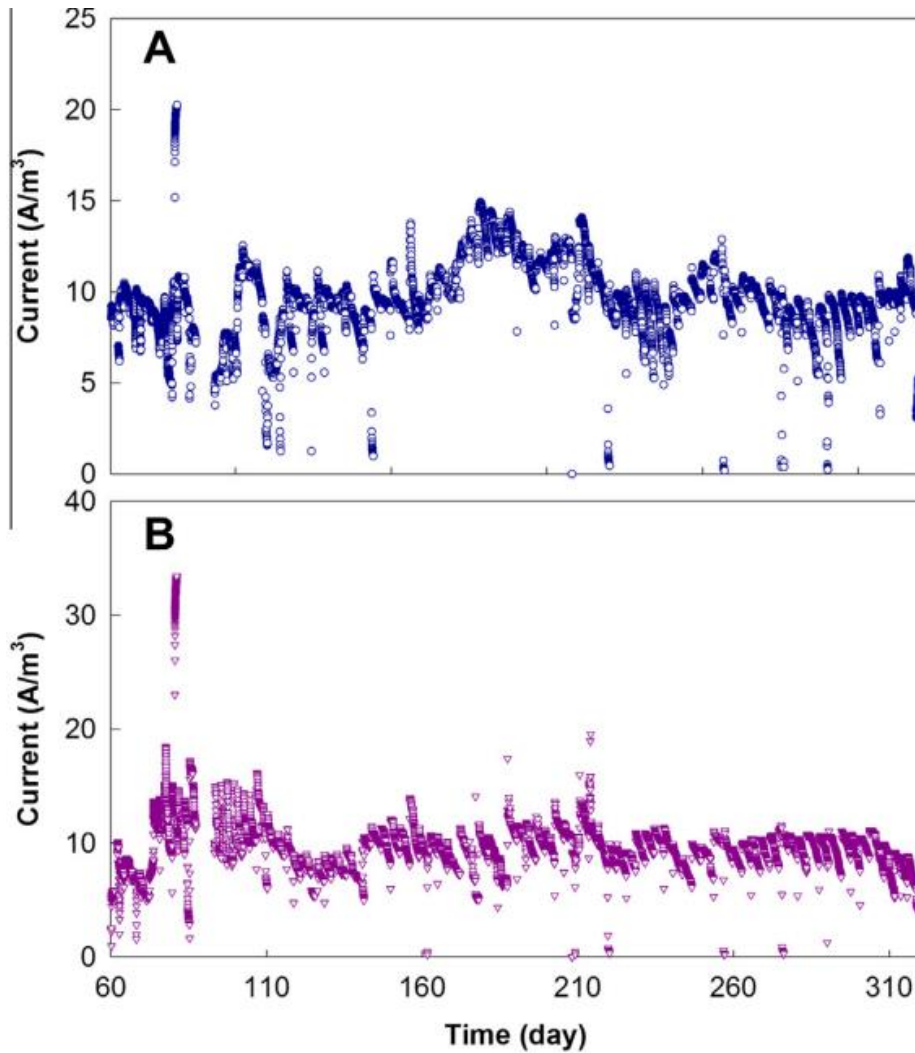


**Figure 6.2** Current generation of individual MFC in Phase I with an HRT of 9 days in each reactor: (A) MFC-1 fed with primary sludge and (B) MFC-2 fed with digested sludge.

**Table 6.1 Characteristics of the primary sludge (PS) and the digested sludge (DS) in the Phase I.**

	<b>PS</b>	<b>DS</b>
TCOD (g/L)	14.2 ± 11.2	16.7 ± 11.4
TSS (g/L)	6.9 ± 5.5	5.8 ± 4.7
VSS (g/L)	6.1 ± 5.0	3.0 ± 2.9
pH	6.0 ± 0.4	7.1 ± 0.6

For sludge treatment, MFC-1 had a higher TCOD removal of  $69.8 \pm 24.1\%$  from the primary sludge compared with  $36.2 \pm 24.4\%$  from the digested sludge in MFC-2. Because of the high concentrations of organic matter in the sludge, both MFCs had relatively low CEs of  $7.2 \pm 8.1\%$  in MFC-1 and  $2.6 \pm 1.4\%$  in MFC-2; MFC-1 also had greater solid reduction than MFC-2. MFC-1 reduced  $63.7 \pm 19.6\%$  of TSS and  $68.4 \pm 17.9\%$  of VSS, while MFC-2 achieved  $42.8 \pm 17.1\%$  of TSS reduction and  $46.1 \pm 19.2\%$  VSS reduction.

In Phase I, the main difference between the two MFCs fed with different sludge was in the reduction of organics/solids, not in electricity generation, although polarization curves did show some difference at the initial period. The primary sludge was better treated in the MFC, because it contained a high fraction of readily degradable compounds; on the other hand, the digested sludge had much less volatile solid and became more stable after anaerobic digestion. Biogas production observed in MFC-1 but not in MFC-2 during the Phase I also indicated the digested sludge had much fewer “useful” organic compounds; even its higher pH than the primary sludge should have favored the growth of methanogens. However, MFC-2 still extracted some electric energy from the digested sludge and further reduced TCOD and VSS, suggesting that MFCs may be used as a post-treatment process

following anaerobic digesters (Pham et al., 2006). However, the high-solid sludge could clog the MFC reactors that contain high surface-area materials as electrodes, and thus its treatment in MFCs may require more maintenance. The supernatant of digested sludge could be a more appropriate substrate for MFCs. In a wastewater treatment facility, digested liquid (supernatant) from anaerobic digesters is usually returned to primary treatment and will eventually be treated by aerobic processes (e.g., activated sludge). If this digested liquid can be further polished in an MFC, the amount of energy needed to remove organic materials will be reduced by eliminating or reducing aeration, and some organics can be directly converted into electric energy in MFCs, thereby decreasing operating expense.

We examined the effects of recirculation rates (mixing intensity) and electrolyte pH on electricity generation in MFC-1. More current production was expected due to better mixing by a higher recirculation rate; however, we did not observe any obvious improvement when adjusting the recirculation rates from 150 to 400 mL/min (Fig. C2). Therefore, to minimize energy consumption by the recirculation, the recirculation rate was fixed at 150 mL/min for the remaining test period. The pH of the anolyte could significantly affect electricity generation by affecting the growth of electrochemically-active bacteria. The anolyte pH of MFC-1 decreased to  $5.48 \pm 0.43$  at the end of each feeding cycle in the absence of any buffering solutions, which was caused by concurrent reactions from acidification process and proton accumulation in the anode compartment. The current generation was not negatively affected by the pH until day 75. When we added phosphate buffer solution (PBS) on day 80 to adjust the pH, the current recovered to  $\sim 12 \text{ A/m}^3$  (Fig.

C3). When  $\text{NaHCO}_3$  was dosed instead of PBS on day 100 to buffer the anolyte, the pH was  $6.5 \pm 0.6$  after each cycle while the electricity generation varied between 6 and 12  $\text{A/m}^3$  (Fig. C3). Unlike the primary sludge, the digested sludge (in MFC-2) had sufficient alkalinity to maintain a pH at  $6.5 \pm 0.4$  at the end of the operating cycle so that no buffer was added into MFC-2.

The limited effect of recirculation rates (mixing intensity) on electricity generation could be due to a sufficient supply of organic compounds with the high-concentration sludge. Previously, we observed a significant improvement in electricity generation at higher recirculation rates with a low-strength anode feeding solution (Zhang et al., 2010 and Zhang et al., 2013). In this study, a high concentration of TCOD was overly supplied to the anode compartment, in which there was no zone with deficiency of organic substrates. Therefore, improving the mixing did not obviously alter the substrate supply to the anode electrode.

### 6.3.2 Two-stage MFC system treating primary sludge

After operating for about 300 days, the two MFCs were changed to a two-stage mode, in which the primary sludge was fed into MFC-1, and then the MFC-1 effluent was transferred into MFC-2. The HRTs were same at 7 days in both MFCs. It took about 50 days to reach a condition of stable current generation due to system clogging, availability of substrate, and other instrumental problems. Fig. 6.3 shows current generation in the two MFCs for more than 120 days. During this phase, the primary sludge was blended and then screened,

resulting in a much higher content of both solids and organics supplied to the MFCs than that of MFC-1 in Phase I (Table 6.2).

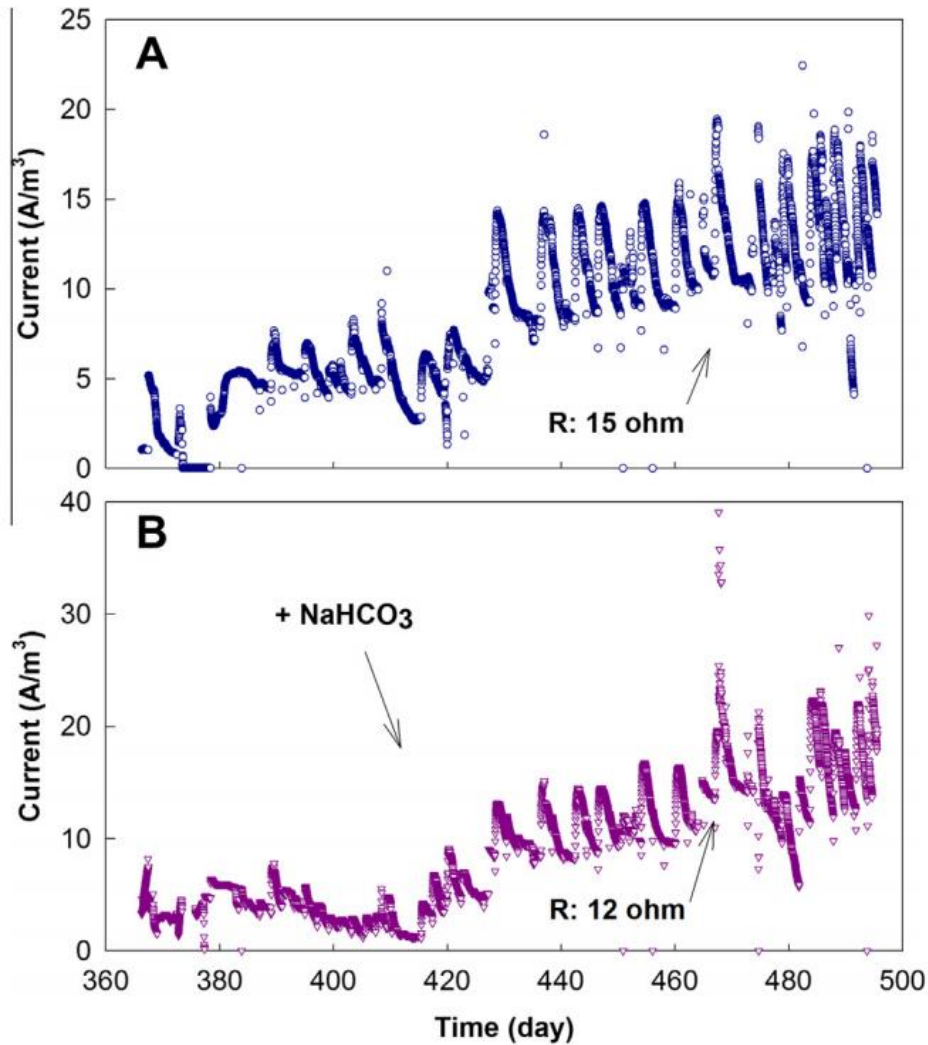


Figure 6.3 Current generation in the two-stage MFC system fed on primary sludge in Phase II with an HRT of 7 days in each reactor: (A) MFC-1 and (B) MFC-2.

Initially, only MFC-1 was buffered by adding NaHCO<sub>3</sub>; its effluent pH was maintained at around 6.5 and the current varied between 6 and 14 A/m<sup>3</sup>. On day 390, the current of the

MFC-2 started to decrease below 6 A/m<sup>3</sup>. On day 415 we added NaHCO<sub>3</sub> to the MFC-2 feeding, which gradually improved the peak current to 17 A/m<sup>3</sup>. In addition, biogas was observed in MFC-2 following the addition of bicarbonate, which will be discussed in the following section. Because of the changes in current generation, we conducted another polarization test and obtained different internal resistances for both MFCs. As a result, the external resistance was changed to 15 Ω for MFC-1 and 12 Ω for MFC-2 on day 467. We also found that the acidified catholyte resulted in maximum power densities of 8.5 and 10.7 W/m<sup>3</sup> for MFC-1 and MFC-2, respectively (Fig. C4A), almost twice the maximum power densities when the catholytes were neutralized (Fig. C4B). The acidified catholytes also resulted in a higher open-circuit voltage (0.2 V) than that with the neutralized catholytes.

**Table 6.2 Characteristics of the primary sludge (PS) and the treatment performance of the two MFCs in the Phase II.**

		PS	MFC-1	MFC-2
Day 380-434	TCOD (g/L)	78.0±12.4	46.7±15.0	24.2±14.2
	TSS (g/L)	58.4±12.0	28.0±5.9	10.4±7.2
	VSS (g/L)	44.8±7.6	19.0±3.2	7.12±3.8
	TCOD Reduction (%)		37.3±23.0	67.0±17.3
	VSS Reduction (%)		54.4±10.5	82.1±9.0
Day 435-470	TCOD (g/L)	52.7±8.8	31.8±7.4	19.6±5.7
	TSS (g/L)	31.8±14.0	19.1±7.6	8.4±4.5
	VSS (g/L)	25.8±14.0	13.1±6.0	5.3±3.5
	TCOD Reduction (%)		41.8±12.6	63.9±10.5
	VSS Reduction (%)		57.4±12.9	79.6±16.3
Day 471-495	TCOD (g/L)	35.0±6.54	19.0±8.8	15.2±3.1
	TSS (g/L)	23.8±4.6	12.4±6.5	8.3±3.6
	VSS (g/L)	25.8±14.0	10.0±5.4	5.7±1.4
	TCOD Reduction (%)		51.1±22.8	60.8±14.2
	VSS Reduction (%)		51.1±27.8	71.7±9.1
pH		5.6±0.1	6.6±0.4	6.4±0.4

The treatment performance of the MFC system in Phase II was divided into three periods: days 380–434, days 435–470, and days 471–495, according to the difference in sludge characteristics from different samplings (Table 6.2). The corresponding removal efficiencies of TCOD in MFC-1 were  $37.3 \pm 23.0\%$ ,  $41.8 \pm 12.6\%$ , and  $51.1 \pm 22.8\%$ , respectively; the total TCOD removal efficiencies after the MFC-2 treatment were  $67.0 \pm 17.3\%$ ,  $63.9 \pm 10.5\%$ , and  $60.8 \pm 14.2\%$ , respectively, during the three periods. In Phase II, the coulombic efficiency was generally low, as the CEs were only  $2 \pm 1\%$  and  $4 \pm 1\%$  for MFC-1 and MFC-2, respectively. For solid reduction, the MFC-1 reduced 51.1–54.4% of VSS; the use of MFC-2 as the second-stage treatment improved solid reduction by about 20% (Table 6.2). The two-stage MFC system had higher reduction efficiencies of both TCOD and VSS at higher initial concentrations.

MFCs may be competitive to anaerobic digesters in terms of primary sludge treatment, especially in reducing volatile solids (VS). A few examples of AD treatment reported in the previous studies include a 56% reduction in VS at an HRT of 15 days (Tchobanoglous et al., 2002), 35% reduction in VS from primary sludge at an HRT 20 days (Ghyoot and Verstraete, 1997), 61.7% reduction in VS from waste-activated sludge at an HRT 15 days (Liu et al., 2012), and 40–50% reduction in VS from sewage sludge (Cao and Pawłowski, 2012). In our study, MFC-1 could reduce 68% of VSS in 9 days in Phase I, and about 50% of VSS in 7 days in Phase II. If we include MFC-2 in the Phase II, the two-stage MFC system could reduce more than 70% of VSS in 14 days. Faster solid reduction in the MFCs was possibly due to two factors: oxygen intrusion into the anode compartment through the

cation exchange membrane, and bioelectrochemical oxidation using oxygen as a terminal electron acceptor that is an “indirect” aerobic reaction. The carbon brush anode electrode with a high specific area provided sites for biofilm formation that could facilitate the growth of robust organisms for organic oxidation; the carbon fibers of the carbon brush might also help with solid–liquid separation that retained organic compounds for microbial use in a longer period of time.

### 6.3.3 Biogas and energy production

Biogas production in the MFCs was observed and analyzed. In Phase I, biogas production occurred only in MFC-1 with the primary sludge, ranging from 190 to 1467 mL/day. MFC-2 was used to treat the digested sludge and did not generate any obvious biogas. During Phase II, biogas was produced in both MFCs (Fig. 6.4). MFC-1 had increasing biogas production that reached the highest rate of about 2200 mL/day during days 435–470. MFC-2, on the other hand, did not produce any biogas at the initial period; after the bicarbonate was added into MFC-2 to buffer the anolyte, biogas was produced subsequently, although not as much as MFC-1. The highest production rate in MFC-2 was about 1175 mL/day. The biogas contained  $62.7 \pm 3.6\%$  and  $51.4 \pm 12.7\%$  of methane from MFC-1 and MFC-2, respectively.

Energy production was analyzed in Phase II as a sum of electric energy from direct electricity generation in the MFCs, and electricity that could be generated from biogas conversion. The direct electric energy was calculated using power production from either a regular operation or the maximum power output from the polarization test. In a regular

operation, electric power was produced at external resistance of  $20 \Omega$  for both MFCs; the average energy production in MFC-1 and MFC-2 was  $0.78$  and  $0.95 \text{ kWh/m}^3$ , respectively, resulting in a total electric energy production of  $1.73 \text{ kWh/m}^3$  in the two-stage MFC system (Table 6.3). At the maximum power output obtained from the polarization curves (Fig. C4A), the energy production will be  $1.43$  and  $1.80 \text{ kWh/m}^3$  from MFC-1 and MFC-2, respectively (Table 6.3); thus, the total electric energy will be  $3.23 \text{ kWh/m}^3$ .

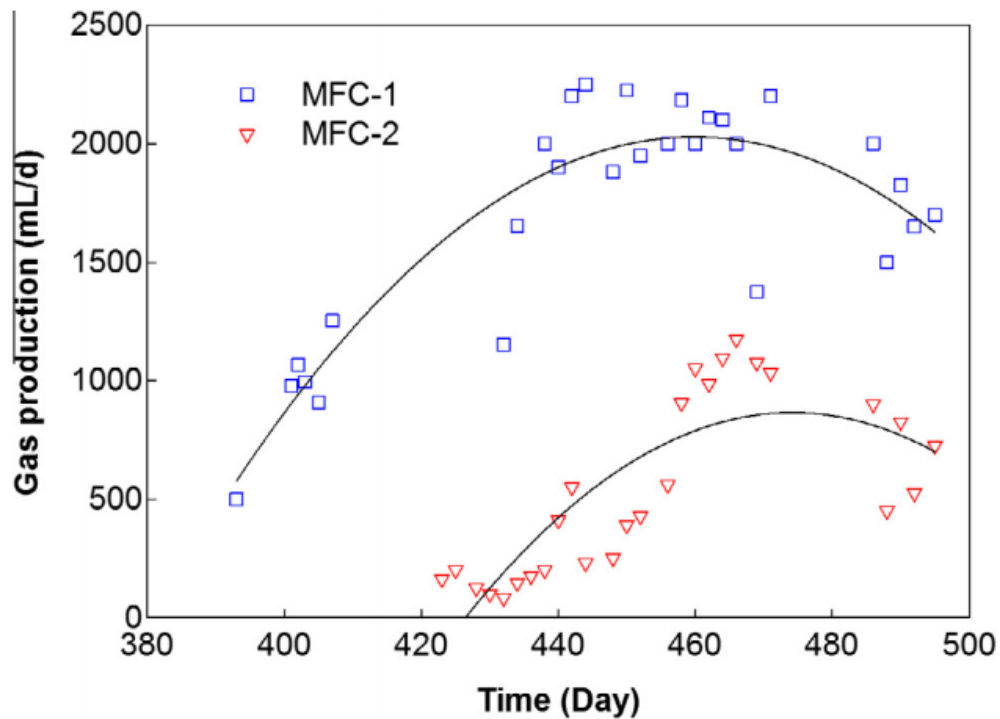


**Figure 6.4 Biogas production in the MFCs during Phase II.**

The energy in biogas was calculated assuming that the methane percentage is 65%, the heating value of methane is  $30 \text{ J/mL}$ , and the conversion efficiency of methane-to-electricity is 34%. We used biogas production of  $2000 \text{ mL/day}$  from MFC-1 and  $1000$

mL/day from MFC-2 for the calculation, and obtained the energy production from biogas as 21.49 kWh/m<sup>3</sup> (sum of 14.33 kWh/m<sup>3</sup> from MFC-1 and 7.16 kWh/m<sup>3</sup> from MFC-2). The results show that the electric energy from direct generation was only 8–15% of the energy from biogas. The total energy production (sum of electric energy and biogas energy) in the two-stage MFC system was 23.22 or 24.72 kWh/m<sup>3</sup>. The energy production in the anaerobic digesters at South Shore Water Reclamation Facility was estimated to be 10.73–38.06 kWh/m<sup>3</sup>. Therefore, the total energy production in the MFC system was comparable with that of anaerobic digesters, but direct electricity generation had a minor contribution (7–13%) to the total energy production.

**Table 6.3 Energy production (kWh/m<sup>3</sup>) from the two-stage MFC system in the Phase II and energy production from biogas at South Shore Water Reclamation Facility.**

MFC Energy	Two-stage MFC system		AD <sup>c</sup>
	Electric energy (Operation) <sup>a</sup>	Methane (Maximum) <sup>b</sup>	Methane
MFC-1	0.78	1.43	10.73-38.06
MFC-2	0.95	1.80	
Total	1.73	3.23	
Total energy (kWh/m <sup>3</sup> ) <sup>d</sup>	22.79	24.29	10.73-38.06

<sup>a</sup> Electricity generation from regular operation of the MFC system with external resistance of 20 Ω for both MFCs.

<sup>b</sup> Electric energy from the maximum power output obtained from polarization tests.

<sup>c</sup> The data of methane production were obtained from four anaerobic digesters at South Shore Water Reclamation Facility.

<sup>d</sup> The total energy is the sum of total electric energy (under one of the conditions) and total energy from methane gas.

Although the MFCs achieved good sludge reduction that is important to sludge treatment, energy production is a key parameter to evaluate whether MFC technology is suitable for treating primary sludge, because primary sludge is usually treated for energy recovery in

anaerobic digesters. Energy production in MFCs, including those treating sludge, has not been properly presented before. Most prior studies only showed power production, which is not an energy parameter. In addition, methane production has not been well monitored in the sludge-fed MFCs. In this study, we analyzed both electric energy and potential energy production from methane gas and presented a better picture of energy production in the sludge-fed MFCs. Although the total energy production in the two-stage MFC system was comparable to that of anaerobic digesters, we do not think MFCs are efficient energy producers from primary sludge at this moment. Our results show that direct production of electric energy has a minor contribution to the overall energy production, which is still dominated by methane gas. The low CEs also confirm that the majority of organic removal was not associated with direct electricity generation; therefore, the MFCs fed with the primary sludge acted mostly as the “modified” anaerobic digesters.

Diverting some organic compounds to direct electricity generation in an MFC could reduce biogas processing and conversion, resulting in some (potentially) economic benefits, but we also need to understand the challenges of MFC application. For example, MFCs generally have much more complex structures and higher capital cost than anaerobic digesters. The use of high surface-area electrodes and high-solid substrate like sludge can create problems such as reactor clogging. Unlike anaerobic digesters that can be constructed in a single reactor with a large volume, MFCs are expected to be built in small-scale modules to form an MFC assembly; a single MFC with a very large volume will have a larger distance between the anode and the cathode electrodes, thereby increasing the

internal resistance and decreasing electricity generation. With multiple small-scale MFC modules, the heating and feeding of the analytes will be very challenging.

Furthermore, there will be losses during harvesting the electricity from MFCs or other bioelectrochemical systems (Zhang and He, 2012), and the “useful” electricity will be less than what was presented here. Therefore, without significant advantages in energy production, MFCs may not be suitable for treating primary sludge; however, as stated earlier, MFCs could function as a post-treatment process to polish the supernatant of digested sludge. In that way, energy production is not a key factor to performance; instead, with satisfactory treatment performance and reduced energy consumption via anaerobic treatment, energy recovery will be an additional benefit.

#### **6.4 Conclusions**

A long-term investigation was conducted on the technical performance of MFCs used to treat sewage sludge. The MFCs satisfactorily reduced of both organics and suspend solids. The total energy production from primary sludge in the two-stage MFC system was comparable to that of anaerobic digesters; however, direct electricity generation had a minor contribution while energy from biogas still dominated the overall energy production. It will be very challenging to apply MFC technology to treat primary sludge; but MFCs may be used to polish the digested effluent from anaerobic digesters, offering potential benefits in energy savings compared with aerobic treatment.

## CHAPTER 7

### **An Effective Dipping Method for Coating Activated Carbon Catalyst on The Cathode Electrodes of Microbial Fuel Cells**

(This section has been published as: Ge, Z. and He, Z.\* (2015) An effective dipping method for coating activated carbon catalysts on the cathode electrodes of microbial fuel cells. **RSC Advances**. Vol 5, pp 36933-36937.)

#### **7.1 Introduction**

Microbial fuel cells (MFCs) offer a promising bioelectrochemical approach for energy-efficient water/wastewater treatment and bioenergy recovery. (Logan et al., 2006; Wang & Ren, 2013; Xiao et al., 2014) MFCs rely on electrochemically-active bacteria to oxidize organic matters and respire with an electrode as an electron acceptor. This oxidation process in the anode produces electrons and protons, both of which move towards the cathode where the electrons and protons are consumed in the reduction reaction with a terminal electron acceptor, such as oxygen. Although oxygen is readily available in a large quantity (in the air), the oxygen reduction reaction (ORR) requires a catalyst to overcome the high energy potential. Many types of catalysts have been studied, including the most commonly used platinum (Pt) and a variety of other materials such as gold, (Kargi & Eker, 2007) cobalt, (Zhao et al., 2006) lead, (Morris et al., 2007) iron, (Zhao et al., 2005) and activated carbon. (Deng et al., 2010; Dong et al., 2012; Rismani-Yazdi et al., 2008; Watson et al., 2013; Zhang et al., 2009; Zhang et al., 2013) In particular, activated carbon (AC) is very attractive as a cathode catalyst for MFCs, because of its low cost, a high specific surface area, and effective ORR catalysis; (Zhang et al., 2009) in addition, AC catalysts have been examined in MFCs for a long period of time and/or with actual wastewater, demonstrating its long-term stability. (Zhang et al., 2013; Zhang et al., 2011) These findings

suggest that AC can be used as an effective (in terms of both cost and performance) ORR catalyst for MFC application.

A widely used method for coating catalysts onto a cathode electrode is brushing, which applied the mixture of catalysts and a binding agent (e.g., Nafion or PTFE) to the surface of the electrode by using a brush (Cheng et al., 2006; Huang et al., 2010). The brushing method is relatively simple and straightforward; however, it leaves a non-homogenous distribution of binder/catalyst mixture on the electrode, and may also cause catalyst loss to the brush (via adsorption). To prepare a large area of electrode, the brushing method will require a significant amount of manual operation. Recently, a rolling method was developed to fabricate the cathode electrodes for MFCs (Dong et al., 2012). Unlike the brushing method, the rolling method omits carbon cloth and instead uses stainless steel mesh as a supporting material. It is possible to have mass production of cathode electrode by using the rolling method; however, it should be noted that the rolling method requires special equipment for operation and the produced electrodes have not been used as widely as the one produced by the brushing method (though the rolling method is receiving increasing attention and interests).

In this study, we have explored an alternative method for catalyst coating, the dipping method, which has been applied in fuel cell study (Zhang et al., 2004). To examine its effectiveness for MFC application, the dipping method, linked to the heat treatment, was studied with mixture of AC powder (catalyst) and polytetrafluoroethylene (PTFE, binding agent). The prepared electrodes were analyzed using electrochemical techniques and examined in two types of MFCs. The effects of dipping concentration and frequency were investigated. The dipping method was compared with the brushing method for catalyst

loading and electrode performance. It should be noted that the cathode electrode prepared by the dipping method is for the application of “wet cathode” as explained in the Experimental section, instead of “air cathode” that is for membrane-less MFCs.

## 7.2 Materials and Methods

To perform the dipping method, 100 mL ethanol was gradually transferred into an air-tight container (150 mL) with selected amount of AC powder (2, 4, 8, or 12 g). Meanwhile, gentle stirring was provided for several seconds to mix and disperse the AC powder. Finally, 2.5 mL of 60% PTFE solution was added with stirring to form the slurry for dipping. The liquid mixture was stored in a 150 mL air-tight container. Dipping duration was fixed to 2 s for each piece of carbon cloth with the same size of 4 cm × 1 cm. Carbon cloth (PANEX 30PW03 at a cost of \$44.4 m<sup>-2</sup>, Zoltek Corporation, St. Louis, MO, USA) was pretreated by acetone as described in a previous study.<sup>18</sup> After dipping, the carbon cloth was dried and heated at 350 °C for 30 min. For comparison, multiple cathode electrodes were coated with AC by using the brushing method described as previous study<sup>18</sup> with a design AC loading rate of 5 and 10 mg cm<sup>-2</sup> (the actual AC loading was determined experimentally). Electrochemical experiments were conducted as described in previous study in a 140 mL glass bottle with 130 mL of 50 mM PBS solution (2.65 g KH<sub>2</sub>PO<sub>4</sub> and 5.35 g K<sub>2</sub>HPO<sub>4</sub> per liter of tap water), where the cathode electrode served as a working electrode, a platinum mesh (002250 platinum gauze electrode 80 mesh, ALS Co., Ltd, Japan) served as a counter electrode, and an Ag/AgCl electrode (CH Instruments, Inc., Austin, TX, USA) functioned as a reference electrode. Air was pumped into the bottle for 30 min before each test to create O<sub>2</sub>-saturated condition. The electrode samples were submerged into 50 mM PBS

solution for 30 min before any electrochemical tests. Tafel plots (scan rate:  $1 \text{ mV s}^{-1}$ ) were carried out by a potentiostat (Reference 600, Gamry Instruments, Warminster, PA, USA).

Two types of MFCs were used for the experiments. First, a two-chamber MFC as described in previous study (Zhang et al., 2014) was used for examining electricity generation with the prepared cathode electrodes. The polarization tests were conducted by using the Gamry potentiostat (scan rate:  $0.2 \text{ mV s}^{-1}$ ). The anode electrode was a 5 cm carbon brush with titanium wire collector. Second, to further examine the performance of dipping cathode, a 15-cm long tubular MFC was setup and operated with a wet cathode, which was coated with AC on carbon cloth; the cathode was exposed to air and rinsed with PBS instead of being submerged into the catholyte (Zhang et al., 2013; Zhang et al., 2010). The catholyte concentration was 50 mM PBS. Both two-chamber and tubular MFCs were inoculated with digested sludge from a local wastewater treatment facility (Peppers Ferry Regional Wastewater Treatment Plant, Radford, VA), and operated in a batch mode with the anolyte containing per liter of tap water: sodium acetate, 2 g;  $\text{NH}_4\text{Cl}$ , 0.15 g;  $\text{NaCl}$ , 0.5 g;  $\text{MgSO}_4$ , 0.015 g;  $\text{CaCl}_2$ , 0.02 g;  $\text{KH}_2\text{PO}_4$ , 2.65 g;  $\text{K}_2\text{HPO}_4$ , 5.35 g; and trace element, 1 mL.<sup>22</sup> The voltage of the MFC (across  $100 \Omega$  in the two-chamber MFC or  $15 \Omega$  in the tubular MFC) was recorded by multimeter (Model 2700; Keithley Instruments, Inc., OH, USA) with 5 min interval.

### **7.3 Results and Discussion**

A commonly designed loading rate of AC by using the brushing method is about  $5 \text{ mg cm}^{-2,8}$  but the exact amount of the AC coated on carbon-base materials (e.g., carbon cloth)

is usually not quantified. By weighing the carbon cathode before and after coating, we found that the actual coated AC using the brushing method was  $1.46 \pm 0.55 \text{ mg cm}^{-2}$ , much lower than the designed loading of  $5 \text{ mg cm}^{-2}$ , indicating that about 70% of AC powder was not loaded onto carbon cloth. By increasing the design loading rate to  $10 \text{ mg cm}^{-2}$  (which means more AC would be applied by the brush), the coated AC reached  $2.45 \pm 0.71 \text{ mg cm}^{-2}$ , which still had over 70% loss. The actual loading rate by using the brushing method could vary depending on the brush used, exact procedure, and skills of the person who performs it. The loss of AC could be due to the use of painting tools (painting brush) whose bristles absorbed a large amount of carbon powder/PTFE mixture. Another possible reason could be due to binding capability of PTFE. A higher concentration of PTFE is able to enhance the attachment of carbon powder with less loss but it also decreases the performance for catalytic reaction. To keep the testing condition consistent, the amount of PTFE (60%) was fixed at 2.5 mL per 100 mL ethanol for dipping, which was equivalent to the dosage applied for the brushing method ( $6.67 \mu\text{L mg}^{-1} \text{ AC}$ ).

The dipping method, on the other hand, has created more uniform distribution of AC with less variance. The actual AC loading by using the dipping method could be increased in two ways, repeated dipping to create multiple layers of AC catalysts and increasing the initial AC concentration in the mixture. Fig. 7.1 shows that both approaches could effectively improve the AC loading on carbon cloth. For example, at an initial AC input of 4 g per 100 mL ethanol, the actual AC loading on carbon cloth was  $1.62 \pm 0.15$ ,  $3.09 \pm 0.21$ , and  $4.60 \pm 0.23 \text{ mg cm}^{-2}$  for dipping 1, 2, and 3 times, respectively. When dipping one time, the coated AC on carbon cloth was increased from  $0.56 \pm 0.23$  to  $5.00 \pm 0.88 \text{ mg}$

$\text{cm}^{-2}$  as the AC concentration was changed from 2 to 12 g per 100 mL ethanol. The concentration of 4 g per 100 mL ethanol had a same PTFE/AC ratio as that used in brushing method ( $6.67 \mu\text{L mg}^{-1}$ ), and it also resulted in a similar actual AC loading of  $1.62 \pm 0.15 \text{ mg cm}^{-2}$  (one time dipping) to that by the brushing method ( $1.46 \pm 0.59 \text{ mg cm}^{-2}$ ) but with obviously less fluctuation. Thus, it is reasonable to conclude that, comparing with the brushing method, the dipping method is better for controlling or adjusting the actual loading of AC on carbon cloth.

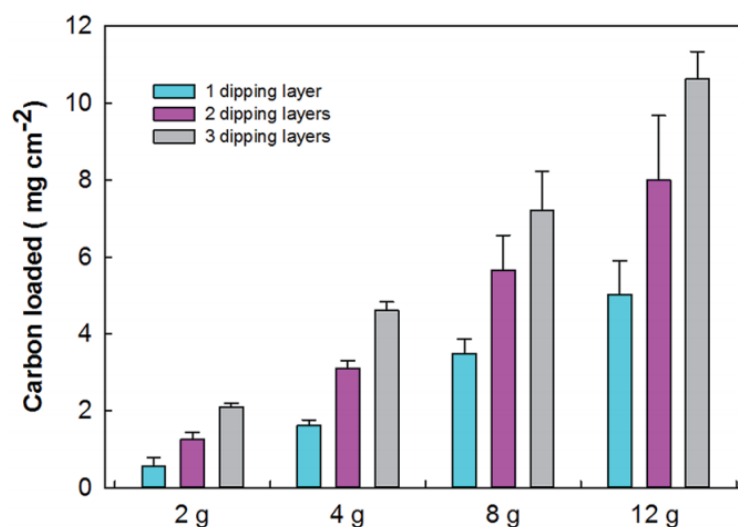


**Figure 7.1** The actual AC loading rates (Y axis) on the electrodes with different initial AC input of 2, 4, 8, and 12 g per 100 mL ethanol, and multiple dipping times.

To determine the relationship between carbon loading and electrochemical kinetics of ORR on the cathode electrode, Tafel plots were constructed to compare electrode reaction rate among the electrodes prepared in different ways. The mechanism of ORR with AC as a cathode catalyst has been investigated in the previous studies (Zhang et al., 2014); thus, it is not the focus of this study and the Tafel results were used to compare the variance based on the numerical magnitude. The ORR on the cathode followed Tafel behavior when

overpotential was larger than 0.118 V.<sup>19</sup> Tafel equation relationship described by eq. (1) (Faulkner, 2000) reveals that current ( $i$ ) can change linearly as overpotential ( $\eta$ ) and exchange current ( $i_0$ ) is involved in constant term as intercept when  $\eta$  is zero (equilibrium status).

$i_0$  can be calculated and compared for its proportional relationship to reaction kinetics, and a high current value indicates a faster reaction rate with a lower overpotential demand, and vice versa (Faulkner, 2000). Because AC was the only catalyst involved and the loading of PTFE was fixed at  $6.67 \mu\text{L mg}^{-1}$  AC, the main difference created by different dipping methods would be the amount of the coated AC and PTFE; the latter may affect the diffusion and adsorption of oxygen for ORR. As shown in Fig. 7.2A, the Tafel plots exhibited significant improvement by increasing the initial concentration of AC in the dipping mixture; the corresponding exchange current ( $i_0$ ) increased almost two-hundred times from  $4 \pm 3$  (2 g) to  $889 \pm 149 \mu\text{A}$  (12 g AC), confirming that increasing the initial AC concentration in the dipping mixture could promote electrode reaction effectively. Apparently, the carbon loading is crucial that the more AC powder is per unit area cathode, the more active sites are for ORR. However, despite increased loading, repeated dipping did not show the expected improved performance; for example, the improvement at the low concentration of 2 g AC in 100 mL ethanol was limited, and for a high initial AC concentration (12 g AC), the extra dipping did not benefit the electron transfer notably (as shown in Fig. 7.2B).

Table 7.1 shows the exchange current extracted from the Tafel plots. The results confirm that a high initial AC concentration could effectively improve the reaction rate with high exchange current, whereas repeated dipping had limited improvement at low AC concentrations. At the initial AC concentration of 8 or 12 g per 100 mL ethanol, the second dipping resulted in improved exchanged current, but one more dipping (third dipping) actually decreased exchange current. For comparison, coating by brushing method with an initial designed loading rate of  $5 \text{ mg cm}^{-2}$  resulted in an exchange current of  $54 \pm 34 \mu\text{A}$  but coating more AC had limited improvement ( $\sim 20\%$ ) when the designed loading rate was doubled ( $10 \text{ mg cm}^{-2}$ ).

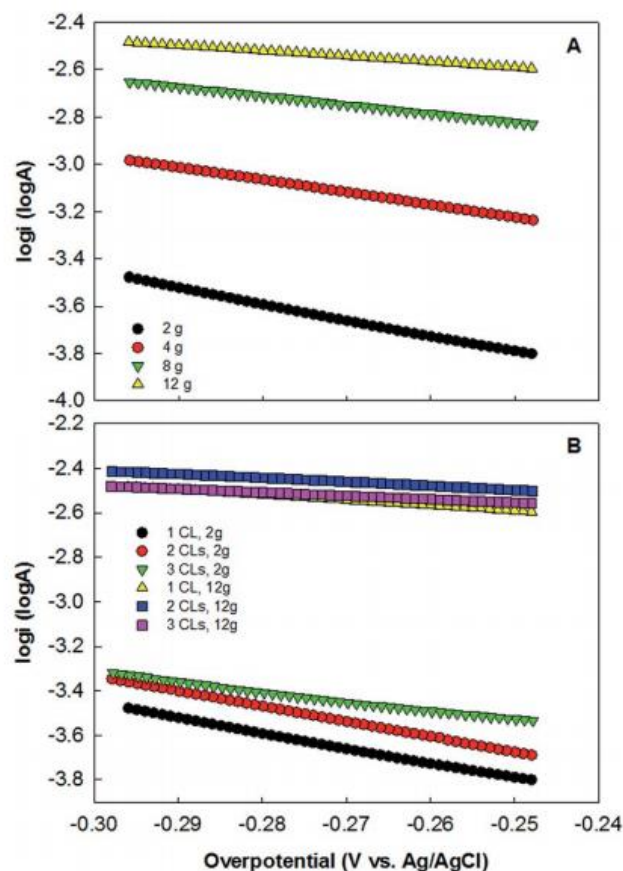


**Figure 7.2 Tafel plots of the cathode electrodes with different initial loading AC load (A) and different coating layers (CLs) by dipping (B).**

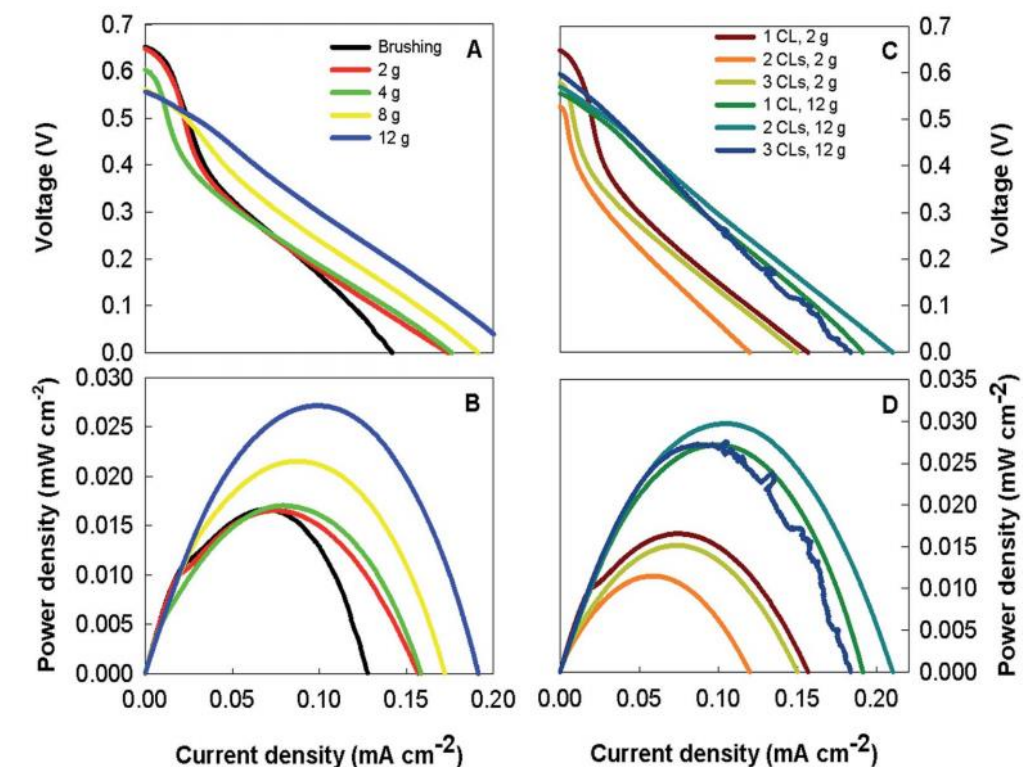


**Figure 7.3** Variation of voltage and power density with current density in the MFC containing cathode electrode prepared in different ways: (A and B) cathode electrode coated with different initial AC input and one prepared by the brushing method for comparison

**Table 7.1** Exchange current generated with the cathode electrodes with different initial AC input and multiple dipping times

Coating methods	Exchange current ( $\mu\text{A}$ )			
	2 <sup>[a]</sup>	4 <sup>[a]</sup>	8 <sup>[a]</sup>	12 <sup>[a]</sup>
One dipping	4 $\pm$ 3	57 $\pm$ 39	601 $\pm$ 424	889 $\pm$ 149
Twice dipping	4 $\pm$ 3	52 $\pm$ 5	669 $\pm$ 78	997 $\pm$ 96
Thrice dipping	4 $\pm$ 3	87 $\pm$ 81	142 $\pm$ 101	613 $\pm$ 230

[a] Initial concentration of AC in the dipping mixture (g per 100 mL ethanol).

The decreased exchange current with repeated dipping likely resulted from overly applied PTFE that could decrease active sites for catalytic reaction and oxygen transfer/adsorption. In addition, more AC layers would also decrease the diffusion of oxygen onto the surface of inner electrode material. Those results indicate that AC loading rate is not the only factor that controls the ORR; the distribution of AC particles and PTFE can also significantly influence ORR and thus current generation. Determining the optimal loading rate will be critical to avoiding overly applying catalysts and/or binding agent, thereby minimizing the amount of catalysts and associated cost.

The cathode electrodes prepared by the dipping method were further examined in a two-chamber H type MFC operated in a batch mode, as shown in Fig. 7.3. A cathode electrode prepared by the brushing method (designed AC loading rate of  $5 \text{ mg cm}^{-2}$ ) was used for comparison. Both power density and current production with the cathode prepared by one-time dipping (Fig. 7.3A and B) increased as the initial AC concentration changed from 2 g to 12 g per 100 mL ethanol, in a good agreement with the electrochemical tests. The electrodes prepared with low initial AC input (2 and 4 g) exhibited similar performance, but a higher AC input at 8 g increased the maximum power density by more than 25%, which was further improved by another 26% with 12 g. The minor difference in power output by the electrode between 2 and 4 g, despite doubled AC loading, indicates that the carbon amount might need to be maintained at a certain level for a linear improvement of electricity generation, but this needs further investigation. The cathode prepared by the

brushing method resulted in a similar maximum power density as that of the dipping with 4 g AC (which had similar actual AC loading as the one by the brushing), but current generation after the maximum power output became much lower, indicating a lower kinetic activity in the high current zone.

The MFC tests showed some difference in electricity by the repeated dipping (Fig. 7.3C and D). At the low initial AC input of 2 g, the single and triple dipping led to better performance than dipping twice, in terms of both maximum power density and current generation. At the high initial AC input of 12 g, the double dipping generated the highest power density. Those results are close to those of Tafel plots with some deviation. However, it is clear that multiple dipping does not always improve ORR and electricity generation, although AC loading is increased. This indication is important to minimizing the use of AC catalyst and the time of electrode preparation.

To further demonstrate the effectiveness of the dipping method, the prepared electrodes were examined in a tubular MFC that had a wet cathode as previously reported.<sup>8,20</sup> Three loading rates, prepared with three different initial AC inputs, 4, 12, and 18 g, were investigated. We could not conduct dipping with an initial AC input higher than 18 g, because carbon powder could not be well dispersed in the solvent. The initial AC input of 18 g could achieve actual loading of  $14.5 \text{ mg cm}^{-2}$  with one-time dipping. As shown in Fig. 7.4, both current density and total coulomb in the tubular MFC became higher at a higher AC loading rate. The current generation with the initial AC input of 18 g was more than twice that with 4 g, while the total charge production presented an approximate linear

increment as the AC loading increased in the 12 hour batch tests. Those results confirm that the dipping method can deliver effective cathode electrodes for application in MFCs.

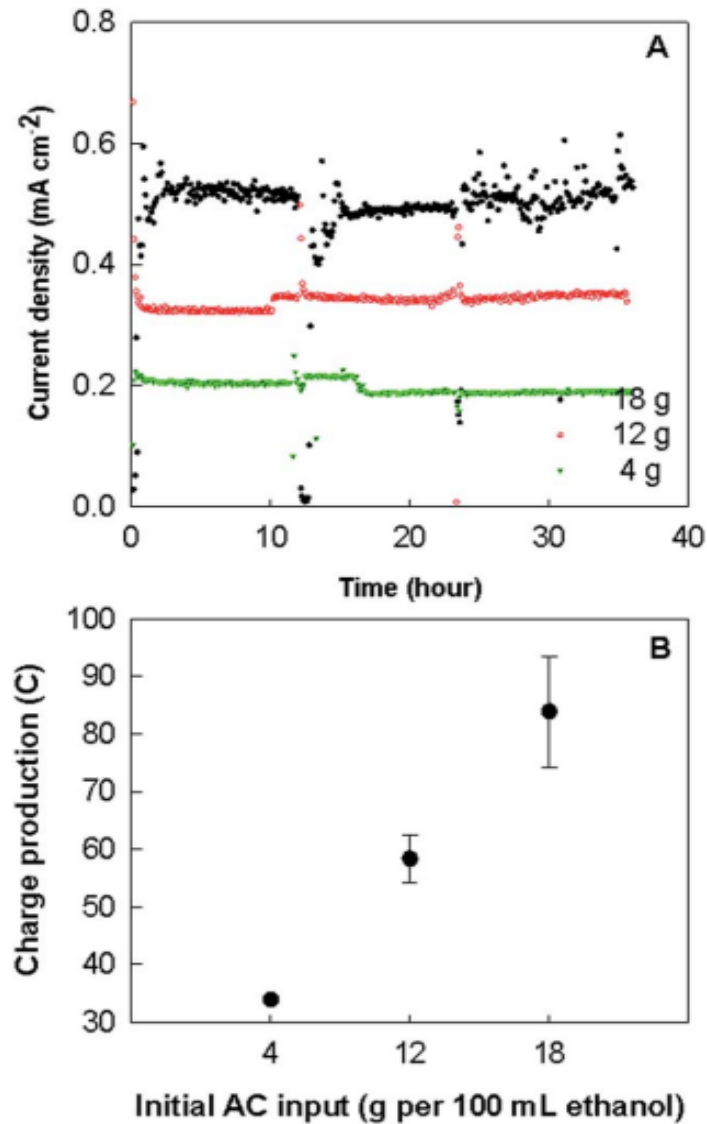


Figure 7.4 Current generation during batch operation (A) and the production of total charge in a batch (B) with different initial AC inputs in a tubular MFC.

## 7.4 Conclusions

To conclude, the dipping method is a promising alternative to coat AC catalysts on the MFC cathode electrode with several advantages. First, the dipping method is much easier and faster to be applied for preparing large-scale electrodes than the brushing method. By using the dipping method, a large piece of carbon cloth can be soaked in a tank containing the AC mixture for coating, while the brushing method requires intensive manpower or development of automatically-controlled brushes for coating. Second, the dipping method will have less loss of AC catalysts during the coating process, since the mixture can be reused with addition of AC catalysts, while the brushing method can result in significant loss of AC powder due to absorption, which also requires extensive cleaning after each coating. Third, the dipping method can deliver a more homogeneous surface coating, which is important to the use of the electrode material (avoiding the dead zones that are short of catalysts due to heterogeneous coating). Last, the dipping method can better control or manipulate the amount of catalyst coating on carbon cloth, which is critical to determining the precise amount of catalysts for large-scale MFC systems. Although some of the above advantages need to be verified with actual large-scale MFC development, the results in this work have demonstrated the effectiveness and promise of the dipping method, and encouraged further investigation.

## CHAPTER 8

### **Energy Extraction from A Large-Scale Microbial Fuel Cell System Treating Municipal Wastewater**

(This section has been published as: Ge, Z., Wu, L., Zhang, F. and He, Z.\* (2015) Energy extraction from a large-scale microbial fuel cell system treating municipal wastewater. **Journal of Power Sources**. Vol 297, pp 260-264.)

#### **8.1 Introduction**

Microbial fuel cells (MFCs) have been intensively studied as an emerging technology for sustainable wastewater treatment with bioenergy recovery. Through interaction between microorganisms and solid electron acceptors/donors, MFCs can directly generate electricity from oxidation of organic contaminants (Li et al., 2014; Logan et al., 2006). With advancement of this technology in various aspects such as microbiology and materials, a key question arises: how to extract and apply the produced energy. While most studies only report the performance of electricity generation in MFCs, some have investigated energy extraction and application to power small electronics such as wireless sensors (Donovan et al., 2008; Shantaram et al., 2005; Tender et al., 2008; Zhang et al., 2011) or charge batteries and capacitors (Erbay et al., 2014; Hatzell et al., 2013; Ieropoulos et al., 2013; Wang et al., 2015; Yang et al., 2012; Zhang & He, 2012). It has been realized that the difficulty of utilizing energy from MFCs is mainly due to the relatively low power and voltage output, which would limit efficiency and application for powering electronics by using commercial power conversion circuits.

Several customized energy harvesting systems have been developed for MFCs applications, such as the ones based on capacitor, charge pump, and boost converter, to increase the

output voltage and power output efficiency (Erbay et al., 2014; Hatzell et al., 2013; Nghia et al., 2015; Wang et al., 2015). However, due to the limitation of the size of single MFC and the number of MFCs in one system, the studies of energy harvesting are still focusing on small-load applications because the output energy is too small to drive electronics with high-power requirement. The electric devices such as DC motors (pumps) with a demand for amp-level current and high voltage input ( $>5$  V) are rarely investigated in the MFC studies except a recent study of a 90 L-scale MFC treating brewery wastewater that a 3-6 V DC pump was successfully used as to feed solution, powered by electricity generated by the MFC (Dong et al.). Clearly, more studies with the MFCs at large scale ( $>50$  L) treating actual wastewater should be conducted for further understanding of the system (and its limitation).

To extract energy from MFCs, maximum power point tracking (MPPT) could be an efficient strategy, which optimizes the power output by tracking the maximum power voltage (MPV) of power sources (e.g., MFCs). The purpose of MPPT is to reduce the power loss by matching the load impedance dynamically (Erbay et al., 2014), and it has been adapted with different algorithms such as perturb and observe (P&O) (Degrenne et al., 2012; Molognoni et al., 2014), partial open circuit voltage (OCV) tracking (Erbay et al., 2014; INSTRUMENTS, 2011), and multiunit optimization (Woodward et al., 2010) (Molognoni et al., 2014; Park & Ren, 2012) for MFCs applications. The system without MPPT could have 50% loss of output power while the voltage reversal might also be avoided by applying MPPT devices for each cell in one system (Boghani et al., 2014; Woodward et al., 2010).

Although multiple high-efficiency energy harvesting devices have been developed for single MFC with low voltage input, they have not been well investigated for an MFC system consisting of multiple modules at a large scale treating actual wastewater, and it is not clear whether one EHS per MFC module would work in a multiple-module MFC system, associated energy loss and maintenance/operation issues. In addition, most of the prior studies were based on bench-scale systems treating synthetic organic solution, or sediment-type MFCs (Xu et al., 2015), and very few of them had MFC systems treating actual wastewater and/or at a large scale (e.g., > 50 L). In this study, energy production and conversion efficiency from a large-scale MFC system treating actual municipal wastewater (installed in a local wastewater treatment plant) was evaluated through parallel and serial electrical connection of 48 MFC modules (total anode volume of ~ 100 L) by using a commercially available device TI BQ 25504 with MPPT using a partial OCV method. Because the efficiency of an EHS may vary as the input of voltage and current fluctuates due to the changes of operation and environmental conditions, it is necessary to examine the final power output, MPPT function, and conversion efficiency when actual wastewater is used as a substrate and multiple MFC modules are involved in one system. The performance of energy extraction from multiple connections with various voltage input ranging from 0.8 to 2.4 V (OCV) were examined as well to determine the optimized electrical connection of MFCs for energy conversion. It should be noted that the present paper focuses on energy extraction with brief introduction of the performance of this MFC system, and its long-term treatment performance will be reported in a separate publication.

## 8.2 Materials and Methods

### 8.2.1 The MFC system

The MFC system consisted of 96 2-L tubular MFCs constructed by using the method described in a previous study (Zhang et al., 2013), except that the cathode catalyst was nitrogen-doped activated carbon prepared by using urea as a nitrogen source. The 96 MFCs were placed as 12 x 8 array with 12 MFCs in each row and 8 rows in total (R1-8) (Fig. D1). The 8 rows were divided into four groups, with 2 rows in each group that had 24 MFCs hydraulically connected through plug-flow feeding. However, only 48 cells (four rows, R1, 3, 5, and 7) were used for this study. The MFC system was started by feeding the effluent from a primary clarifier (Peppers Ferry wastewater treatment plant, Radford, VA, USA) continuously at a hydraulic retention time (HRT) of 6 h. The anode effluent was collected in a 100-L rectangular tank placed under the MFC system and then pumped to the top of the cell array to wet the cathode. When the performance of the MFC system became stable, the HRT was adjusted to 18 h including 12 h for the MFCs and 6 h for the collection tank. For electricity connection, the 12 MFCs in the same row were connected in parallel with an external circuit across a resistor of 2.2  $\Omega$ , and then, R1, R3, R5, R7 were connected in serial (R1357) while R2, R4, R6, R8 were connected in serial (R2468), both of which had 15  $\Omega$  resistor as external load. The reason why the adjacent rows were not connected in serial was to avoid short circuit connection.

### 8.2.2 Electronic connections and energy harvesting device

Four rows of the MFCs (R1, 3, 5, and 7) were used in this study and 4 types of serial connections (S1-4) were examined based on the number of the MFC rows in connection

(Fig. D2). S1 had only 1 row as a power source and S4 had all 4 rows connected in serial. S2 (R3 and R7) and S3 (R3, R5, and R7) were the connection with 2 and 3 rows, respectively. To extract electric energy from the MFCs, BQ25504 battery management evaluation module (EVM) board (TI Instruments, TX, USA) was used and modified with a MPPT ratio of 0.5, because the ratio of MPV to OCV is close to a constant (0.5 in most cases) for a functioning MFC system (Fig. 8.1 and S8.3). The overvoltage was set at 5 V so that the circuit would stop when the output voltage reached the value (INSTRUMENTS, 2011). Two serial-connected 5-F ultracapacitors (Maxwell, 2.7V) were used as energy storage media for charging and discharging tests. Fig. D2 shows the schematic of the circuit connection with BQ 25504 EVM and ultracapacitors.

### 8.2.3 Measurement and analysis

The voltage and current of the MFC output and the PMS output was recorded every 10 sec by a digital multimeter (2700, Keithley Instruments, Inc., Cleveland, OH, USA). Polarization tests were conducted using a potentiostat (Reference 600, Gamry Instruments, Warminster, PA, USA) at a scan rate of  $1 \text{ mV s}^{-1}$ . The concentration of chemical oxygen demand (COD) was measured using a colorimeter according to the manufacturer's instructions (Hach Company, Loveland, CO, USA). Total suspended solids (TSS) was measured using standard methods (L.S. Clesceri, 1998). The power was calculated by eq. (8.1):

$$P = VI \tag{8.1}$$

where P is power (W), V is voltage (V), and I is current (A). The conversion efficiency of BQ 25504 was calculated based on eq. (8.2):

$$\eta = P_{MFC}/P_{BQ} \quad (8.2)$$

where  $\eta$  is efficiency (%),  $P_{MFC}$  and  $P_{BQ}$  are power output of MFC and BQ 25504, respectively, based on eq. (8.1).

## 8.3 Results and Discussion

### 8.3.1 Performance of the MFC system

The performance of the MFC system was briefly summarized in Table 8.1. The system effectively removed more than 75% organics and 80% solid content. The current generation during regular operation from the S4 connection of the R1357 ranged from 75 to 93 mA with a power output between 84 and 130 mW. Polarization curves with four types of connection are shown in Fig. 8.1. Among the single row of the MFCs, the R1 produced a maximum power of ~17 mW with a short-circuit current of ~110 mA, lower than that of the R3, R5 and R7 (55, 50, and 65 mW, Fig. D3). When two rows of the MFCs were connected as the S2 (containing R5 and R7), the power output was improved 40% from the S1 (R5 only). When more rows of the MFCs connected to the circuit (S3 and S4), the OCV was increased from 1.6 to 2.4 V but the power was only improved by 10%; the performance of the S3 was even better than the S4. The voltage reversal was not observed as reported from other studies on single MFCs (An et al., 2015; Boghani et al., 2014; Oh & Logan, 2007). It seems that the power output of serial connection of multiple MFC rows was affected by the limitation of the weakest current production in each row. In addition, the large difference between the R1 and the other three rows could result in little improvement in the S4 connection.

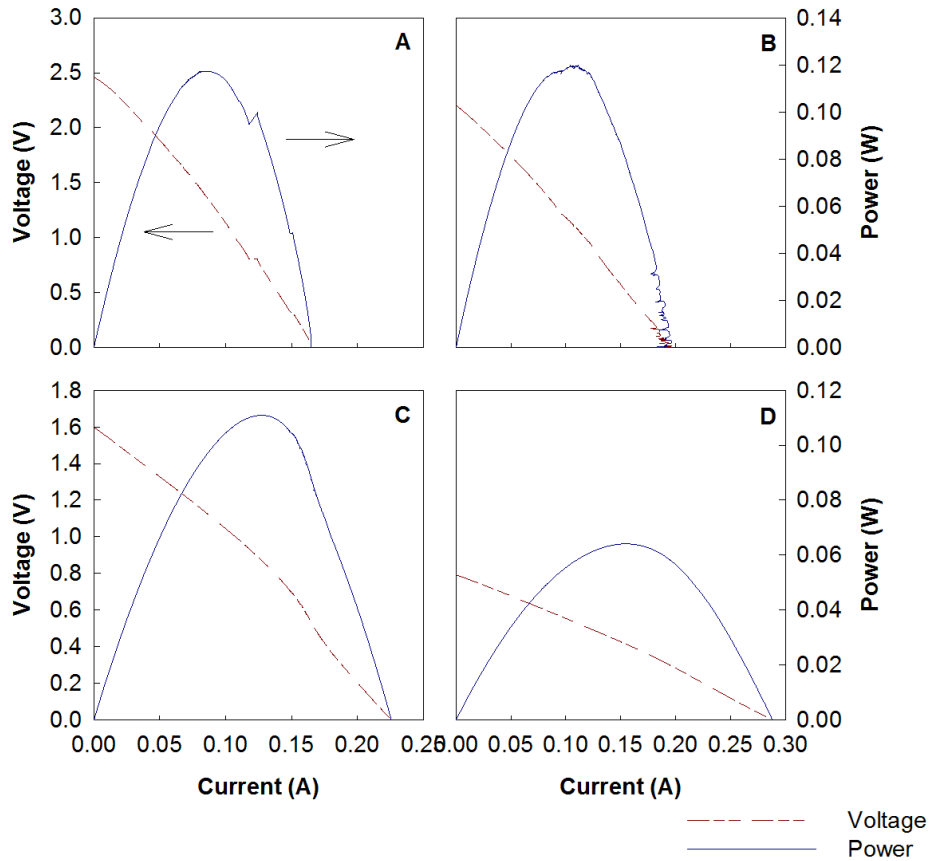


**Figure 8.1 Polarization curves of the MFCs with four types of serial connection: (A) S4 (R1357), (B) S3 (R 357), (C) S2 (R57), and (D) S1 (R5).**

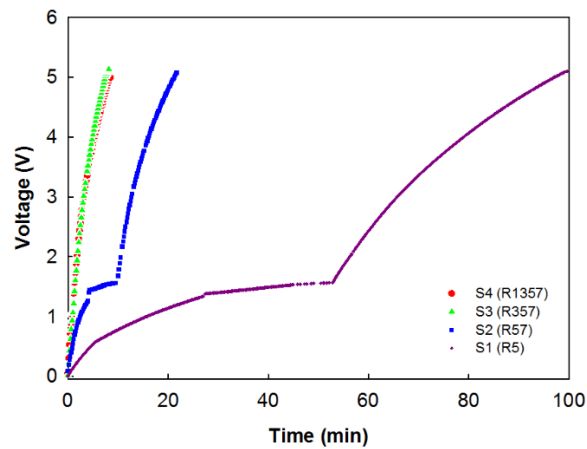
### 8.3.2 Energy extraction and conversion efficiency by using BQ 25504

BQ 25504 was applied to extract energy from the MFC system under four types of connection and to charge the ultracapacitors with charging kinetics shown in Fig. 8.2. It is obvious that more MFC modules could accelerate the charging process. It took almost 100 min to charge the 5-F ultracapacitors to 5 V with the S1 connection, while the S3 and the S4 connection achieved the same voltage in 8 min. The S3 exhibited better performance than the S4, likely due to the limitation of the R1 on current and voltage (the S3 did not

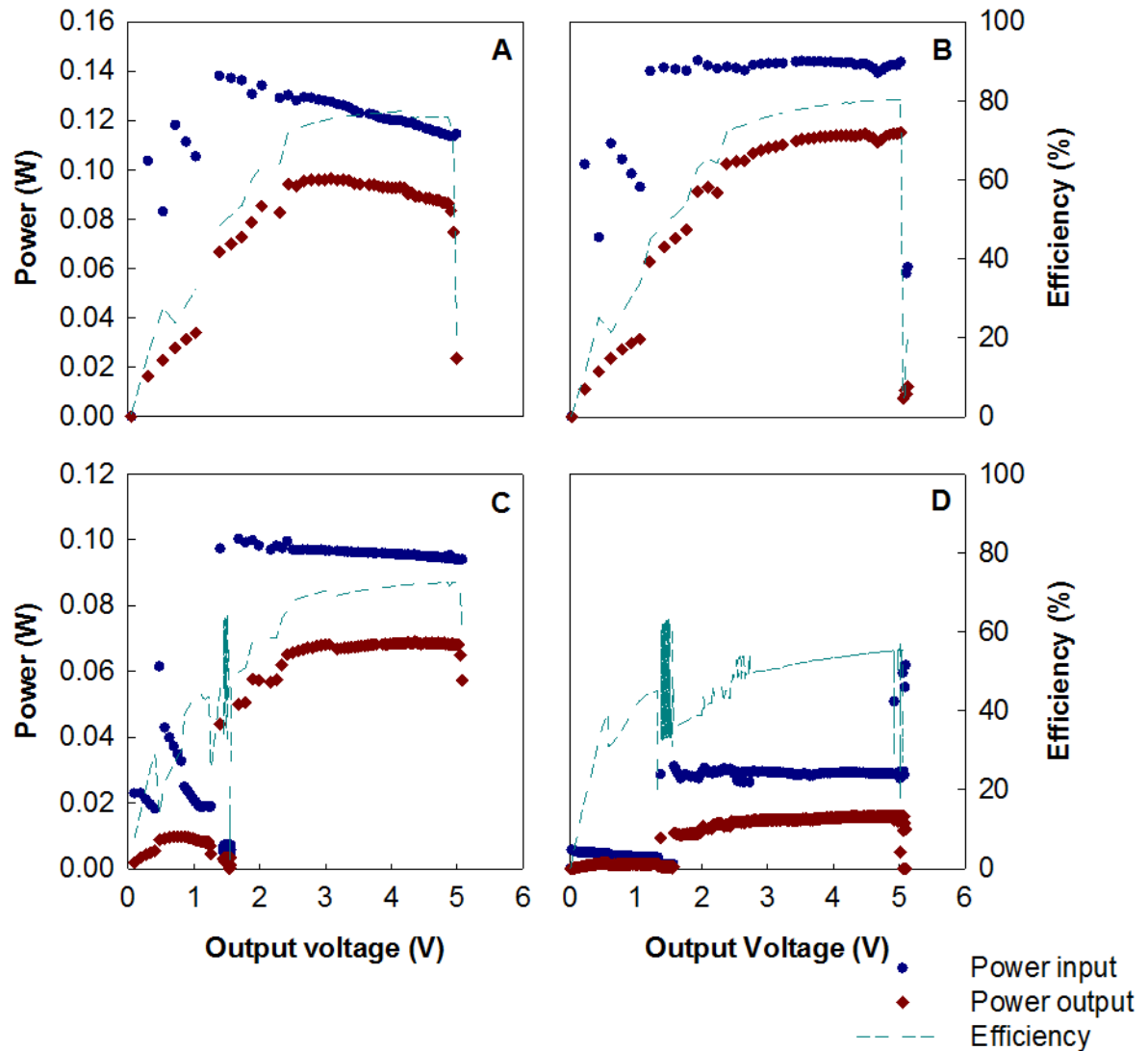
contain the R1). As more MFC modules increased the power output (which was the power input of BQ 25504), the “cold-start” period was significantly shortened from 52 min (S1) to 1 min (S3). The MPPT did not function until the voltage reached ~1.6 V, which was the end point of the warm-up period for self-starting when the input voltage was higher than 300 mV (Texas Instruments, 2011). Therefore, the S1 and the S2 may not have advantage for charging a depleted energy storage element because of a long pre-charging period and a slow charging rate.

**Table 8.1. Performance of the MFC system (four groups in serial connection) in contaminants removal and current production.**

Parameters	Influent	Effluent
TCOD (mg L <sup>-1</sup> )	156 ± 42	33 ± 15
SCOD (mg L <sup>-1</sup> )	67 ± 26	27 ± 8
TSS (mg L <sup>-1</sup> )	94 ± 61	14 ± 13
Current production (mA)	75-93	
Power output (mW)	84-130	



**Figure 8.2 Charging profiles of the ultracapacitors by the MFCs with four types of serial connection using BQ 25504.**



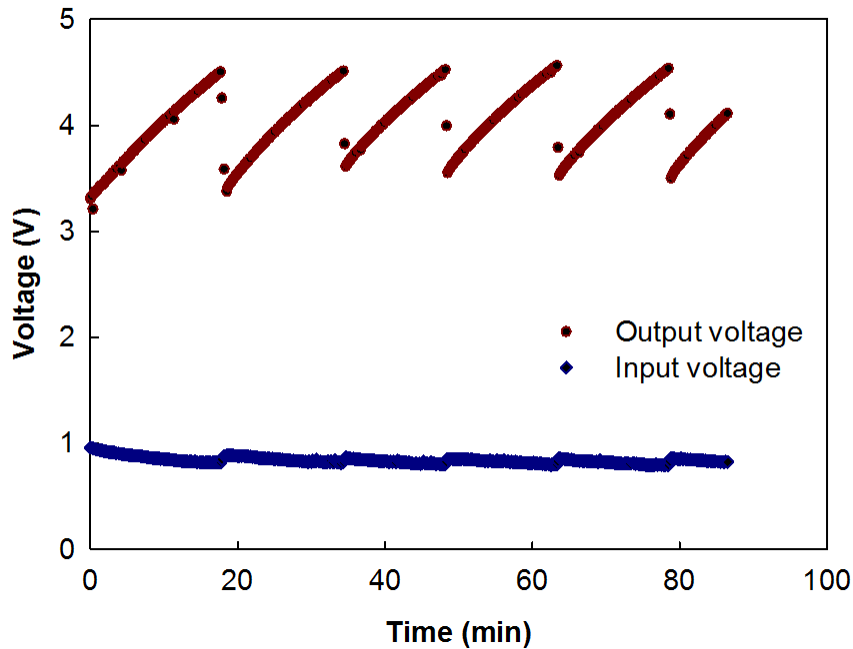
**Figure 8.3** The efficiency of the BQ25504 with different voltage input under four types of connection: (A) S4 (R1357), (B) S3 (R 357), (C) S2 (R57), and (D) S1 (R5).

Fig. 8.3 shows the power output from BQ 25504 and its conversion efficiency applied for different types of serial connection. The S1 (containing only R5) supplied ~30 mW when the MPPT functioned and about 55% power was transferred to charge the ultracapacitors. The S2 (R5 and R7) produced 1.6 V OCV and ~100 mW power with much higher

efficiency of ~72% in BQ 25504. It was expected that BQ 25504 would be more efficient with a higher input voltage from the S2, not only because of the higher conversion efficiency but also due to the better capability to extract energy from the MFCs with higher power input to BQ 25504. The power production of the S2 was very close to the MPP obtained from the polarization curve, which was ~110 mW and about 9% lower than the total power production of R5 and R7 (Fig. 8.1C and Fig. D3). The S3 (R3, R5, and R7) generated an even higher power input of ~140 mW, which is about 12% lower than the sum of maximum power output from group R3, R5, and R7 (Fig. D3), but 17% higher than that of the S4 (~120 mW). The conversion efficiency with the S3 was over 80%, which is comparable with many other customized converters (McBride et al., 2006; Wang et al., 2012a; Wang et al., 2012b; Zhang & He, 2012). Higher conversion efficiency of BQ 25504 with the S2 and the S3 indicates that a weak power source (e.g., R1 in this study) could negatively affect the power transfer. In general, BQ 25504 has promoted higher power output at a point close the MPP of the MFCs but could not reduce the negative impact from the weak power source. Therefore, it is critical to cautiously select (grouped) MFCs with similar electrochemical performance as power source when they are connected in serial, and there are many non-global factors causing the variance of power output from the single MFC such as bioactivity, difference in reactor manufacturing, distribution and gradient of substrate concentration, etc.

### 8.3.3 Charging and discharging

Because the S3 (R357) exhibited the best performance, this connection was examined with the 25 F ultracapacitors for charging/discharging test. The undervoltage and overvoltage for charging was set as 3.5 and 4.5 V, respectively, according to the working voltage of a



**Figure 8.4 Charging and discharging of the ultracapacitors by the MFC system (S3 connection) and BQ25504.**

DC motor (3-5V). As shown in Fig. 8.4, when the voltage of the ultracapacitors reached 4.5 V, it was discharged by powering the motor and when the voltage was lower than 3.5 V, they were disconnected from the motor and charged by the MFCs until the voltage was 4.5 V. It took ~15 min for the MFC system (S3) to charge the ultracapacitor from 3.5 to 4.5 V during each cycle while the input voltage was maintained at ~1 V, which was close to the half value of OCV as shown in Fig. 8.1B. BQ 25504 worked well for the MFCs with

good conversion efficiency and flexible power management function to charge capacitors. In addition, because the voltage increment by connecting 3 or more MFCs may become less efficient (Oh & Logan, 2007), BQ 25504 can be used to stabilize the output voltage level with 3 or less rows of MFCs connected in serial. Although BQ 25504 EVM is designed specifically for DC sources like solar and thermal electric generators and the efficiency can be over 90% as reported by manufacturer, the large variation in current and voltage from the MFCs would result in unsteady MPP that causes the MPPT to function imperfectly with MFCs. It is possible to use this approach to boost output voltage to a higher level like 12 V by a secondary converter system rather than connect 20 or more (grouped) MFCs to minimize the negative effects from weak power source in serial connection.

#### **8.4 Conclusions**

Energy can be effectively extracted from a large-scale MFC system treating municipal wastewater. The power was efficiently converted through BQ 25504 to charge ultracapacitors and run a DC motor. The use of the MPPT promoted energy extraction from the MFCs. The presence of weakly performed MFC modules could negatively impact the performance of the whole MFC system and thus energy extraction/transfer. The successful extraction of the energy from such a large-scale MFC system operated with actual wastewater will encourage further development of this technology for sustainable and energy efficient wastewater treatment. Future investigation will focus on application of the produced energy to offset energy consumption by the MFC system.

## CHAPTER 9

### Perspectives

Through the studies included in this dissertation, MFCs was proofed to be effective for removing organic contaminants and solid content from domestic wastewater. However, MFCs cannot be used as a standalone process that post treatment is necessary for further COD reduction and nitrification. The residual organic content could be higher than discharge limit under 12 h HRT. The increase of HRT may reduce the final effluent COD but low COD concentration and high concentration gradient along the reactor are not beneficial for electricity energy collection. From the results of this dissertation, ~100 mg/L COD could be a set point for effluent COD from anode chamber that either aerobic treatment or anaerobic ammonia oxidation (ANAMMOX) could be alternative polish treatment after MFCs to achieve ammonia removal. However, the significant benefit from MFCs system could be a very low demand of sludge treatment and disposal. Throughout over 300-day operation, little sludge were wasted from the system, which means the general sludge handling facilities used in activated sludge based wastewater treatment plant could be significant simplified with much smaller digester and dewatering equipment. In addition, the future work could focus on treating domestic wastewater without primary clarification that primary sludge may not be by-product appeared in MFCs based treatment process.

For energy recovery, the commercialized DC-DC converter such as BQ 25504 was evaluated and demonstrated to be efficient to extract and stabilize the electricity energy

output from multiple MFC units. Therefore, the strategy of using converter would be appropriate for large-scale MFCs with multiple cells instead of connecting too many MFCs in serial to rise voltage output. The serial connection must be operated cautiously because it is the major reason for most voltage reversal cases reported in MFCs studies due to the variation in MFCs. The weakest MFC in one connection could limit the current production and would be overdraw due to the limitation of mass transfer or electrode reaction. When certain MFC cannot generate enough electron to maintain the current flow in the whole circuit, this cell would transform from power generator to energy consumer. It was found that three serial-connected units could be the optimized connection to provide enough voltage input for DC-DC converter with less risk of reversing the electrode potential. On the other side, although parallel connection uniform the voltage output from MFCs and increase the current capacity to avoid voltage reversal to some extent, the MFC units in one connection should be identical to minimize the energy loss from uniformization, which also means the MFCs selected for one parallel connection should be operated similarly.

It should be noticed that there are still several obstacles prevent MFCs from practical applications. Till now, there is no commercialized-scale system developed for wastewater treatment. Even though multiple configurations have been designed for scaling-up efforts, little progress has been achieved due to the complexity of “fuel cell” concept. Besides, the capital costs of MFCs system would be another concern for practical application that catalyst, electrodes, separators, and wires for electrical connection are all specialized in MFCs comparing with conventional treatment equipment.

## Reference

- Achilli, A., Cath, T., Childress, A. 2010. Selection of inorganic-based draw solutions for forward osmosis applications. *Journal of Membrane Science*, **364**(1-2), 233-241.
- Achilli, A., Cath, T.Y., Marchand, E.A., Childress, A.E. 2009. The forward osmosis membrane bioreactor: A low fouling alternative to MBR processes. *Desalination*, **239**, 10-21.
- Aelterman, P., Rabaey, K., Pham, H.T., Boon, N., Verstraete, W. 2006. Continuous Electricity Generation at High Voltages and Currents Using Stacked Microbial Fuel Cells. *Environmental Science & Technology*, **40**(10), 3388-3394.
- An, J., Kim, B., Chang, I.S., Lee, H.-S. 2015. Shift of voltage reversal in stacked microbial fuel cells. *Journal of Power Sources*, **278**(0), 534-539.
- Anderson, J. 2003. The environmental benefits of water recycling and reuse. *Water Science and Technology: Water Supply*, **3**(4), 1-10.
- Angenent, L.T., Karim, K., Al-Dahhan, M.H., Wrenn, B.A., Domiguez-Espinosa, R. 2004. Production of bioenergy and biochemicals from industrial and agricultural wastewater. *Trends in Biotechnology*, **22**(9), 477-485.
- Angenent, L.T., Sung, S. 2001. Development of anaerobic migrating blanket reactor (AMBR), a novel anaerobic treatment system. *Water Research*, **35**(7), 1739-1747.
- Appels, L., Baeyens, J., Degrève, J., Dewil, R. 2008. Principles and potential of the anaerobic digestion of waste-activated sludge. *Progress in Energy and Combustion Science*, **34**(6), 755-781.
- Arends, J.B.A., Verstraete, W. 2012. 100 years of microbial electricity production: three concepts for the future. *Microbial Biotechnology*, **5**(3), 333-346.
- Boghani, H.C., Papaharalabos, G., Michie, I., Fradler, K.R., Dinsdale, R.M., Guwy, A.J., Ieropoulos, I., Greenman, J., Premier, G.C. 2014. Controlling for peak power extraction from microbial fuel cells can increase stack voltage and avoid cell reversal. *Journal of Power Sources*, **269**(0), 363-369.
- Brindle, K., Stephenson, T. 1996. The application of membrane biological reactors for the treatment of wastewaters. *Biotechnology and Bioengineering*, **49**(6), 601-610.
- Cao, X., Huang, X., Liang, P., Xiao, K., Zhou, Y., Zhang, X., Logan, B.E. 2009. A new method for water desalination using microbial desalination cells. *Environmental Science & Technology*, **43**(18), 7148-52.
- Cao, Y., Pawłowski, A. 2012. Sewage sludge-to-energy approaches based on anaerobic digestion and pyrolysis: Brief overview and energy efficiency assessment. *Renewable and Sustainable Energy Reviews*, **16**(3), 1657-1665.
- Cath, T.Y., Childress, A.E., Elimelech, M. 2006. Forward osmosis: principles, applications, and recent developments. *Journal of Membrane Science* **281**, 70-87.
- Cath, T.Y., Nathan T. Hancock, Carl D. Lundin, Christiane Hoppe-Jones, Drewes, J.E. 2010. A multi-barrier osmotic dilution process for simultaneous desalination and purification of impaired water. *Journal of Membrane Science*, **362**, 417-426.
- Çetinkaya, A.Y., Köroğlu, E.O., Demir, N.M., Baysoy, D.Y., Özkaya, B., Çakmakçı, M. 2015. Electricity production by a microbial fuel cell fueled by brewery wastewater and the factors in its membrane deterioration. *Chinese Journal of Catalysis*, **36**(7), 1068-1076.

- Cheng, S., Liu, H., Logan, B.E. 2006. Increased performance of single-chamber microbial fuel cells using an improved cathode structure. *Electrochemistry Communications*, **8**(3), 489-494.
- Choi, J., Ahn, Y. 2013. Continuous electricity generation in stacked air cathode microbial fuel cell treating domestic wastewater. *Journal of Environmental Management*, **130**, 146-152.
- Chung, T.-S., Zhang, S., Wang, K.Y., Su, J., Ling, M.M. 2011. Forward osmosis processes: yesterday, today and tomorrow *Desalination*, **doi:10.1016/j.desal.2010.12.019**.
- Chung, T.-S., Zhang, S., Wang, K.Y., Su, J., Ling, M.M. 2012. Forward osmosis processes: yesterday, today and tomorrow *Desalination*, **287**, 78–81.
- Clauwaert, P., Rabaey, K., Aelterman, P., Schampelaire, L.D., Pham, T.H., Boeckx, P., Boon, N., Verstraete, W. 2007. Biological denitrification in microbial fuel cells. *Environmental Science and Technology*, **41**(9), 3354-3360.
- Clesceri, L.S., Greenberg, A.E., Eaton, A.D. 1998. *Standard Methods for the Examination of Water and Wastewater*. 20th ed. American Public Health Association, Washington, DC.
- Cord-Ruwisch, R., Law, Y., Cheng, K.Y. 2011. Ammonium as a sustainable proton shuttle in bioelectrochemical systems. *Bioresource Technology*, **102**(20), 9691-9696
- Degrenne, N., Buret, F., Allard, B., Bevilacqua, P. 2012. Electrical energy generation from a large number of microbial fuel cells operating at maximum power point electrical load. *Journal of Power Sources*, **205**(0), 188-193.
- Deng, Q., Li, X., Zuo, J., Ling, A., Logan, B.E. 2010. Power generation using an activated carbon fiber felt cathode in an upflow microbial fuel cell. *Journal of Power Sources*, **195**(4), 1130-1135.
- Dong, H., Yu, H., Wang, X., Zhou, Q., Feng, J. 2012. A novel structure of scalable air-cathode without Nafion and Pt by rolling activated carbon and PTFE as catalyst layer in microbial fuel cells. *Water Research*, **46**(17), 5777-5787.
- Dong, Y., Qu, Y., He, W., Du, Y., Liu, J., Han, X., Feng, Y. 2015. A 90-liter stackable baffled microbial fuel cell for brewery wastewater treatment based on energy self-sufficient mode. *Bioresource Technology*, **195**, 66-72.
- Dong, Y., Qu, Y., He, W., Du, Y., Liu, J., Han, X., Feng, Y. A 90-liter stackable baffled microbial fuel cell for brewery wastewater treatment based on energy self-sufficient mode. *Bioresource Technology*(0).
- Donovan, C., Dewan, A., Heo, D., Beyenal, H. 2008. Batteryless, Wireless Sensor Powered by a Sediment Microbial Fuel Cell. *Environmental Science & Technology*, **42**(22), 8591-8596.
- Douglas C. Montgomery, G.C.R. 2011. *Applied Statistics and Probability for Engineers*. 5th ed. John Wiley & Sons, Inc.
- Erbay, C., Carreon-Bautista, S., Sanchez-Sinencio, E., Han, A. 2014. High Performance Monolithic Power Management System with Dynamic Maximum Power Point Tracking for Microbial Fuel Cells. *Environmental Science & Technology*, **48**(23), 13992-13999.

- Fang, Z., Song, H.-l., Cang, N., Li, X.-n. 2015. Electricity production from Azo dye wastewater using a microbial fuel cell coupled constructed wetland operating under different operating conditions. *Biosensors and Bioelectronics*, **68**, 135-141.
- Faulkner, A.J.B.a.L.R. 2000. *Electrochemical Methods: Fundamentals and Applications*. 2nd ed. Wiley.
- Feng, Y., He, W., Liu, J., Wang, X., Qu, Y., Ren, N. 2014a. A horizontal plug flow and stackable pilot microbial fuel cell for municipal wastewater treatment. *Bioresour Technol*, **156**(0), 132-138.
- Feng, Y., He, W., Liu, J., Wang, X., Qu, Y., Ren, N. 2014b. A horizontal plug flow and stackable pilot microbial fuel cell for municipal wastewater treatment. *Bioresour Technol*, **156**, 132-138.
- Gander, M., Jefferson, B., Judd, S. 2000. Aerobic MBRs for domestic wastewater treatment: a review with cost considerations. *Separation and Purification Technology*, **18**, 119–130.
- Gao, D., Peng, Y., Li, B., Liang, H. 2009. Shortcut nitrification-denitrification by real-time control strategies. *Bioresour Technol*, **100**(7), 2298-300.
- Ge, Z., He, Z. 2012. Effects of draw solutions and membrane conditions on electricity generation and water flux in osmotic microbial fuel cells. *Bioresour Technol*, **109**, 70-76.
- Ge, Z., Li, J., Xiao, L., Tong, Y., He, Z. 2013a. Recovery of Electrical Energy in Microbial Fuel Cells. *Environmental Science & Technology Letters*, **1**(2), 137-141.
- Ge, Z., Ping, Q., He, Z. 2013b. Hollow-fiber membrane bioelectrochemical reactor for domestic wastewater treatment. *Journal of Chemical Technology & Biotechnology*, DOI: 10.1002/jctb.4009.
- Ge, Z., Ping, Q., Xiao, L., He, Z. 2013c. Reducing effluent discharge and recovering bioenergy in an osmotic microbial fuel cell treating domestic wastewater. *Desalination*, **312**, 52–59.
- Ge, Z., Wu, L., Zhang, F., He, Z. 2015. Energy extraction from a large-scale microbial fuel cell system treating municipal wastewater. *Journal of Power Sources*, **297**, 260-264.
- Ge, Z., Zhang, F., Grimaud, J., Hurst, J., He, Z. 2013d. Long-term investigation of microbial fuel cells treating primary sludge or digested sludge. *Bioresour Technol*, **136**, 509-514.
- Ghyoot, W., Verstraete, W. 1997. Anaerobic digestion of primary sludge from chemical pre-precipitation. *Water Science and Technology*, **36**, 357–365.
- Gil, G.C., Chang, I.S., Kim, B.H., Kim, M., Jang, J.K., Park, H.S., Kim, H.J. 2003. Operational parameters affecting the performance of a mediator-less microbial fuel cell. *Biosens. Bioelectron.*, **18**(4), 327-334.
- Halalshah, M., Kassab, G., Yazajeen, H., Qumsieh, S., Field, J. 2011. Effect of increasing the surface area of primary sludge on anaerobic digestion at low temperature. *Bioresour Technol*, **102**(2), 748–752.
- Hancock, N.T., Cath, T.Y. 2009. Solute coupled diffusion in osmotically driven membrane processes. *Environ Sci Technol*, **43**(17), 6769-75.

- Hatzell, M.C., Kim, Y., Logan, B.E. 2013. Powering microbial electrolysis cells by capacitor circuits charged using microbial fuel cell. *Journal of Power Sources*, **229**(0), 198-202.
- He, Z. 2013. Microbial fuel cells: now let us talk about energy. *Environmental Science & Technology*, **47**, 332-333.
- He, Z. 2012. One more function for microbial fuel cells in treating wastewater: producing high-quality water. *CHEMIK*, **66**, 7-10.
- He, Z., Wagner, N., Minteer, S., Angenent, L. 2006a. An upflow microbial fuel cell with an interior cathode: Assessment of the internal resistance by impedance Spectroscopy. *Environmental Science & Technology*, **40**(17), 5212-5217.
- He, Z., Wagner, N., Minteer, S.D., Angenent, L.T. 2006b. An upflow microbial fuel cell with an interior cathode: assessment of the internal resistance by impedance spectroscopy. *Environmental Science & Technology*, **40**(17), 5212-5217.
- Heidrich, E.S., Curtis, T.P., Dolfing, J. 2011. Determination of the Internal Chemical Energy of Wastewater. *Environmental Science & Technology*, **45**(2), 827-832.
- Hoover, L.A., Phillip, W.A., Tiraferri, A., Yip, N.Y., Elimelech, M. 2011. Forward with osmosis: emerging applications for greater sustainability. *Environ Sci Technol*, **45**(23), 9824-30.
- Hu, Z. 2008. Electricity generation by a baffle-chamber membraneless microbial fuel cell. *Journal of Power Sources*, **179**(1), 27–33.
- Huang, Y., He, Z., Mansfeld, F. 2010. Performance of microbial fuel cells with and without Nafion solution as cathode binding agent. *Bioelectrochemistry*, **79**(2), 261-264.
- Huang, Z., Ong, S.L., Ng, H.Y. 2011. Submerged anaerobic membrane bioreactor for low-strength wastewater treatment: effect of HRT and SRT on treatment performance and membrane fouling. *Water Res*, **45**(2), 705-13.
- Ieropoulos, I.A., Ledezma, P., Stinchcombe, A., Papaharalabos, G., Melhuish, C., Greenman, J. 2013. Waste to real energy: the first MFC powered mobile phone. *Physical Chemistry Chemical Physics*, **15**(37), 15312-15316.
- Inglesby, A.E., Fisher, A.C. 2012. Enhanced methane yields from anaerobic digestion of *Arthrospira maxima* biomass in an advanced flow-through reactor with an integrated recirculation loop microbial fuel cell. *Energy & Environmental Science*, **5**, 7996-8006.
- INSTRUMENTS, T. 2011. bq25504 EVM – Ultra Low Power Boost Converter with Battery Management for Energy Harvester Applications.
- Jacobson, K.S., Drew, D., He, Z. 2011. Use of a liter-scale microbial desalination cell as a platform to study bioelectrochemical desalination with salt solution or artificial seawater. *Environmental Science & Technology*, **45**, 4652-4657.
- Jiang, J., Zhao, Q., Zhang, J., Zhang, G., Lee, D.-J. 2009. Electricity generation from bio-treatment of sewage sludge with microbial fuel cell. *Bioresour Technol*, **100**, 5808–5812.
- Jiang, J.Q., Zhao, Q.L., Wang, K., Wei, L.L., Zhang, G.D., Zhang, J.N. 2010. Effect of ultrasonic and alkaline pretreatment on sludge degradation and electricity generation by microbial fuel cell. *Water Science and Technology*, **61**(11), 2915-2921.

- Judd, S. 2008. The status of membrane bioreactor technology. *Trends in Biotechnology*, **26**(2), 109–116.
- Kargi, F., Eker, S. 2007. Electricity generation with simultaneous wastewater treatment by a microbial fuel cell (MFC) with Cu and Cu–Au electrodes. *Journal of Chemical Technology & Biotechnology*, **82**(7), 658-662.
- Kim, J., Kim, K., Ye, H., Lee, E., Shin, C., McCarty, P.L., Bae, J. 2011a. Anaerobic fluidized bed membrane bioreactor for wastewater treatment. *Environ Sci Technol*, **45**(2), 576-81.
- Kim, J., Kim, K., Ye, H., Lee, E., Shin, C., McCarty, P.L., Bae, J. 2011b. Anaerobic Fluidized Bed Membrane Bioreactor for Wastewater Treatment. *Environmental Science & Technology*, **45**(2), 576-581.
- Kim, J.R., Premier, G.C., Hawkes, F.R., Rodríguez, J., Dinsdale, R.M., Guwy, A.J. 2010a. Modular tubular microbial fuel cells for energy recovery during sucrose wastewater treatment at low organic loading rate. *Bioresource Technology*, **101**(4), 1190–1198.
- Kim, J.R., Premier, G.C., Hawkes, F.R., Rodríguez, J., Dinsdale, R.M., Guwy, A.J. 2010b. Modular tubular microbial fuel cells for energy recovery during sucrose wastewater treatment at low organic loading rate. *Bioresource Technology*, **101**(4), 1190-1198.
- Kim, J.R., Zuo, Y., Regan, J.M., Logan, B.E. 2008. Analysis of ammonia loss mechanisms in microbial fuel cells treating animal wastewater. *Biotechnology and Bioengineering*, **99**(5), 1120-1127.
- Kim, Y., Logan, B.E. 2013. Microbial desalination cells for energy production and desalination. *Desalination*, **308**, 122–130.
- Kuntke, P., Smiech, K.M., Bruning, H., Zeeman, G., Saakes, M., Sleutels, T.H., Hamelers, H.V., Buisman, C.J. 2012. Ammonium recovery and energy production from urine by a microbial fuel cell. *Water Res*, **46**(8), 2627-36.
- L.S. Clesceri, A.E.G., A.D. Eaton. 1998. Standard Methods for the Examination of Water and Wastewater. 20th ed. ed, American Public Health Association. Washington, DC.
- Lackner, S., Gilbert, E.M., Vlaeminck, S.E., Joss, A., Horn, H., van Loosdrecht, M.C.M. 2014. Full-scale partial nitrification/anammox experiences – An application survey. *Water Research*, **55**, 292-303.
- Ledezma, P., Stinchcombe, A., Greenman, J., Ieropoulos, I. 2013. The first self-sustainable microbial fuel cell stack. *Physical Chemistry Chemical Physics*, **15**(7), 2278-2281.
- Lee, S., Boo, C., Elimelech, M., Hong, S. 2010. Comparison of fouling behavior in forward osmosis (FO) and reverse osmosis (RO). *Journal of Membrane Science*, **1-2**, 34–39.
- Li, W.-W., Sheng, G.-P., Liu, X.-W., Yu, H.-Q. 2011. Recent advances in the separators for microbial fuel cells. *Bioresource Technology*, **102**, 244-252.
- Li, W.-W., Yu, H.-Q., He, Z. 2014a. Towards sustainable wastewater treatment by using microbial fuel cells-centered technologies. *Energy Environ. Sci.*, **7**(3), 911-924.
- Li, W.-W., Yu, H.-Q., He, Z. 2014b. Towards sustainable wastewater treatment by using microbial fuel cells-centered technologies. *Energy & Environmental Science*, **7**(3), 911-924.

- Li, Z.Y., Yangali-Quintanilla, V., Valladares-Linares, R., Li, Q., Zhan, T., Amy, G. 2012. Flux patterns and membrane fouling propensity during desalination of seawater by forward osmosis. *Water Res*, **46**(1), 195-204.
- Liang, P., Wei, J., Li, M., Huang, X. 2013. Scaling up a novel denitrifying microbial fuel cell with an oxic-anoxic two stage biocathode. *Frontiers of Environmental Science & Engineering*, **7**(6), 913-919.
- Liao, B.-Q., Kraemer, J.T., Bagley, D.M. 2006. Anaerobic Membrane Bioreactors: Applications and Research Directions. *Critical Reviews in Environmental Science and Technology*, **36**(6), 489-530.
- Ling, M.M., Wang, K.Y., Chung, T.-S. 2010. Highly water-soluble magnetic nanoparticles as novel draw solutes in forward osmosis for water reuse. *Industrial & Engineering Chemistry Research*, **49**(12), 5869–5876.
- Liu, H., Logan, B.E. 2004. Electricity Generation Using an Air-Cathode Single Chamber Microbial Fuel Cell in the Presence and Absence of a Proton Exchange Membrane. *Environmental Science & Technology*, **38**(14), 4040-4046.
- Liu, X., Wang, W., Shi, Y., Zheng, L., Gao, X., Qiao, W., Zhou, Y. 2012. Pilot-scale anaerobic co-digestion of municipal biomass waste and waste activated sludge in China: effect of organic loading rate. *Waste Manag*, **32**(11), 2056-60.
- Logan, B., Rabaey, K. 2012. Conversion of wastes into bioelectricity and chemicals using microbial electrochemical technologies. *Science*, **337**, 686-690.
- Logan, B., Regan, J. 2006. Electricity-producing bacterial communities in microbial fuel cells. *Trends in Microbiology*, **14**(12), 512-518.
- Logan, B.E. 2010. Scaling up microbial fuel cells and other bioelectrochemical systems. *Applied Microbiology and Biotechnology*, **85**(6), 1665-1671.
- Logan, B.E., Call, D., Cheng, S., Hamelers, H.V., Sleutels, T.H., Jeremiasse, A.W., Rozendal, R.A. 2008. Microbial electrolysis cells for high yield hydrogen gas production from organic matter. *Environmental Science & Technology*, **42**(23), 8630-40.
- Logan, B.E., Hamelers, B., Rozendal, R., Schröder, U., Keller, J., Freguia, S., Aelterman, P., Verstraete, W., Rabaey, K. 2006a. Microbial Fuel Cells: Methodology and Technology†. *Environmental Science & Technology*, **40**(17), 5181-5192.
- Logan, B.E., Hamelers, B., Rozendal, R.A., Schroder, U., Keller, J., Freguia, S., Aelterman, P., Verstraete, W., Rabaey, K. 2006b. Microbial fuel cells: methodology and technology. *Environmental Science and Technology*, **40**(17), 5181-5192.
- Logan, B.E., Hamelers, B., Rozendal, R.A., Schroder, U., Keller, J., Freguia, S., Aelterman, P., Verstraete, W., Rabaey, K. 2006c. Microbial fuel cells: Methodology and technology. *Environmental Science & Technology*, **40**(17), 5181-5192.
- Logan, B.E., Murano, C., Scott, K., Gray, N.D., Head, I.M. 2005. Electricity generation from cysteine in a microbial fuel cell. *Water Research*, **39**(5), 942-952.
- Marrot, B., Barrios-Martinez, A., Moulin, P., Roche, N. 2004. Industrial wastewater treatment in a membrane bioreactor: A review. *Environmental Progress*, **23**(1), 59-68.
- Masters, G.M., Ela, W.P. 2008. *Introduction to environmental engineering and science. Third ed.* Prentice-Hall, Inc., Upper Saddle River, New Jersey.

- Mata-Alvarez, J., Mac é S., Llabrés, P. 2000. Anaerobic digestion of organic solid wastes. An overview of research achievements and perspectives. *Bioresource Technology*, **74**(1), 3-16.
- McBride, L.R., Girguis, P., Reimers, C.E. 2006. Power Storage and Conversion from an Ocean Microbial Energy Source. *OCEANS 2006*, 18-21 Sept. 2006. pp. 1-5.
- McCarty, P.L., Bae, J., Kim, J. 2011a. Domestic Wastewater Treatment as a Net Energy Producer—Can This be Achieved? *Environ. Sci. Technol.*, **45**(17), 7100–7106.
- McCarty, P.L., Bae, J., Kim, J. 2011b. Domestic Wastewater Treatment as a Net Energy Producer—Can This be Achieved? *Environmental Science & Technology*, **45**(17), 7100-7106.
- McCutcheon, J.R., McGinnis, R.L., Elimelech, M. 2005. A novel ammonia—carbon dioxide forward (direct) osmosis desalination process *Desalination*, **174**(1), 1-11.
- Mi, B., Elimelech, M. 2008. Chemical and physical aspects of organic fouling of forward osmosis membranes. *Journal of Membrane Science*, **320**, 292–302.
- Molognoni, D., Puig, S., Balaguer, M.D., Liberale, A., Capodaglio, A.G., Callegari, A., Colprim, J. 2014. Reducing start-up time and minimizing energy losses of Microbial Fuel Cells using Maximum Power Point Tracking strategy. *Journal of Power Sources*, **269**(0), 403-411.
- Morris, J.M., Jin, S., Wang, J., Zhu, C., Urynowicz, M.A. 2007. Lead dioxide as an alternative catalyst to platinum in microbial fuel cells. *Electrochemistry Communications*, **9**(7), 1730-1734.
- Nghia, T., Wookpyo, H., Ewing, T., Beyenal, H., Jong-Hoon, K., Deukhyoun, H. 2015. A Self-Sustainable Power Management System for Reliable Power Scaling Up of Sediment Microbial Fuel Cells. *Power Electronics, IEEE Transactions on*, **30**(9), 4626-4632.
- Oh, S.E., Logan, B.E. 2007. Voltage reversal during microbial fuel cell stack operation. *Journal of Power Sources*, **167**(1), 11-17.
- Pant, D., Van Bogaert, G., Diels, L., Vanbroekhoven, K. 2010. A review of the substrates used in microbial fuel cells (MFCs) for sustainable energy production *Bioresource Technology*, **101**(6), 1533-1543
- Park, J.-D., Ren, Z. 2012. Hysteresis controller based maximum power point tracking energy harvesting system for microbial fuel cells. *Journal of Power Sources*, **205**(0), 151-156.
- Pham, T.H., Rabaey, K., Aelterman, P., Clauwaert, P., De Schamphelaire, L., Boon, N., Verstraete, W. 2006. Microbial fuel cells in relation to conventional anaerobic digestion technology. *Engineering in Life Sciences*, **6**(3), 285-292.
- Phillip, W.A., Yong, J.S., Elimelech, M. 2010. Reverse draw solute permeation in forward osmosis: modeling and experiments. *Environmental Science & Technology*, **44**(13), 5170-6.
- Phuntsho, S., Shon, H.K., Hong, S., Lee, S., Vigneswaran, S. 2011. A novel low energy fertilizer driven forward osmosis desalination for direct fertigation: Evaluating the performance of fertilizer draw solutions. *Journal of Membrane Science*, **375**, 172-181.
- Plappally, A.K., Lienhard V, J.H. 2012a. Energy requirements for water production, treatment, end use, reclamation, and disposal. *Renewable and Sustainable Energy Reviews*, **16**(7), 4818-4848.

- Plappally, A.K., Lienhard V, J.H. 2012b. Energy requirements for water production, treatment, end use, reclamation, and disposal. *Renewable & Sustainable Energy Reviews*, **16**(7), 4818–4848.
- Prieto, A.L. 2011. Sequential Anaerobic and Algal Membrane Bioreactor (A2MBR) System for Sustainable Sanitation and Resource Recovery from Domestic Wastewater. in: *Civil and Environmental Engineering*, Vol. PhD, University of South Florida. Tampa, FL, pp. 3296.
- Quan, X., Wang, F., Zhao, Q., Zhao, T., Xiang, J. 2009. Air stripping of ammonia in a water-sparged aerocyclone reactor. *Journal of Hazardous Materials*, **170**(2-3), 983-8.
- Rabaey, K., Boon, N., Höfte, M., Verstraete, W. 2005a. Microbial Phenazine Production Enhances Electron Transfer in Biofuel Cells. *Environmental Science & Technology*, **39**(9), 3401-3408.
- Rabaey, K., Butzer, S., Brown, S., Keller, J., Rozendal, R.A. 2010. High current generation coupled to caustic production using a lamellar bioelectrochemical system. *Environmental Science & Technology*, **44**(11), 4315-21.
- Rabaey, K., Clauwaert, P., Aelterman, P., Verstraete, W. 2005b. Tubular Microbial Fuel Cells for Efficient Electricity Generation. *Environmental Science & Technology*, **39**(20), 8077-8082.
- Rabaey, K., Verstraete, W. 2005. Microbial fuel cells: novel biotechnology for energy generation. *Trends Biotechnol.*, **23**(6), 291-298.
- Rabiller-Baudry, M., Maux, M.L., Chaufer, B., Begoin, L. 2002. Characterisation of cleaned and fouled membrane by ATR—FTIR and EDX analysis coupled with SEM: application to UF of skimmed milk with a PES membrane. *Desalination*, **146**(1-3), 123–128.
- Rinaldi, A., Mecheri, B., Garavaglia, V., Licoccia, S., Di Nardo, P., Traversa, E. 2008. Engineering materials and biology to boost performance of microbial fuel cells: a critical review. *Energy & Environmental Science*, **1**(4), 417-429.
- Rismani-Yazdi, H., Carver, S.M., Christy, A.D., Tuovinen, O.H. 2008. Cathodic limitations in microbial fuel cells: An overview. *Journal of Power Sources*, **180**(2), 683-694.
- Rozendal, R.A., Hamelers, H.V.M., Buisman, C.J.N. 2006. Effects of membrane cation transport on pH and microbial fuel cell performance. *Environmental Science and Technology*, **40**(17), 5206-5211.
- Rozendal, R.A., Leone, E., Keller, J., Rabaey, K. 2009. Efficient hydrogen peroxide generation from organic matter in a bioelectrochemical system. *Electrochemistry Communications*, **11**(9), 1752-1755.
- Samsudeen, N., Radhakrishnan, T.K., Matheswaran, M. 2015. Performance comparison of triple and dual chamber microbial fuel cell using distillery wastewater as a substrate. *Environmental Progress & Sustainable Energy*, **34**(2), 589-594.
- Shannon, M.A., Bohn, P.W., Elimelech, M., Georgiadis, J.G., Marinas, B.J., Mayes, A.M. 2008. Science and technology for water purification in the coming decades. *Nature*, **452**(7185), 301-10.
- Shantaram, A., Beyenal, H., Veluchamy, R.R.A., Lewandowski, Z. 2005. Wireless Sensors Powered by Microbial Fuel Cells. *Environmental Science & Technology*, **39**(13), 5037-5042.

- Smith, A.L., Stadler, L.B., Love, N.G., Skerlos, S.J., Raskin, L. 2012. Perspectives of anaerobic membrane bioreactor treatment of domestic wastewater: a critical review. *Bioresource Technology*, DOI: [10.1016/j.biortech.2012.04.055](https://doi.org/10.1016/j.biortech.2012.04.055).
- Smith, R.G.W. 2002. U.S. Electricity Consumption for Water Supply & Treatment - The Next Half Century. in: *Water & Sustainability*, Vol. 4.
- Sun, J., Hu, Y., Bi, Z., Cao, Y. 2009. Improved performance of air-cathode single chamber microbial fuel cell for wastewater treatment using microfiltration membranes and multiple sludge inoculation. *Journal of Power Sources*, **187**(2), 471-479.
- Sun, G., Thygesen, A., Ale, M., Mensah, M., Poulsen, F., Meyer, A. 2014. The significance of the initiation process parameters and reactor design for maximizing the efficiency of microbial fuel cells. *Applied Microbiology and Biotechnology*, **98**(6), 2415-2427
- Sung, S., Liu, T. 2003. Ammonia inhibition on thermophilic anaerobic digestion. *Chemosphere*, **53**(1), 43-52.
- Tchobanoglous, G., Burton, F.L., Stensel, H.D. 2002. *Wastewater Engineering: Treatment and Reuse. 4th ed.* McGraw-Hill.
- Tender, L.M., Gray, S.A., Groveman, E., Lowy, D.A., Kauffman, P., Melhado, J., Tyce, R.C., Flynn, D., Petrecca, R., Dobarro, J. 2008. The first demonstration of a microbial fuel cell as a viable power supply: Powering a meteorological buoy. *Journal of Power Sources*, **179**(2), 571-575.
- Ting, C.H., Lee, D.J. 2007. Production of hydrogen and methane from wastewater sludge using anaerobic fermentation. *International Journal of Hydrogen Energy*, **32**, 677 – 682.
- Tugtas, A.E., Cavdar, P., Calli, B. 2011. Continuous flow membrane-less air cathode microbial fuel cell with spunbonded olefin diffusion layer. *Bioresource Technology*, **102**(22), 10425–10430.
- van Nieuwenhuijzen, A.F., Evenblij, H., Uijterlinde, C.A., Schulting, F.L. 2008. Review on the state of science on membrane bioreactors for municipal wastewater treatment. *Water Science and Technology*, **57**(7), 979-986.
- Wang, H., Park, J.-D., Ren, Z. 2012a. Active Energy Harvesting from Microbial Fuel Cells at the Maximum Power Point without Using Resistors. *Environmental Science & Technology*, **46**(9), 5247-5252.
- Wang, H., Park, J.-D., Ren, Z.J. 2015. Practical Energy Harvesting for Microbial Fuel Cells: A Review. *Environmental Science & Technology*, **49**(6), 3267-3277.
- Wang, H., Park, J.D., Ren, Z. 2012b. Active energy harvesting from microbial fuel cells at the maximum power point without using resistors. *Environ Sci Technol*, **46**(9), 5247-52.
- Wang, H., Ren, Z., Park, J.-D. 2012c. Power electronic converters for microbial fuel cell energy extraction: Effects of inductance, duty ratio, and switching frequency. *Journal of Power Sources*, **220**(0), 89-94.
- Wang, H., Ren, Z.J. 2013. A comprehensive review of microbial electrochemical systems as a platform technology. *Biotechnology Advances*, **31**(8), 1796-1807.
- Wang, X., Cheng, S., Feng, Y., Merrill, M.D., Saito, T., Logan, B.E. 2009. Use of carbon mesh anodes and the effect of different pretreatment methods on power

- production in microbial fuel cells. *Environmental Science & Technology*, **43**(17), 6870-6874.
- Wang, Y.-K., Sheng, G.-P., Li, W.-W., Huang, Y.-X., Yu, Y.-Y., Zeng, R.J., Yu, H.-Q. 2011. Development of a novel bioelectrochemical membrane reactor for wastewater treatment. *Environmental Science and Technology*, **45**(21), 9256–9261.
- Wang, Y.-P., Liu, X.-W., Li, W.-W., Li, F., Wang, Y.-K., Sheng, G.-P., Zeng, R.J., Yu, H.-Q. 2012d. A microbial fuel cell–membrane bioreactor integrated system for cost-effective wastewater treatment. *Applied Energy*, **98**, 230–235.
- Wang, Z., Mei, X., Ma, J., Wu, Z. 2012e. Recent Advances in Microbial Fuel Cells Integrated with Sludge Treatment. *Chemical Engineering & Technology*, **35**(10), 1733–1743.
- Watson, V.J., Nieto Delgado, C., Logan, B.E. 2013. Influence of Chemical and Physical Properties of Activated Carbon Powders on Oxygen Reduction and Microbial Fuel Cell Performance. *Environmental Science & Technology*, **47**(12), 6704-6710.
- Woodward, L., Perrier, M., Srinivasan, B., Pinto, R.P., Tartakovsky, B. 2010. Comparison of real-time methods for maximizing power output in microbial fuel cells. *AIChE Journal*, **56**(10), 2742-2750.
- Xiao, B., Yang, F., Liu, J. 2011. Enhancing simultaneous electricity production and reduction of sewage sludge in two-chamber MFC by aerobic sludge digestion and sludge pretreatments. *J Hazard Mater*, **189**(1-2), 444-9.
- Xiao, L., Ge, Z., Kelly, P., Zhang, F., He, Z. 2014. Evaluation of normalized energy recovery (NER) in microbial fuel cells affected by reactor dimensions and substrates. *Bioresource Technology*, **157**(0), 77-83.
- Xiao, L., Young, E.B., Berges, J.A., He, Z. 2012. Integrated photo-bioelectrochemical system for contaminants removal and bioenergy production. *Environmental Science & Technology*, **46**, 11459-11466.
- Xu, B., Ge, Z., He, Z. 2015. Sediment microbial fuel cells for wastewater treatment: challenges and opportunities. *Environmental Science: Water Research & Technology*, **1**(3), 279-284.
- Yang, F., Ren, L., Pu, Y., Logan, B.E. 2013. Electricity generation from fermentation solution of primary sludge using single-chambered air-cathode microbial fuel cells. *Bioresource Technology*, DOI: **10.1016/j.biortech.2012.10.021**.
- Yang, F., Zhang, D., Shimotori, T., Wang, K.-C., Huang, Y. 2012. Study of transformer-based power management system and its performance optimization for microbial fuel cells. *Journal of Power Sources*, **205**(0), 86-92.
- Yang, Q., Wang, K.Y., Chung, T.S. 2009. Dual-layer hollow fibers with enhanced flux as novel forward osmosis membranes for water production. *Environmental Science & Technology*, **43**(8), 2800-5.
- Yang, W., Cicek, N., Ilg, J. 2006. State-of-the-art of membrane bioreactors: Worldwide research and commercial applications in North America. *Journal of Membrane Science*, **270**, 201–211.
- Ye, Z., Zhang, B., Liu, Y., Wang, Z., Tian, C. 2014. Continuous electricity generation with piggery wastewater treatment using an anaerobic baffled stacking microbial fuel cell. *Desalination and Water Treatment*, **55**(8), 2079-2087.

- Yip, N.Y., Tiraferri, A., Phillip, W.A., Schiffman, J.D., Elimelech, M. 2010. High performance thin-film composite forward osmosis membrane. *Environmental Science & Technology*, **44**(10), 3812-8.
- Yuan, H., Li, J., Yuan, C., He, Z. 2014. Facile Synthesis of MoS<sub>2</sub>@CNT as an Effective Catalyst for Hydrogen Production in Microbial Electrolysis Cells. *ChemElectroChem*, **1**(11), 1828-1833.
- Zhang, B., He, Z. 2012a. Energy production, use and saving in a bioelectrochemical desalination system. *RSC Advances*, **2**(28), 10673-10679.
- Zhang, B., He, Z. 2012b. Integrated salinity reduction and water recovery in an osmotic microbial desalination cells. *RSC Advances*, **2**, 3265-3269.
- Zhang, B., Wen, Z., Ci, S., Mao, S., Chen, J., He, Z. 2014. Synthesizing Nitrogen-Doped Activated Carbon and Probing its Active Sites for Oxygen Reduction Reaction in Microbial Fuel Cells. *ACS Applied Materials & Interfaces*, **6**(10), 7464-7470.
- Zhang, F., Brastad, K., He, Z. 2011a. Integrating forward osmosis into microbial fuel cells for wastewater treatment, water extraction and bioelectricity generation. *Environmental Science & Technology*, **45**, 6690-6696.
- Zhang, F., Cheng, S., Pant, D., Bogaert, G.V., Logan, B.E. 2009. Power generation using an activated carbon and metal mesh cathode in a microbial fuel cell. *Electrochemistry Communications*, **11**(11), 2177-2179.
- Zhang, F., Ge, Z., Grimaud, J., Hurst, J., He, Z. 2013a. Improving electricity production in tubular microbial fuel cells through optimizing the anolyte flow with spiral spacers. *Bioresource Technology*, **Under review**.
- Zhang, F., Ge, Z., Grimaud, J., Hurst, J., He, Z. 2013b. Long-term performance of liter-scale microbial fuel cells installed in a municipal wastewater treatment facility. *Environmental Science & Technology*, **47**, 4941-4948.
- Zhang, F., Ge, Z., Grimaud, J., Hurst, J., He, Z. 2013c. Long-Term Performance of Liter-Scale Microbial Fuel Cells Treating Primary Effluent Installed in a Municipal Wastewater Treatment Facility. *Environmental Science & Technology*, **47**(9), 4941-4948.
- Zhang, F., Jacobson, K.S., Torres, P., He, Z. 2010a. Effects of anolyte recirculation rates and catholytes on electricity generation in a liter-scale upflow microbial fuel cell. *Energy & Environmental Science*, **3**, 1347-1352.
- Zhang, F., Jacobson, K.S., Torres, P., He, Z. 2010b. Effects of anolyte recirculation rates and catholytes on electricity generation in a litre-scale upflow microbial fuel cell. *Energy & Environmental Science*, **3**(9), 1347-1352.
- Zhang, F., Pant, D., Logan, B.E. 2011b. Long-term performance of activated carbon air cathodes with different diffusion layer porosities in microbial fuel cells. *Biosensors and Bioelectronics*, **30**(1), 49-55.
- Zhang, F., Tian, L., He, Z. 2011c. Powering a wireless temperature sensor using sediment microbial fuel cells with vertical arrangement of electrodes. *Journal of Power Sources*, **196**(22), 9568-9573.
- Zhang, Y., Gao, J., Peng, D., Guangyao, M., Liu, X. 2004. Dip-coating thin yttria-stabilized zirconia films for solid oxide fuel cell applications. *Ceramics International*, **30**(6), 1049-1053.

- Zhao, F., Harnisch, F., Schroder, U., Scholz, F., Bogdanoff, P., Herrmann, I. 2006a. Challenges and constraints of using oxygen cathodes in microbial fuel cells. *Environmental Science and Technology*, **40**(17), 5193-5199.
- Zhao, F., Harnisch, F., Schröder, U., Scholz, F., Bogdanoff, P., Herrmann, I. 2005. Application of pyrolysed iron(II) phthalocyanine and CoTMPP based oxygen reduction catalysts as cathode materials in microbial fuel cells. *Electrochemistry Communications*, **7**(12), 1405-1410.
- Zhao, F., Harnisch, F., Schröder, U., Scholz, F., Bogdanoff, P., Herrmann, I. 2006b. Challenges and Constraints of Using Oxygen Cathodes in Microbial Fuel Cells. *Environmental Science & Technology*, **40**(17), 5193-5199.
- Zhao, F., Slade, R.C.T., Varcoe, J.R. 2009. Techniques for the study and development of microbial fuel cells: an electrochemical perspective *Chemical Society Reviews* **38**, 1926-1939.
- Zhou, M., Chi, M., Luo, J., He, H., Jin, T. 2011. An overview of electrode materials in microbial fuel cells. *Journal of Power Sources*, **196**, 4427-4435.
- Zou, S., Gu, Y., Xiao, D., Tang, C.Y. 2011. The role of physical and chemical parameters on forward osmosis membrane fouling during algae separation *Journal of Membrane Science*, **366**(1-2), 356-362
- Zuo, Y., Cheng, S., Call, D., Logan, B.E. 2007. Tubular membrane cathodes for scalable power generation in microbial fuel cells. *Environ Sci Technol*, **41**(9), 3347-53.

## Appendices

### Appendix A Supplemental Information to Chapter 4

#### Additional Measurement and Analysis

Elemental analysis was performed on an X-ray energy dispersive spectrometer (EDS) (TopCon ABT-32). The EDS was conducted with an accelerating voltage of 15 kV and a working distance of 30 mm. The target elements included nitrogen, oxygen, sodium, magnesium, aluminum, silicon, phosphate, calcium, and copper.

The electrochemical impedance spectroscopy (EIS) measurements were performed in a cell of two compartments separated by the FO membrane. The impedance across the membrane was measured by using a potentiostat (Gamry reference 600) in a four-electrode mode. The four-electrode system includes two platinum electrodes as the working electrode and the counter electrode, respectively, and two Ag/AgCl electrodes as the reference electrodes (according to Gamry technical note). The frequency was set at the range of 0.01Hz~100kHz. The electrolyte used was NaCl solution of 30g/L. The resistance measured at high frequency represents the combined solution and membrane resistance  $R_{m+s}$ . To obtain the pure membrane resistance  $R_m$ , the combined resistance is deducted by the solution resistance  $R_s$  obtained from a blank experiment that did not contain the membrane over the same frequency range.

For scanning electron microscopy (SEM), small pieces of the FO membrane were fixed with glutaraldehyde for one night and OsO<sub>4</sub> for one hour, and then dehydrated with a

graded ethanol series: 10%, 25%, 50%, 75%, 95%, 100% and 100%. The samples were critical-point dried via liquid CO<sub>2</sub> in a Balzers CPD 020 critical point drying apparatus (Balzers Union, Liechtenstein). After drying, the samples were glued on the specimens and then coated with 5.0 nm Iridium in the Emitech K575X Sputter Coater (Emitech, Polaron, Britain). The morphology of microorganisms was observed by SEM (S-4800 Hitachi, Japan).

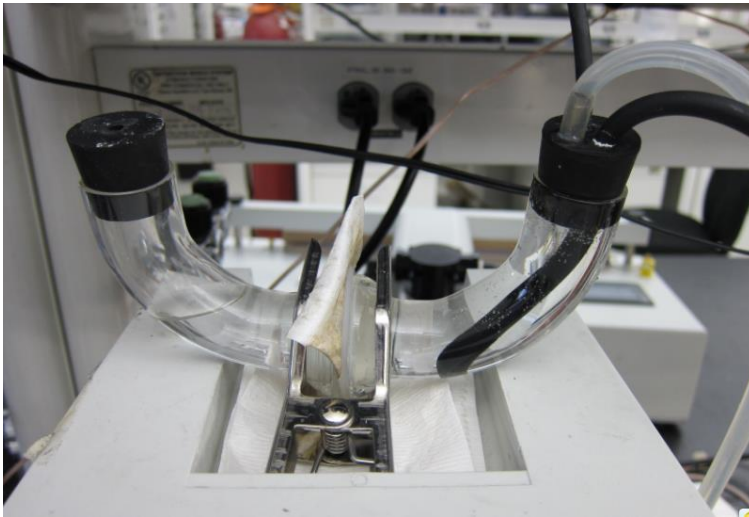


**Figure A1. The U-shape reactor used for the water flux test.** Water flux tests were carried out at the end of this study to examine the membrane fouling using a U-shape two-chamber reactor (Figure S1). Both new and fouled membranes were tested for baseline and fouling flux tests, respectively. The active layer of membrane was facing the feed solution; there was no recirculation in the feed chamber. The recirculation rate was 500 mL/min to enhance the mixture in the draw solution chamber. The excess water drawn through membrane was collected in a conical flask and weighed by a digital balance. During the 4-hr test, the weight was recorded every hour for flux calculation. DI water was used as feed

solution; the draw solution was 2M NaCl stored in a 1-L glass bottle that had a total volume of 1050 mL, while the volume of the feed solution was 50 mL.

**Table A1 The composition of the scaling compounds on the side of the FO membrane facing the anode (wastewater)**

Elements:	WT%	AT%	K_A	K_F	K_Z	Intensity	P/bkg
N K	23.86	38.29	0.099	1	1.056	9.142	0.6
O K	15.35	21.57	0.13	1	1.047	11.691	0.7
NaK	0.98	0.96	0.449	1.002	0.976	5.016	0.2
MgK	0.16	0.15	0.593	1.005	1	1.29	0
AlK	2.21	1.84	0.736	1.009	0.97	22.829	0.7
SiK	3.18	2.55	0.815	1.015	0.996	36.82	1.1
P K	20.06	14.56	0.867	1.01	0.961	177.491	5.8
S K	14.35	10.06	0.792	1.003	0.984	115.087	3.3
CaK	14.52	8.14	0.931	1	0.964	89.531	4.3
CuK	5.32	1.88	0.999	1	0.834	6.452	0.7

**Table A2 The composition of the scaling compounds on the side of the FO membrane facing the cathode (draw solution)**

Elements:	WT%	AT%	K_A	K_F	K_Z	Intensity	P/bkg
N K	29.25	42.3	0.141	1	1.049	7.048	0.9
O K	21.76	27.54	0.151	1	1.039	8.538	0.9
NaK	3.36	2.96	0.446	1.002	0.969	7.552	0.3
MgK	0.44	0.37	0.567	1.004	0.993	1.539	0.1
AlK	3.7	2.78	0.712	1.007	0.962	16.33	0.6
SiK	4.13	2.98	0.784	1.01	0.987	20.274	0.8
P K	20.93	13.68	0.837	1.002	0.952	78.595	3
S K	2.05	1.3	0.769	1.002	0.976	7.071	0.2
CaK	8.12	4.1	0.951	1.001	0.956	22.679	1.3
CuK	6.25	1.99	1.003	1	0.826	3.367	0.4

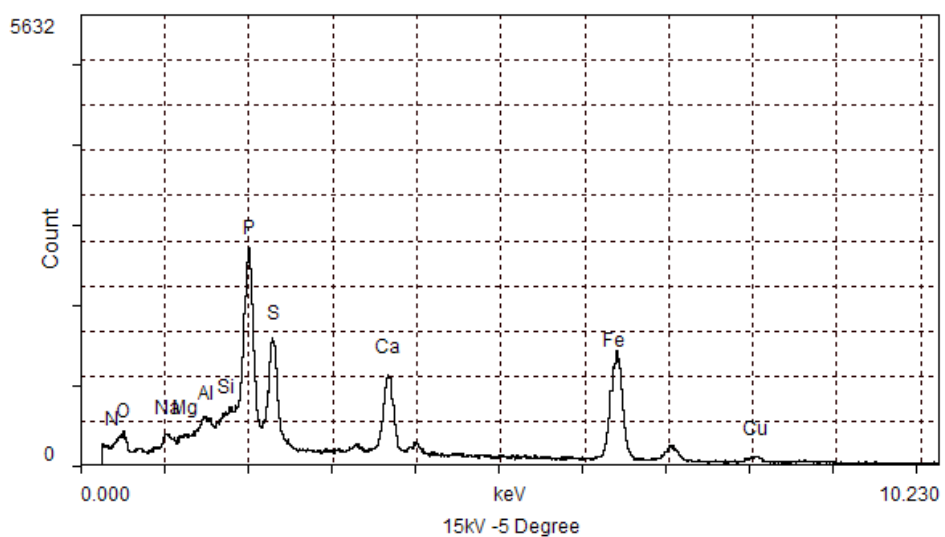


**Figure A2 EDS spectrum of the scaling compounds on the side of the FO membrane facing the anode (wastewater).**

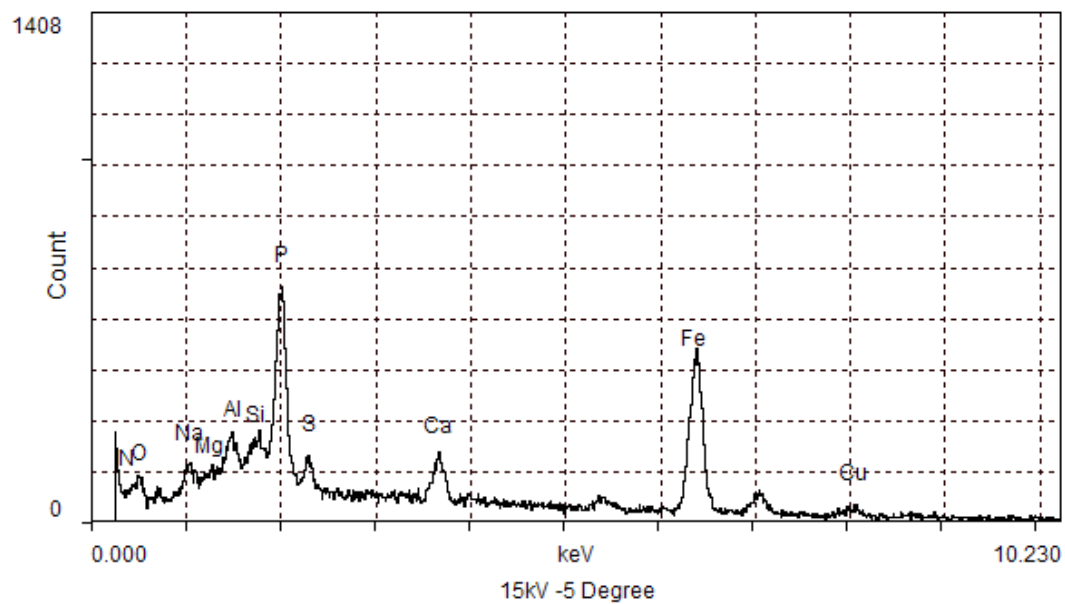


**Figure A3 EDS spectrum of the scaling compounds on the side of the FO membrane facing the cathode (draw solution).**

## Appendix B Supplemental Information to Chapter 5

**Table B1. Power consumption by the pumping system at different HRTs.**

Substrate	HRT (h)	Power Consumption (kW)			
		Influent	Permeate	Recirculation	Total
Acetate Solution	27	$3.20 \times 10^{-8}$	$1.83 \times 10^{-7}$	$9.00 \times 10^{-7}$	$1.11 \times 10^{-6}$
Acetate Solution	19	$4.57 \times 10^{-8}$	$3.92 \times 10^{-7}$	$9.00 \times 10^{-7}$	$1.34 \times 10^{-6}$
Primary Effluent	36	$2.45 \times 10^{-8}$	$1.03 \times 10^{-7}$	$9.00 \times 10^{-7}$	$1.03 \times 10^{-6}$
Primary Effluent	26	$3.35 \times 10^{-8}$	$2.06 \times 10^{-7}$	$9.00 \times 10^{-7}$	$1.14 \times 10^{-6}$
Primary Effluent	19	$4.73 \times 10^{-8}$	$4.31 \times 10^{-7}$	$9.00 \times 10^{-7}$	$1.38 \times 10^{-6}$
Primary Effluent	15	$5.83 \times 10^{-8}$	$6.96 \times 10^{-7}$	$9.00 \times 10^{-7}$	$1.65 \times 10^{-6}$

**TABLE B2 Analysis of energy production and consumption of the MBER with different substrates and HRTs.**

Substrate	HRT (h)	Energy Production (kWh/m <sup>3</sup> )	Energy Consumption (kWh/m <sup>3</sup> )			
			Influent	Permeate	Recirculation	Total
Acetate Solution	27	0.038	$9.53 \times 10^{-4}$	$5.44 \times 10^{-3}$	$2.68 \times 10^{-2}$	0.033
Acetate Solution	19	0.035	$9.53 \times 10^{-4}$	$8.17 \times 10^{-3}$	$1.87 \times 10^{-2}$	0.028
Primary Effluent	36	0.003	$9.53 \times 10^{-4}$	$4.02 \times 10^{-3}$	$3.51 \times 10^{-2}$	0.040
Primary Effluent	26	0.010	$9.53 \times 10^{-4}$	$5.85 \times 10^{-3}$	$2.56 \times 10^{-2}$	0.032
Primary Effluent	19	0.021	$9.53 \times 10^{-4}$	$8.69 \times 10^{-3}$	$1.81 \times 10^{-2}$	0.028
Primary Effluent	15	0.025	$9.53 \times 10^{-4}$	$1.14 \times 10^{-2}$	$1.47 \times 10^{-2}$	0.027

**Table B3 Membrane cleaning methods and water flux during treatment of primary effluent.**

Time	Cleaning methods	Testing Flux (LMH)	
		Before	After
Day 120	pH 12, submerged for 30 min, backwash for 30 min	117 at 25.8 °C	154 at 25.7 °C
Day 163		106 at 25.1 °C	138 at 25.3 °C
Day 178		93 at 25.3 °C	146 at 25.3 °C
Day 192	pH 12, 100 ppm NaClO submerged for 30 min, backwash for 30 min	53 at 25.1 °C	93 at 25.2 °C
Day 202	pH 12, 400 ppm NaClO submerged for 30 min, backwash for 30 min	96 at 25.3 °C	146 at 25.7 °C

**Table B4 The mass ratio of the new and the fouled membrane.**

Membrane		Nitrogen	C/F	O/F
New	Interior	0	0.83	0.49
	Exterior	0	1.01	0.53
Fouled	Interior	18.1 ± 1.7 %	0.88	0.68
	Exterior	16.2 ± 2.1 %	1.16	0.68

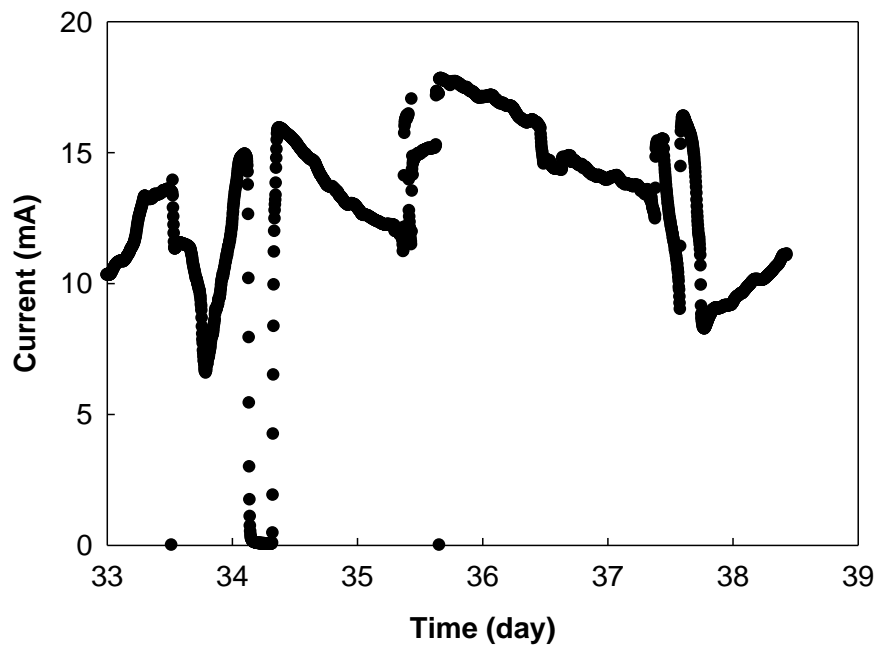


Figure B1 Current generation in the MBER fed with the acetate solution at HRT 19 h.

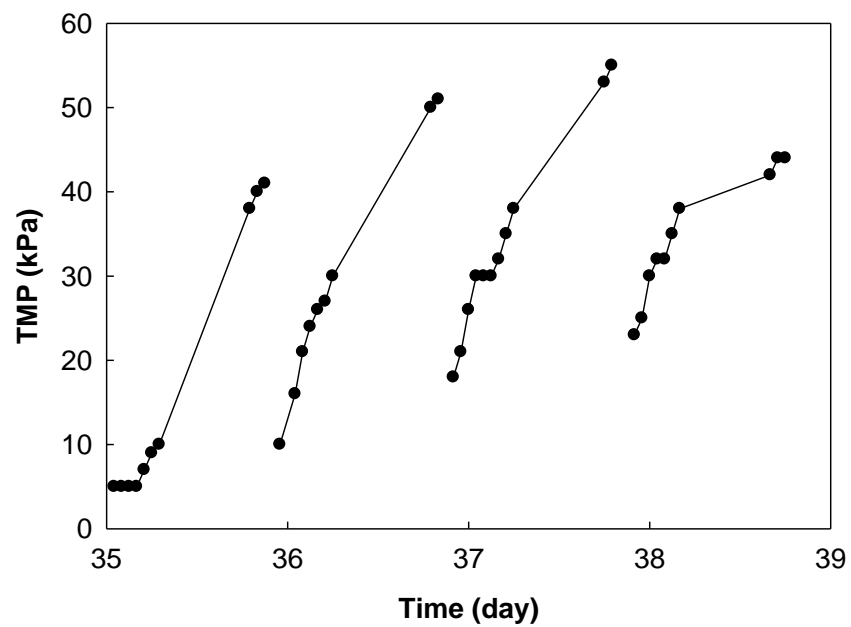
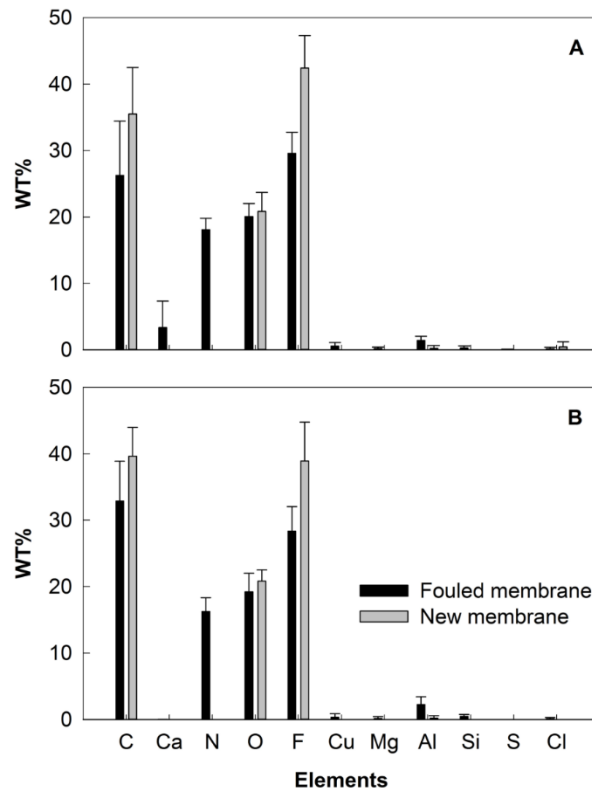


Figure B2 The TMP increase in the MBER fed with the acetate solution at HRT 19 h



**Figure B3 Hollow-fiber membranes before (left) and after (right) chemical cleaning (day 202).**



**Figure B4 The weight percentages (WT%) of the elements in the new and the fouled membrane from EDS analysis: A) the interior and B) the exterior.**

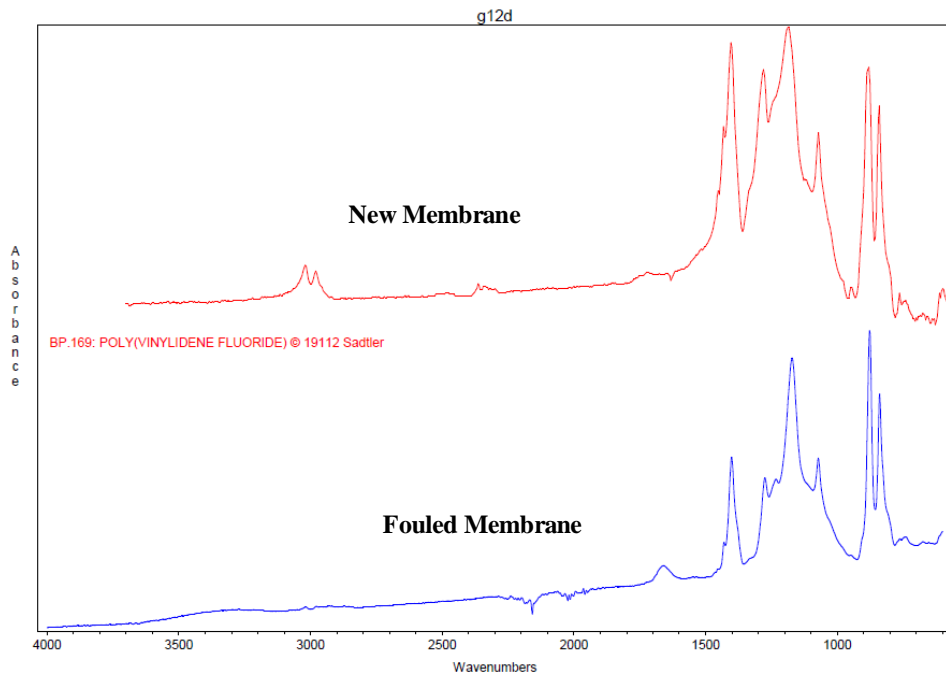


**Figure B5 FTIR spectra of the new and the fouled membranes.**

## Appendix C Supplemental Information to Chapter 6

### Energy Calculation

Energy is calculated from power according to the following equation:

$$E = P \times t$$

Where, E is the energy (J), P is the power (W) and t is the time (s).

To convert energy from J to kWh, we can use the following relationship:

$$1 \text{ kWh} = 3.6 \times 10^6 \text{ J}$$

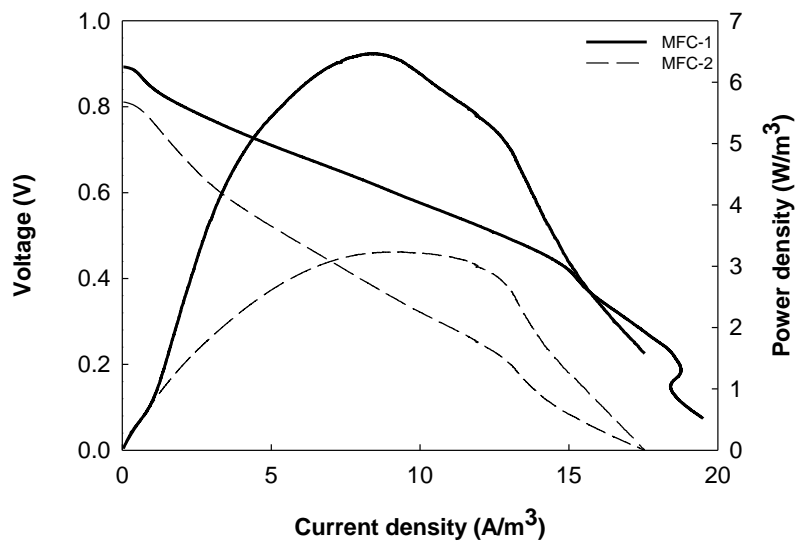


**Figure C1** Power and voltage curves of the two MFCs during Phase I. MFC-1 was fed with the primary sludge and MFC-2 was supplied with the digested sludge. The scan rate was 0.1 mV/s.

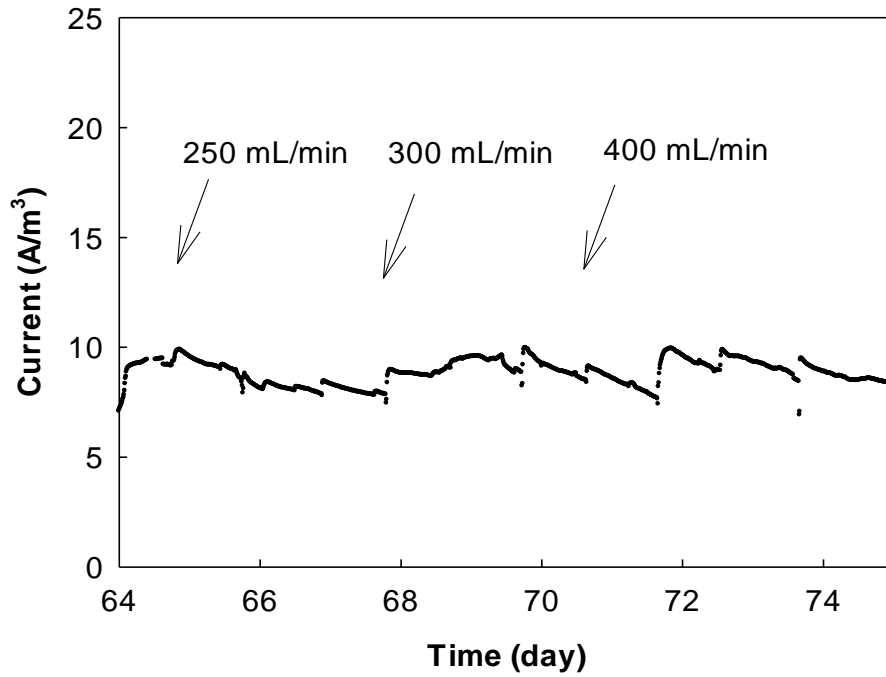


Figure C2 Current generation of MFC-1 with different recirculation rates in Phase I.

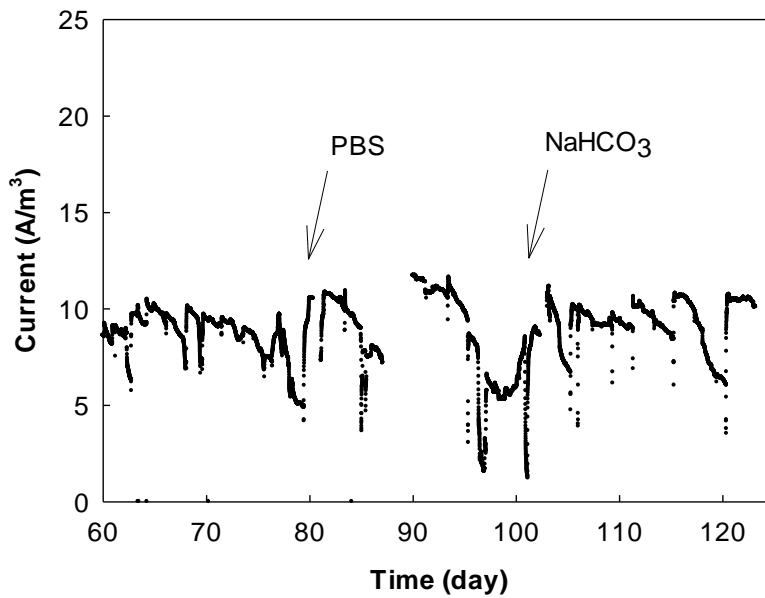
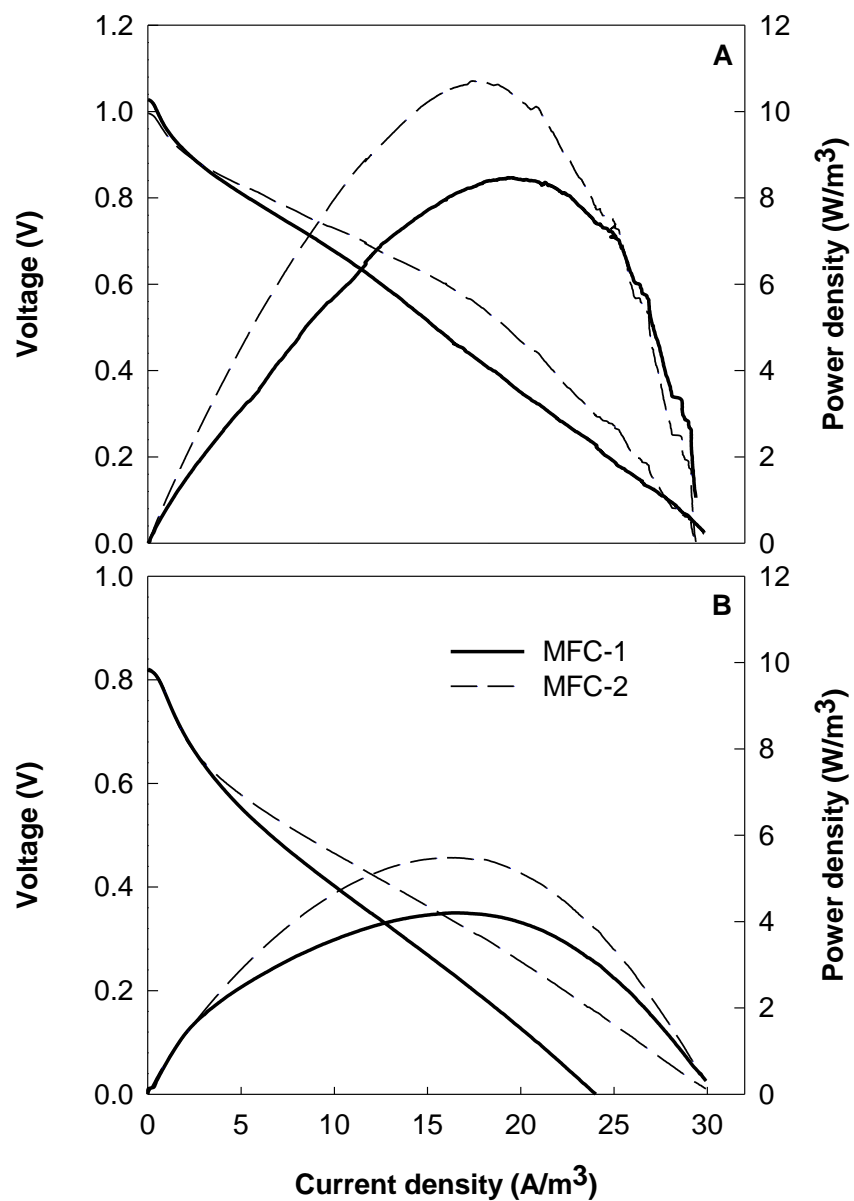


Figure C3 Current generation of MFC-1 buffered with two different solutions in Phase I.



**Figure C4 Power and voltage curves of the two MFCs during Phase II: (A) using acidified water as a catholyte; and (B) using neutralized water as a catholyte. The scan rate was 0.1 mV/s.**

## Appendix D Supplemental Information to Chapter 8

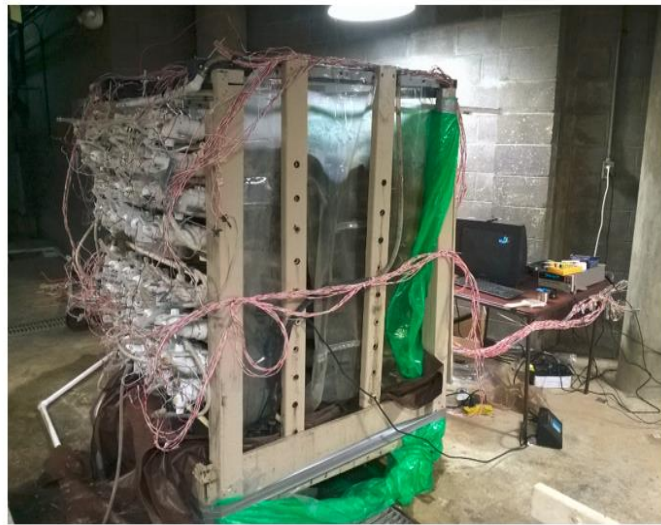
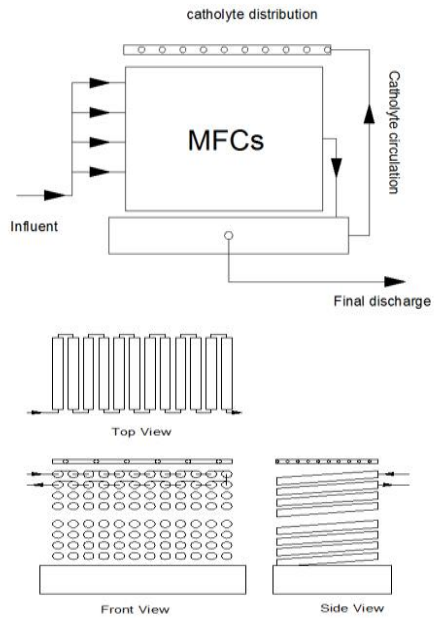


Figure D1. Schematic of MFCs system.

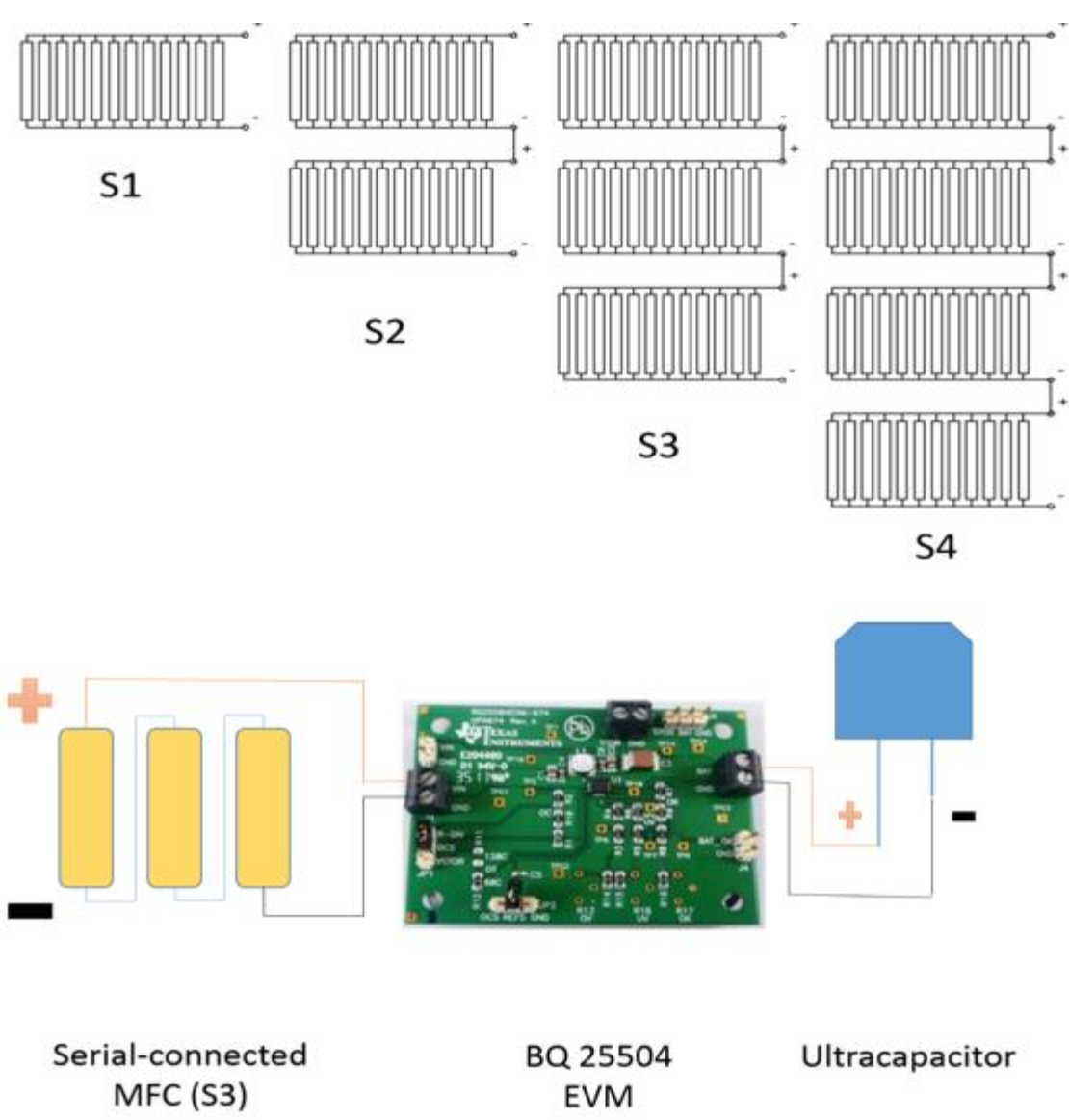
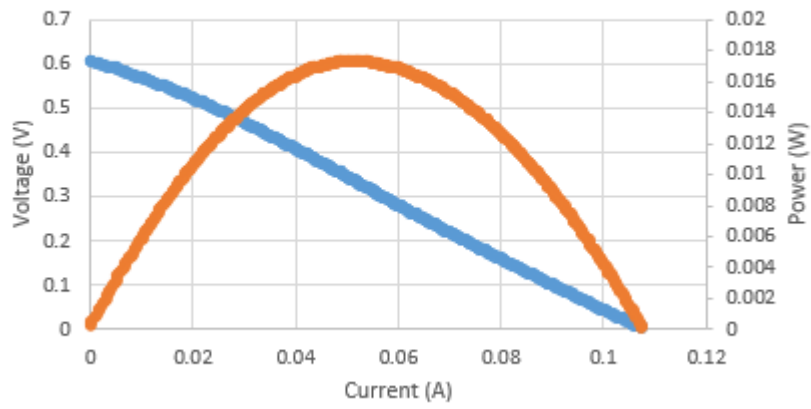
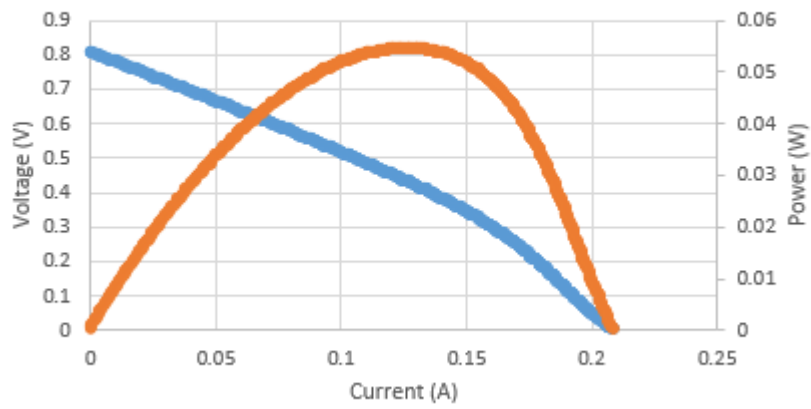


Figure D2 Schematic of electric connections: serial connections (top) and charging/discharging circuit connection (bottom).

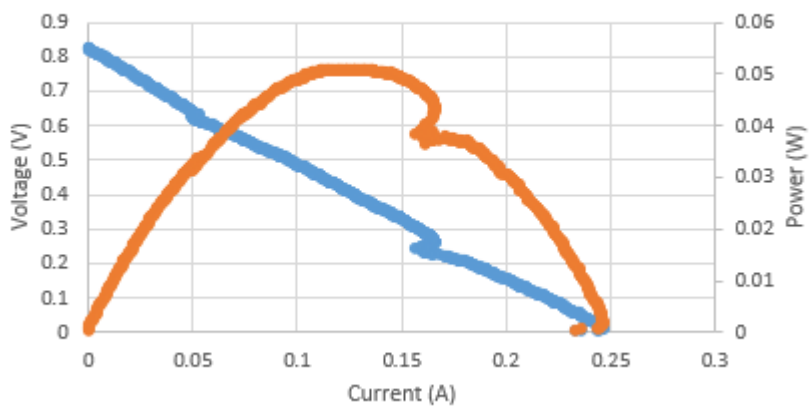
### S1 - R1



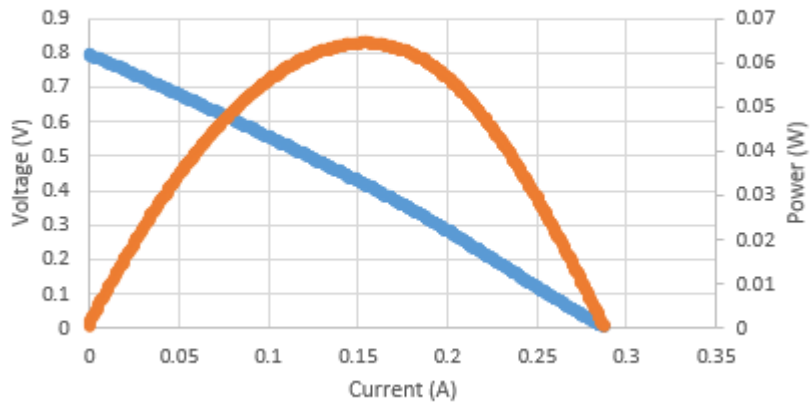
### S1 - R3



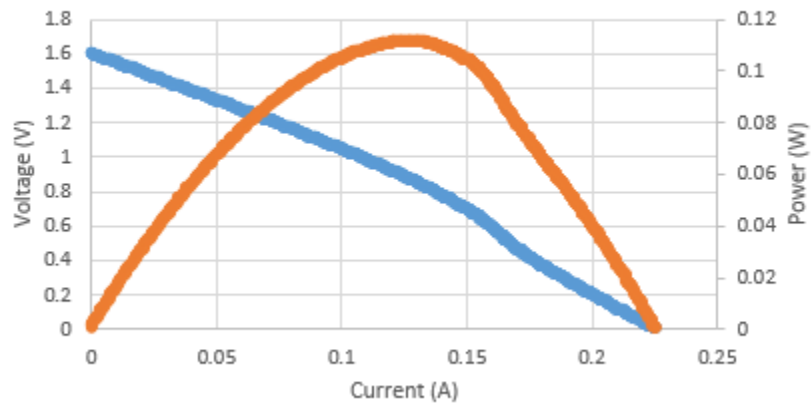
### S1-R5



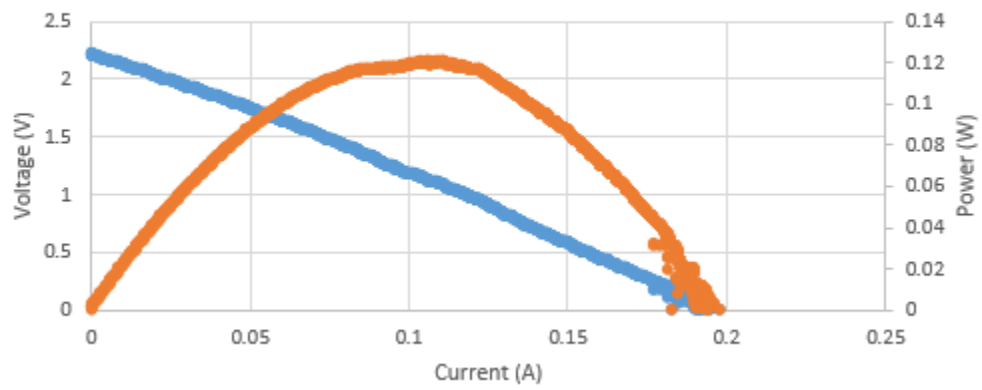
### S1 - R7



### S2 - R37



### S3 - R357



### S4 - R1357

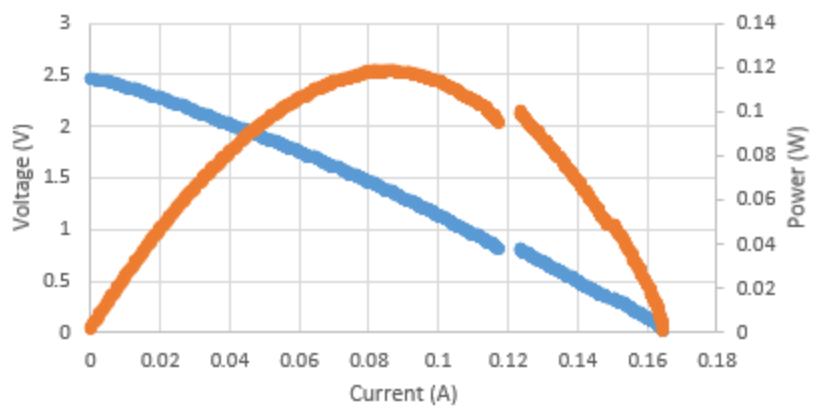


Figure D3 Polarization curves of MFCs with various serial connections.

## CURRICULUM VITAE

### Zheng Ge

Department of Civil and Environmental Engineering  
Virginia Polytechnic Institute and State University  
1303 University City BLVD., APT. 11  
Blacksburg, VA 24060  
Cell phone: (540)-577-6888  
Email: zheng9@vt.edu  
Webpage: <https://sites.google.com/a/vt.edu/zhengge/>

### Education

- **Ph.D. Environmental Engineering**  
Virginia Tech 08/2013-present
- **M.S. Environmental Engineering**  
Polytechnic Institute of NYU 08/2009-05/2011
- **B.S. Environmental Science**  
Wuhan University of Technology, China 09/2004-07/2008

### Intern and Work experience

- **Teaching assistant**  
Virginia Tech 08/2015 – present
- **Summer Intern**  
CHA Companies 05/2015 – 08/2015
- **Research assistant**  
Virginia Tech 08/2013 – 05/2015
- **Research assistant**  
University of Wisconsin – Milwaukee 06/2011 – 06/2013
- **Water treatment technician**  
Aqucell Membrane Technology Co., Ltd, Wuhan, China 07/2008 – 02/2009
- **Design intern**  
Wuhuan Engineering Co., Ltd, Wuhan, China Summer, 2007

## Research interest

Biological wastewater treatment, membrane separation, desalination, nutrients removal and recovery, bioenergy production, bioelectrochemical systems,

## Honors and awards

- Sussman Foundation Scholarship 05/2015
- WaterJAM, the 10th Annual Student Water Challenge, first place 09/2013
- UWM CEAS annual graduate student poster competition, third place 05/2012
- R. E. Speece Fellowship for the anaerobic treatment short course at Marquette University 09/2011
- UWM Chancellor Rewards 2011-2013
- Poly NYU Grade merit scholarships 2009 – 2011

## Publications

1. **Ge, Z.**, Wu, L., Zhang, F. and He, Z.\* (2015) Energy extraction from a large-scale microbial fuel cell system treating municipal wastewater. *Journal of Power Sources*. Vol 297, pp 260-264.
2. **Ge, Z.** and He, Z.\* (2015) An effective dipping method for coating activated carbon catalysts on the cathode electrodes of microbial fuel cells. *RSC Advances*. Vol 5, pp 36933-36937.
3. Xu, B., **Ge, Z.** and He, Z.\* (2015) Sediment microbial fuel cells for wastewater treatment: challenges and opportunities. *Environmental Science: Water Research & Technology*. Vol 1, pp 279-284.
4. Zhi, W., **Ge, Z.**, He, Z. and Zhang H.\* (2014) Methods for understanding microbial community structure and functions in microbial fuel cells: a review. *Bioresource Technology*. Vol 171, pp 461-468.
5. Li, J., **Ge, Z.** and He, Z.\* (2014) A fluidized bed membrane bioelectrochemical reactor for energy-efficient wastewater treatment. *Bioresource Technology*. Vol 167, pp 310-315
6. **Ge, Z.**, Dosoretz, C. and He, Z.\* (2014) Effects of numbers of cell pairs on the performance of microbial desalination cells. *Desalination*. Vol 341, pp 101-106.
7. Xiao, L., **Ge, Z.**, Kelly P., Zhang, F. and He, Z.\* (2014) Evaluation of normalized energy recovery (NER) in microbial fuel cells affected by reactor dimension and substrates. *Bioresource Technology*. Vol 157, pp 77-83.
8. Li, J., **Ge, Z.** and He, Z.\* (2014) Advancing membrane bioelectrochemical reactor (MBER) with hollow-fiber membranes installed in the cathode compartment. *Journal of Chemical Technology & Biotechnology*. Vol 89, pp 1330-1336.
9. **Ge, Z.**, Li, J., Xiao, L., Tong, Y. and He, Z.\* (2014) Recovery of electrical energy in microbial fuel cells. *Environmental Science & Technology Letters*. Vol 1, pp 137-141.
10. Zhang, F., **Ge, Z.**, Grimaud, J., Hurst, J. and He, Z.\* (2013) Long-term performance of liter-scale microbial fuel cells installed in a municipal wastewater treatment

- facility. *Environmental Science & Technology*. Vol 47, pp 4941-4948.
11. Zhang, F., **Ge, Z.**, Grimaud, J., Hurst, J. and He, Z.\* (2013) In situ investigation of tubular microbial fuel cell deployed in an aeration tank at a municipal wastewater treatment plant. *Bioresource Technology*. Vol 136, pp 316-321.
  12. **Ge, Z.**, Zhang, F., Grimaud, J., Hurst, J. and He, Z.\* (2013) Long-term investigation of microbial fuel cells treating primary sludge or digested sludge. *Bioresource Technology*. In press
  13. Zhang, F., **Ge, Z.**, Grimaud, J., Hurst, J. and He, Z.\* (2013) Improving electricity production in tubular microbial fuel cell system through optimizing the anode flow with spiral spacers. *Bioresource Technology*. Vol 134, pp 251-256.
  14. **Ge, Z.**, Ping, Q. and He, Z.\* (2013) Hollow-fiber membrane bioelectrochemical reactor for domestic wastewater treatment. *Journal of Chemical Technology & Biotechnology*. In press.
  15. **Ge, Z.**, Ping, Q., Xiao, L. and He, Z.\* (2013) Reducing effluent discharge and recovering bioenergy in an osmotic microbial fuel cell treating domestic wastewater. *Desalination*. Vol 312, pp 52-59. (Special Issue: Recent Advances in Forward Osmosis)
  16. **Ge, Z.** and He, Z.\* (2012) Effects of draw solutions and membrane conditions on electricity generation and water flux in osmotic microbial fuel cells. *Bioresource Technology*. Vol 109, pp 70-76.

### **Conference Presentations and Posters (\*Presenter)**

1. **Ge, Z.\***, Zhang, F., and He, Z. Microbial Fuel Cells for Energy-efficient Wastewater Treatment: can we do it? VA AWWA & VWEA Water JAM 2015, Virginia Beach, VA.
2. **Ge, Z.\***, Veltman, S., and He, Z. Treatability Evaluation of N-Methyl-2-Pyrrolidone under Anaerobic Condition. VA AWWA & VWEA Water JAM 2015, Virginia Beach, VA (Poster)
3. **Ge, Z.\***, Zhang, F., and He, Z. Development of large-scale Microbial Fuel Cells. The North American Meeting of the ISMET. May 13-15, 2014, State College, PA. (Poster)
4. **Ge, Z.\***, Zhang, F., and He, Z. Development of Microbial Fuel Cells for Energy-efficient Wastewater Treatment. Borchardt Conference, Feb 25-26, 2014, Ann Arbor, MI. (Poster)
5. Jacobson, K., Xiao, Li., **Ge, Z.**, Brastad, K. and He, Z. Development of Photo-Bioelectrochemical Systems for Wastewater Treatment and Bioenergy Production. National Sustainable Design Expo, April 18-19, 2013, Washington D.C.
6. **Ge, Z.\*** and He, Z. Reducing effluent discharge and recovering bioenergy in an osmotic microbial fuel cell treating domestic wastewater. The North American Meeting of the ISMET. October 9-10, 2012, Ithaca, NY.